DISCRETE-TIME CONTROL OF A SPACECRAFT WITH RETARGETABLE FLEXIBLE ANTENNAS

by

Martin E.B. France

Dissertation submitted to the Faculty of the
Virginia Polytechnic Institute and State University
in partial fulfillment of the requirements for the degree of

DOCTOR OF PHILOSOPHY
in
Engineering Mechanics

APPROVED:

L. Meirovitch, Chairman

D. Frederick

D.P. Telionis

M.A. Norris

H.F. VanLandingham

25 May 1989
Blacksburg, Virginia

DISCRETE-TIME CONTROL OF A SPACECRAFT WITH RETARGETABLE FLEXIBLE ANTENNAS

by

Martin E.B. France

L. Meirovitch, Chairman

Engineering Mechanics

(ABSTRACT)

This dissertation considers the discrete-time control of a spacecraft consisting of a rigid-platform with retargetable flexible antennas. The mission consists of independent minimum-time maneuvers of each antenna to coincide with predetermined lines of sight, while the platform is stabilized in an inertial space and elastic vibration of the antennas is suppressed. The system is governed by a set of linearized, time-varying equations of motion. A discrete-time approach permits consideration of the time-varying nature of the system in designing the control law.

Both global and decentralized controls are proposed for a noise-free system with full-state feedback. Initially, a time-varying linear-quadratic regulator (LQR) is implemented, followed by two types of decentralized controllers. First, a collocated control law is devised in which actuator forces are based on the position and velocity at the actuator locations. Next, a new method called Substructure-Decentralized Control is proposed, where each flexible substructure is controlled

based on state measurements associated with the substructure modes of the separately modeled appendages.

In both global and decentralized cases, a linear control law is first implemented coupled with an open-loop disturbance-accommodating control based on the known inertial disturbances caused by the maneuver. Elastic motion is next controlled using nonlinear (on-off) antenna controllers for each decentralized case. For Substructure-Decentralized Control, the controls translate into quantized actual controls. Lastly, nonlinear (on-off) control laws are also used to control the rigid-body motion for each case.

Next, the problem of controlling the time-varying system in the presence of noisy actuators and sensors is examined. It is assumed that only displacements, not velocities, are sensed for both rigid-body and elastic motion, making state reconstruction also necessary. A discrete-time, full-order Kalman filter is constructed for the time-varying system. A pseudo-decentralized control is proposed whereby feedback controls are based on system state estimates. As before, both linear and nonlinear controls are implemented. For each case mentioned, a numerical example is presented involving a spacecraft with a single flexible maneuvering antenna.

ACKNOWLEDGEMENTS

Thanking all who have played a vital role in the completion of this work is no small task. I'm sure most of those mentioned below are at least as happy as I that this day has come - for a variety of reasons!

I would first like to thank the U.S. Air Force Academy, particularly Head of the Department of Astronautics, for providing me with the opportunity to pursue my PhD, as well as his confidence in me as a student and teacher.

I am very grateful to Dr Leonard Meirovitch for the inspiration and guidance he provided as my major advisor. It has been an rare honor to learn from someone who so embodies professionalism and academic achievement.

I'd like to thank the members of my committee, Drs Frederick, VanLandingham, Telionis and Norris, for their advice on this work and in the classroom and Drs Henneke and Smith for taking the time to serve on my final exam committee. I'm particularly indebted to Dr Mark Norris for office space, his undying motivation, patience with my questions and tolerance of my whining and complaining during those all too common 'dark' moments on the research road.

Other VPI&SU people whose friendship and advice have cushioned the blows and helped make our stay in Blacksburg enjoyable and productive include Dr M.K. Kwak,

and

and - all current and former students in the ESM Department. I'd also like to thank

and for their clerical support, encouragement and occasional baked goods.

To my wonderful wife, and terrific sons and

words cannot describe the positive effect your love, support, patience and laughter have had on me. You, more than others, always believed in me even when I doubted.

To my hero, and younger brother,

I thank you for 30 years of friendship and good-natured competition. As our careers have taken different paths, you've enabled me to "slip the surly bonds," albeit vicariously, whenever you strap on your F-16.

Finally, I'd like to dedicate this work to my parents,

and The greatest teachers I've ever known, their love and lessons have played a crucial part in my every successful decision, and that has made all the difference.

TABLE OF CONTENTS

LIST OF ILLUSTRATIONS

1 INTRODUCTION

As the complexity of future space systems and missions increases, e.g., NASA's Space Station, the problem of maneuver and control of flexible spacecraft takes on added importance. The orientation of simple flexible spacecraft along a desired line of sight has been generally addressed by slewing the entire vehicle and suppressing vibration in the flexible components during and/or after maneuver completion. However, instances arise in which it is more efficient to reorient specific components, e.g., an antenna, relative to a main body while stabilizing the main body in an inertial space and suppressing elastic motion of the flexible parts of the spacecraft. Such an approach becomes particularly attractive in the case of spacecraft consisting of a main rigid-body and several flexible substructures, each requiring independent, simultaneous retargeting. This dissertation addresses the control of such a system.

1.1 Background

Since the beginning of the "Space Age" more than 30 years ago, the dynamics and control of flexible spacecraft have been

a growing concern (Ref. 39). The problem of efficient derivation of the equations of motion for complex spacecraft has been a constant goal in the analysis of systems such as the one considered in this dissertation. Indeed, equations of motion for flexible spacecraft are typically very complicated, leading to many recent attempts to develop more convenient expressions for spacecraft motion. Several of these are compared in Ref. 16. Another effective modeling technique using Lagrange's equations of motion for flexible bodies in terms of quasi-coordinates (Ref. 23) was proposed by Meirovitch (Ref. 33).

As the complexity of missions has grown beyond simple station keeping to include maneuvering, control design has also become more difficult. The control of large flexible structures in general is treated in several works, e.g. Refs. 2,4,15,16,22,25-27,51. Studies involving single-axis maneuvers of simple spacecraft consisting of a main rigid-body and a number of flexible appendages with fixed orientation relative to the main body provided important insights into problems confronting engineers (Refs. 5,7,8,30,31,42,44,47,48). Turner and Junkins (Ref. 47), Turner and Chun (Ref. 48) and Breakwell (Ref. 8) proposed methods for simultaneous maneuver and vibration suppression of such systems, while Baruh and Silverberg (Refs. 5 and 7) separated the maneuver and vibration suppression tasks. More recent work has centered on NASA's Spacecraft Control Laboratory Experiment (SCOLE) and the

possibility of missions involving control of flexible structures carried into orbit by the space shuttle (Refs. 29,42,49). The objective of SCOLE is to reorient the structure line of sight in minimum time with limited control authority. As in the case of simpler systems, the SCOLE is concerned with reorienting the entire spacecraft.

For more complex systems involving rotational maneuvering, the derivation of the equations of motion by means of Lagrange's equations for flexible bodies in terms of quasi-coordinates is particularly attractive. The beauty of this method is that the equations of motion are based on body-fixed coordinates, hence it is convenient to design a control law based on these body-fixed coordinates. This approach was successfully applied by Meirovitch and Kwak (Ref. 35) to multi-body systems in which individual substructures are reoriented to coincide with desired lines of sight. Figure 1 shows a typical spacecraft of the type described above consisting of a rigid main body and several flexible appendages.

The control design problem for a system of the type shown in Fig. 1 was first treated by a continuous-time approach by Meirovitch and Kwak (Ref. 32) under the assumption that the time-varying terms in the coefficients are sufficiently small that they can be ignored for the purpose of control design. This is based on the premise that the appendages are relatively small and that the maneuvers are "slow." Reference 32 also

assumed noise-free, continuous, full-state feedback by means of perfect actuators and that each antenna maneuver is carried out open-loop using a bang-bang control law, while platform inertial stabilization and appendage vibration suppression are performed simultaneously. Reference 19 contains a summary of Refs. 32, 34, and 35 that propose a disturbance-minimization technique, a proportional-plus-integral (PI) control and a perturbation method, respectively, to control the spacecraft. A perturbation method was applied to the time-varying system in Ref. 34 using both an "adiabatic approximation" (Ref. 12) and an integral method to update the system parameters and calculate feedback control gains at discrete intervals during a maneuver while employing a continuous time controller. Gains calculated using both techniques are held constant between updates.

The time-varying nature of the system was considered by Meirovitch and France (Ref. 36) using a discrete-time approach. The resulting control laws assumed noise-free, full-state feedback and perfect actuators. Both decentralized and global linear control laws were demonstrated, as well as a combination of linear and nonlinear decentralized controls to stabilize the rigid-body motions and elastic deformations, respectively. Reference 38 extended the work of Ref. 36 by considering noisy actuators and sensors, where the sensors measure elastic deformations of the antennas relative to local coordinate

frames. This sensor output is then processed by a Kalman filter that provides current estimates of the system states, upon which each antenna's pseudo-decentralized control input is based.

The use of strain gauges in measuring elastic motions has been discussed in several papers (Refs. 9,15,18,41). Reference 18 demonstrated that strain gauges could be used to measure very high frequency phenomena. Optical sensors also show great promise in low-noise sensing of elastic motions (Refs. 43,49) as well as in distributed sensing (Refs. 40,50).

Nonlinear control of flexible structures using quantized controls was proposed in Ref. 28, while on-off attitude control of spacecraft, and rigid-body systems in general, is discussed in many sources (e.g., Refs. 1,17,46). Several decentralized control techniques for control of large flexible structures have also been proposed (Refs. 3,22,45). Uniform Damping, developed by Silverberg (Ref. 45) is attractive because control forces at discrete actuator points can be determined independently of stiffness properties given position and velocity information at the actuator location. A method of substructure control based on the Component Mode Synthesis method has been proposed by Young (Ref. 51). Reference 36 demonstrates the use of Uniform Damping in a discrete-time formulation for the system in question, and it proposes a Substructure-Decentralized Control.

The design of both continuous-time and discrete-time full-order Kalman filters to estimate states in a system with incomplete and noisy measurements is well known (Refs. 11,13,20,27). In the case in which some measurements are noise-free and others are not, i.e., a singular sensor noise covariance matrix, some attempts have been made to define a reduced order Kalman filter (Refs. 10,21), although the computational savings when applied to real systems remains in question.

Much of this dissertation is based on the work presented in Refs. 36 and 38. It extends this earlier work by including the use of a nonlinear (bang-off-bang) control law to stabilize the rigid-body motions and by considering a pseudo-collocated control to suppress vibration of the flexible appendages. As before, each additional approach is demonstrated by means of a numerical example involving a spacecraft with a single flexible antenna undergoing a 45^{o} reorientation relative to the platform, while the platform is stabilized relative to an inertial space. Results for the various cases are then compared and discussed.

1.2 Organization of the Dissertation

Chapter 2 gives a summary of the equations of motion for a spacecraft consisting of a main rigid-body and several independently retargetable flexible antennas developed in Ref.

26. Coefficient matrices for these equations are shown in detail in Appendix B.

Chapter 3 presents both global and decentralized control laws for the deterministic (noise-free) system assuming full-state feedback. First, a discrete-time version of the linear disturbance-accommodating control derived in Ref. 32 is presented based on the inertial disturbances caused by the known antenna maneuver. Then, a step-varying linear quadratic regulator is proposed. Both linear and nonlinear collocated controllers are discussed, with the linear case based on the concept of Uniform Damping. A new approach, Substructure-Decentralized Control, is then presented using both linear and nonlinear control.

The problems associated with controlling a noisy system with incomplete measurements is addressed in Chapter 4. First, the unique problems associated with sensor selection and output processing are discussed, as are the advantages and disadvantages of several specific sensor types. Design of an appropriate step-varying, full-order Kalman filter is then presented, followed by a discussion of the effects of such a global estimation on controller design. Next, the concept of pseudo-decentralized control is addressed for each of the decentralized control techniques presented in Chapter 3.

Chapter 5 presents numerical examples of each control law considered for both the deterministic and stochastic systems.

Each case is evaluated on a system consisting of a main rigid-body and one flexible antenna undergoing a 45^{o} reorientation relative to the platform, while the platform is stabilized relative to an inertial space. Finally, in Chapter 6, the work contained in this dissertation is summarized and the results of the numerical examples are compared and discussed.

2 EQUATIONS OF MOTION

The equations of motion for the system shown in Fig. 1 were derived in Ref. 32 using a new formulation of Lagrange's equations for flexible bodies in terms of quasi-coordinates (Ref. 33). Following is a brief summary of these equations. Referring to Fig. 1, we identify a set of inertial axes XYZ, a set of body axes xyz attached to the rigid platform and a set of body axes $x_e y_e z_e$ embedded in the typical flexible appendage e, $(e = 1,2,\ldots,N)$. The position vector of a point in the rigid body is given by $\underline{R}_r = \underline{R}_o + \underline{r}$ and that in the appendage e can be written as $\underline{R}_e = \underline{R}_o + \underline{r}_{o_e} + \underline{r}_e + \underline{u}_e$, $(e = 1,2,\ldots,N)$, where $\underline{R}_o$ is the radius vector from O to o, $\underline{r}$ is the position vector of a point in the rigid body relative to xyz, $\underline{r}_{o_e}$ is the radius vector from o to e, $\underline{r}_e$ is the position vector of a nominal point in the undeformed appendage relative to $x_e y_e z_e$ and $\underline{u}_e$ is the elastic displacement of that point. Vector $\underline{R}_o$ is expressed in terms of components along XYZ, $\underline{r}$ and $\underline{r}_{o_e}$ in terms of components along xyz and $\underline{r}_e$ and $\underline{u}_e$ in terms of components along $x_e y_e z_e$. The velocity vector of o can be written in terms of components along xyz in the form $\underline{V}_o = C\,\dot{\underline{R}}_o$, where C is the matrix of direction cosines between xyz and XYZ and $\dot{\underline{R}}_o$ is the velocity vector of o in terms of components along XYZ. The angular velocity

vector of axes xyz in terms of components along xyz is given by $\underline{\omega} = \mathcal{D}\dot{\underline{\theta}}$, where $\dot{\underline{\theta}}$ is a vector of angular velocities $\dot{\theta}_i$ and D is a matrix depending on the angular displacements θ_i $(i = 1,2,3)$. In view of the above, the velocity vector of a point on the rigid body in terms of components along xyz is

$$\underline{V}_r = \underline{V}_o + \underline{\omega} \times \underline{r} \tag{2-1}$$

and that of a point in appendage e in terms of components along $x_e y_e z_e$ is

$$\underline{V}_e = E_e(\underline{V}_o + \underline{\omega} \times \underline{r}_{oe}) + (E_e\underline{\omega} + \underline{\omega}_e) \times (\underline{r}_e + \underline{u}_e) + \underline{v}_e, \quad e = 1,2,\ldots,N \tag{2-2}$$

where $\underline{\omega}_e$ is the angular velocity of axes $x_e y_e z_e$, E_e is a matrix of direction cosines between axes $x_e y_e z_e$ and xyz and $\underline{v}_e$ is the elastic velocity of the point in the appendage relative to $x_e y_e z_e$, $\underline{v}_e = \dot{\underline{u}}_e$. For the proposed maneuver, the angular velocity vectors $\underline{\omega}_e$ of $x_e y_e z_e$ relative to xyz are given, so that the rotational motions of the appendages relative to the platform do not add degrees of freedom to the system.

The equations describing the rigid-body translations and rotations of the system are ordinary differential equations and those for the elastic motions of the appendages are partial differential equations, so that the equations of motion are hybrid. Because control design for systems described by hybrid

equations is not feasible, we must discretize the system in space. This is accomplished by expressing the elastic displacements as linear combinations of space-dependent admissible functions multiplied by time-dependent generalized coordinates of the form

$$\underline{u}_e(\underline{r}_e,t)=\Phi_e(\underline{r}_e)\underline{q}_e(t), \quad e=1,2,\ldots,N \tag{2-3}$$

where Φ_e is a matrix of admissible functions and $\underline{q}_e$ is a vector of generalized coordinates. The equations of motion, discretized in space, are given in Ref. 32 and will not be repeated here in full. Assuming small motions of the stabilized rigid platform, a linearized version of these equations has the state form

$$\dot{\underline{x}}(t)=\mathbf{A}(t)\underline{x}(t)+\mathbf{B}(t)\underline{f}(t)+\mathbf{D}(t)\underline{d}(t) \tag{2-4}$$

where $\underline{x}(t)=[\underline{R}_o^T\underline{\theta}^T\underline{q}_1^T\underline{q}_2^T\ldots\underline{q}_N^T\underline{V}_o^T\underline{\omega}^T\dot{\underline{q}}_1^T\dot{\underline{q}}_2^T\ldots\dot{\underline{q}}_N^T]^T$ is a state vector, in which $\underline{\theta}$ is a symbolic vector of angular displacements of the platform and

$$\mathbf{A}(t)=\begin{bmatrix}\mathbf{0} & \mathbf{I}\\ -\mathbf{M}^{-1}(t)\mathbf{K}(t) & -\mathbf{M}^{-1}(t)\mathbf{G}(t)\end{bmatrix} \tag{2-5a}$$

$$\mathbf{B}(t)=\begin{bmatrix}\mathbf{0}\\ \mathbf{M}^{-1}(t)\mathbf{B}^*(t)\end{bmatrix} \qquad \mathbf{D}(t)=\begin{bmatrix}\mathbf{0}\\ \mathbf{M}^{-1}(t)\end{bmatrix} \tag{2-5b,c}$$

are coefficient matrices. Moreover, $\underline{d}(t)$ is a vector of disturbances caused by the maneuver and $\underline{f}(t) = [\underline{F}_o^{*T}\, \underline{M}_o^{*T}\, \underline{f}_{11}^T\, \underline{f}_{12}^T \cdots \underline{f}_{1n_1}^T\, \underline{f}_{21}^T\, \underline{f}_{22}^T \cdots \underline{f}_{2n_2}^T\, \underline{f}_{31}^T \cdots \underline{f}_{Nn_N}^T]^T$ is the control force vector, in which $\underline{F}_o^*$ and $\underline{M}_o^*$ are actuator force and torque vectors acting on the rigid platform and $\underline{f}_{en_t}$ are the actuator forces acting on appendage e at point n_t, where appendage e has n_e actuators. Explicit expressions for the matrices $\mathrm{M}(t)$, $\mathrm{K}(t)$, $\mathrm{G}(t)$ and $\mathrm{B}(t)$ are given in Appendix A.

3 DETERMINISTIC DISCRETE-TIME CONTROL

3.1 Introduction

For the system considered in this dissertation, maneuvering of each antenna is carried out open-loop using a bang-bang control law, while simultaneously performing platform stabilization and appendage vibration suppression. To this end, the control law design process begins by considering a discrete-time approach that permits consideration of the time-varying nature of the system. The resulting step-varying controller can then be applied to the time-varying spacecraft. It is initially assumed that, as in Refs. 32 and 34, the sensors and actuators are noise free, i.e., that the system is deterministic, and all the states necessary to compute the feedback controls are available. Therefore, no state estimation or filtering is required.

In this section, the control process is divided into open- and closed-loop components for linear control. The open-loop control is a the discrete-time adaptation of the continuous-time disturbance-accommodating controller presented in Ref. 32. Next, both global and decentralized control laws are considered.

The global control is a discrete-time linear quadratic regulator. Two different decentralized approaches are discussed: Colocated Control and Substructure-Decentralized Control. In the case of decentralized control, both linear and nonlinear controllers are proposed for rigid-body stabilization and vibration suppression.

3.2 Disturbance-Accommodating Control

We propose to control the system by means of a combination of open- and closed-loop controllers, taking into account the time-varying nature of the coefficient matrices and the fact that for an open-loop maneuver the inertial disturbances are known. Hence, the control is separated into open and closed-loop components as follows:

$$\underline{f}(t) = \underline{f}_o(t) + \underline{f}_c(t) \tag{3-1}$$

Then, with reference to Eq. (2-4), the open-loop control is chosen to satisfy

$$\mathbf{B}(t)\underline{f}_o(t) + \mathbf{D}(t)\underline{d}(t) = \underline{0} \tag{3-2}$$

Considering Eqs. (2-5b,c), then

$$\mathbf{B}^*(t)\underline{f}_o(t) + \underline{d}(t) = \underline{0} \tag{3-3}$$

so that the open-loop disturbance-accommodating control is given by

$$\underline{f}_o(t) = -[\mathbf{B}^*(t)]^\dagger \underline{d}(t) \tag{3-4}$$

where

$$[\mathbf{B}^*(t)]^\dagger = [(\mathbf{B}^*(t))^T \mathbf{B}^*(t)]^{-1} [\mathbf{B}^*(t)]^T \tag{3-5}$$

is the pseudo-inverse of $\mathbf{B}^*(t)$.

In the case of a discrete-time system, the open-loop control at step k becomes

$$\underline{f}_o(k) = -[\mathbf{B}^*(k)]^\dagger \underline{d}(k) \tag{3-6}$$

where each of the terms in Eq. (3-6) are evaluated at time $t = kT$ as described in the next section. This open-loop control can be implemented in conjunction with any linear closed-loop control.

3.3 Global Control

For closed-loop control, we first consider a discrete-time linear quadratic regulator. The discrete-time equivalent of the state equations, Eq. (2-4) is (Ref. 11)

$$\underline{x}(k+1) = \mathcal{A}(k)\underline{x}(k) + \mathcal{B}(k)\underline{u}(k), \quad k = 0, 1, 2, \ldots \tag{3-7}$$

where k denotes the time $t = t_k = kT$, in which T is the sampling period, and

$$\mathcal{A}(k) = e^{\mathrm{A}(k)T} = \mathrm{I} + \frac{\mathrm{A}(k)T}{1!} + \frac{\mathrm{A}^2(k)T^2}{2!} + \cdots + \frac{\mathrm{A}^i(k)T^i}{i!} + \cdots \qquad (3-8)$$

$$\mathcal{B}(k) = \left[\mathrm{I}T + \frac{\mathrm{A}(k)T^2}{2!} + \frac{\mathrm{A}^2(k)T^3}{3!} + \cdots + \frac{\mathrm{A}^i(k)T^{i+1}}{(i+1)!} + \cdots \right] \mathrm{B}(k) \qquad (3-9)$$

are discrete-time coefficient matrices. Equations (3-8) and (3-9) are obtained by regarding $\mathrm{A}(t)$ and $\mathrm{B}(t)$, Eqs. (2-5a,b), as constant over the steps $kT < t < kT + T$, $(k = 0, 1, 2, \ldots)$. The discrete-time optimal feedback control can be written as

$$\underline{u}(k) = \mathcal{K}(k)\underline{x}(k), \quad k = 0, 1, 2, \ldots \qquad (3-10)$$

where $\mathcal{K}(k)$ is the discrete-time control gain matrix, obtained by minimizing the discrete-time quadratic cost function (Ref. 13)

$$J = \underline{x}^T(N)\mathrm{P}(N)\underline{x}(N) + \sum_{k=0}^{N-1} [\underline{x}^T(k)\mathrm{Q}(k)\underline{x}(k) + \underline{u}^T(k)\mathrm{R}(k)\underline{u}(k)] \qquad (3-11)$$

The weighting matrices $\mathrm{P}(N), \mathrm{Q}(0), \mathrm{Q}(1), \ldots, \mathrm{Q}(N-1)$ and $\mathrm{R}(0), \mathrm{R}(1), \ldots, \mathrm{R}(N-1)$ are symmetric. Moreover, $\mathrm{Q}(k)$ and $\mathrm{R}(k)$ are positive definite and $\mathrm{P}(N)$ is positive semidefinite, and for our purposes they are assumed to be constant and diagonal for all N control steps with $\mathrm{P}(N) = \mathrm{Q}(N-1)$. Also, it is assumed throughout this

chapter that all system states are available for feedback, and that there is no estimation error involved.

The solution to this state-feedback problem is based on the work of either Kalman or Bellman and can be found in a variety of texts . Following the procedure based on Bellman's Principle of Optimality described in Ref. 13, the optimal feedback gains are calculated backwards in step. Beginning with $i = 1$ and the known $\mathrm{P}(N)$, we write

$$\mathcal{K}(N-i) = -[\mathcal{B}^T(N-i)\mathrm{P}(N+1-i)\mathcal{B}(N-i) + \mathbf{R}(N-i)]^{-1} \times \mathcal{B}^T(N-i)\mathrm{P}(N+1-i)\mathcal{A}(N-i) \tag{3-12}$$

$$\mathrm{P}(N-i) = [\mathcal{A}(N-i) + \mathcal{B}(N-i)\mathcal{K}(N-i)]^T\mathrm{P}(N+1-i)[\mathcal{A}(N-i) + \mathcal{B}(N-i)\mathcal{K}(N-i)] + \mathcal{K}^T(N-i)\mathbf{R}(N-i)\mathcal{K}(N-i) + \mathbf{Q}(N-i) \tag{3-13}$$

and continue until $\mathcal{K}(0)$ is calculated. For our system, the final step occurs several time steps after the slewing maneuver is completed, at which time the system can be regarded as time-invariant. Therefore, the gains calculated soon after the completion of the maneuver will be treated as constant, leading to steady-state regulation.

If the system complexity results in computational requirements in excess of the controller's capacity, given the desired control frequency, then in implementing such a control law the LQR gains can be calculated prior to maneuver execution,

based on the known system parameters and slewing profile, and stored in the computer for use during and after the maneuver. The disturbance-accommodating open-loop control is calculated during the maneuver and updated with each time step.

In evaluating the utility of such a control law versus the time-invariant approximation, we must weigh the improvements in the time response of the spacecraft against the added computational complexity involved in a time-varying plant.

3.4 Decentralized Control

Implemention of a decentralized control law has many significant advantages for the type of system under investigation. Especially in the case of a spacecraft with several antennas, using many simple independent controllers reduces the computational requirements significantly compared to a global control system. The computations can also be performed completely "on-line," as opposed to a significant amount of premaneuver computations required by global controls. This computational savings could allow for faster, more accurate sampling in the case of discrete-time control.

In this dissertation, two different types of decentralized control are investigated: the first in which individual points on the antennas are controlled with collocated sensors and actuators (Collocated Control) and the second in which individual modes of the independently modeled substructures are

controlled (Substructure-Decentralized Control). In the case of Collocated Control, it is assumed that both displacements and velocities at the sensor locations, measured relative to the appendage body axes, are available. In the case of Substructure-Decentralized Control, each appendage has an individual controller whose actuator forces are based solely on the generalized displacement and velocity of the substructure modes corresponding to that appendage. In both cases, the rigid-body motions of the entire system are controlled independently via actuators and sensors located on the main platform. As in Collocated Control, in the case of Substructure-Decentralized Control, all states associated with the flexible motion of the antennas are available. Although the controls are designed using a decentralized approach, the response in both cases is calculated by applying the decentralized control law to the full spacecraft.

3.4.1 Collocated Control

3.4.1.1 Linear Control - Uniform Damping

In this case, a linear control law is first considered for the controllers at all points. Control gains for each controller are designed and implemented using a discrete-time approach considering the time-varying nature of the plant. Each of the six controllers responsible for the rigid body motion of the spacecraft are designed separately, each with

a closed-loop frequency chosen well above the fundamental frequency of the flexible appendage and damping equal to 70% of the critical damping. The controllers are designed on the basis of the discrete-time version of the state equations. The continuous-time equations for the rigid-body motions are

$$\frac{d}{dt}\begin{bmatrix} x_i(t) \\ \dot{x}_i(t) \end{bmatrix} = \mathbf{A}_i \begin{bmatrix} x_i(t) \\ \dot{x}_i(t) \end{bmatrix} + \mathbf{B}_i(t) u_i(t), \quad i = 1,2,\ldots,6 \tag{3-14}$$

where

$$\mathbf{A}_i = \begin{bmatrix} 0 & 1 \\ 0 & 0 \end{bmatrix}, \quad \mathbf{B}_i(t) = \begin{bmatrix} 0 \\ m_{ii}^{-1}(t) \end{bmatrix}, \quad i = 1,2,\ldots,6 \tag{3-15a,b}$$

in which m_{ii} is mass or moment of inertia corresponding to the rigid body mode i. Using full state feedback for each controller, the closed-loop difference equation is

$$\underline{x}(k+1) = [\mathcal{A}(k) + \mathcal{B}(k)\mathcal{K}(k)]\underline{x}(k), \quad k = 0,1,2,\ldots \tag{3-16}$$

where $\mathcal{K}(k)$ is chosen to yield satisfactory closed-loop response.

For the point controllers located on the appendage(s), the control law is based on the concept of Uniform Damping Control (Ref. 45). This technique is attractive because the control design is independent of the system stiffness. When n discrete actuators are used on an antenna, the control forces at points P_r are given by

$$\underline{F}_r(t) = -\alpha^2 M_r \underline{U}_r(t) - 2\alpha M_r \dot{\underline{U}}_r(t), \quad r = 1,2,\ldots,n \tag{3-17}$$

where $\underline{U}_r(t) = \underline{u}(P_r,t)$ and $\dot{\underline{U}}_r(t) = \dot{\underline{u}}(P_r,t)$ are measurements of displacement and velocity, respectively, at points P_r and $M_r = \int_{D_r} \rho(P)\,dD_r$ is the mass associated with the region on which $\underline{F}_r(t)$ acts; α is the desired exponential decay rate of the closed-loop response.

3.4.1.2 Mixed Control

Next, we implement a nonlinear (bang-off-bang) control law for the point controllers on the appendage. A combination of velocity and position feedback is used in conjunction with a control deadzone. A dual elliptical deadzone is used to reduce control interaction between subsystems and slow limit-cycle behavior, thus conserving fuel. The two deadzones are such that the "off" deadzone is smaller and lies completely within the "on" deadzone (Ref. 37). The "off" deadzone is defined by

$$\frac{\dot{U}_{\theta_\ell}^2}{a_{\text{off}}^2} + \frac{U_{\theta_\ell}^2}{b_{\text{off}}^2} \leq 1 \tag{3-18}$$

Once turned off, the control remains off until the "on" criterion

$$\frac{\dot{U}_{\theta_\ell}^2}{a_{\text{on}}^2} + \frac{U_{\theta_\ell}^2}{b_{\text{on}}^2} \geq 1 \tag{3-19}$$

is met. A state-plane description of the control law is shown in Fig. 2.

3.4.1.3 Nonlinear Control

As in the linear control case, each rigid-body mode is considered separately, with its own control law and actuator. However in this case, nonlinear controls are used to stabilize the rigid-body motions as well. The state-plane switching curve used for each rigid-body mode is that of a time-optimal, discrete-time controller for a double-integrator system as described in Ref. 17. The mass and inertia terms, and thus the switching curve for each mode, are updated at each control step. However, because in reality the system modes are coupled, the resulting system control is suboptimal. Figure 3 shows these new switching curves with control deadzones in the state plane. The appendage controllers are of the same type as in the previous case, in which linear rigid-body controls were used.

3.4.2 Substructure-Decentralized Control

Next, we propose is to control each flexible substructure by means of actuator forces depending on state measurements associated with a given substructure alone. For example, in the case of a system modeled as one or more flexible antennas hinged to a rigid platform, a controller is implemented in which each antenna's feedback forces are based on displacement

and velocity information taken at discrete points on that antenna. Therefore, each antenna is modeled separately as a cantilever beam with a substructure control law designed to control a finite number of antenna modes.

3.4.2.1 Linear Control

As in the case of Collocated Control, a linear control for both the rigid-body and the flexible motions is employed first. The control law used for rigid-body motions is unchanged from the Collocated Control cases. The equations of motion for substructure e can be expressed as the infinite set of decoupled second-order substructure modal equations

$$\ddot{q}_i(t) + \omega_i^2 q_i(t) = Q_i(t), \quad i = 1, 2, \ldots \tag{3-20}$$

or as the set of first-order state equations

$$\frac{d}{dt}\begin{bmatrix} q_i(t) \\ \dot{q}_i(t) \end{bmatrix} = \begin{bmatrix} 0 & 1 \\ -\omega_i^2 & 0 \end{bmatrix}\begin{bmatrix} q_i(t) \\ \dot{q}_i(t) \end{bmatrix} + \begin{bmatrix} 0 \\ Q_i(t) \end{bmatrix}, \quad i = 1, 2, \ldots \tag{3-21}$$

where ω_i is the natural frequency and $Q_i(t)$ the generalized control force, each associated with the ith substructure mode.

Of course, it is neither necessary nor possible to control all substructure modes using discrete controllers. Hence, the first step is to truncate these equations, controlling enough modes to simulate the motion adequately and to minimize control

spillover into the uncontrolled substructure modes. Using a number of actuators larger than or equal to the number of controlled modes helps reduce spillover (Ref. 6). Feedback gains are chosen for the equations of the controlled substructure modes so that the discrete-time formulation of these equations yields a damping factor and settling time for the fundamental substructure mode of each appendage comparable to the settling time for the uniform damping case. Lower factors for the higher modes are chosen so as to yield a settling time for each equation comparable to that of the fundamental mode for that appendage. The discrete-time closed-loop system matrix can then be constructed and the eigenvalues checked at key points in the maneuver to assure convergence. The resulting η_e generalized control forces can then be transformed to n_e actual control forces for antenna e using the transformation

$$\underline{f}_e(k) = \left[\Phi_e^T\left(\underline{r}_{e_1}\right) \quad \Phi_e^T\left(\underline{r}_{e_2}\right) \quad \cdots \quad \Phi_e^T\left(\underline{r}_{e_{n_e}}\right)\right]^{-1} \underline{Q}_e(k) \tag{3-22}$$

where $\Phi_e^T(z_{e_\ell})$ is the substructure participation matrix, i.e., a matrix of admisssible functions evaluated at the location of actuator e_ℓ, and $\underline{Q}_e(t) = \left[Q_{e_1} Q_{e_2} \cdots Q_{e_{n_e}}\right]^T$ is the vector of generalized controls. If the matrix multiplying $\underline{Q}_e(t)$ is not square, then the pseudo-inverse, described earlier for the

disturbance accommodation control, should be used. The coefficient matrix for the closed-loop system can then be expressed as

$$\mathcal{A}_{cl}(k) = \mathcal{A}(k) + \mathcal{B}(k)\mathcal{K} \tag{3-23}$$

where

$$\mathcal{K} = \begin{bmatrix} \mathcal{K}_{11} & \mathbf{0} & \mathcal{K}_{13} & \mathbf{0} \\ \mathbf{0} & \mathcal{K}_{22} & \mathbf{0} & \mathcal{K}_{24} \end{bmatrix} \tag{3-24}$$

in which $\mathcal{K}_{11}$ and $\mathcal{K}_{13}$ are diagonal 6×6 matrices, the first with elements $c_{ii}(t)$ $(i = 1,2,\ldots,6)$ corresponding to discrete-time position feedback gains for the ith rigid-body mode and the second with elements $b_{ii}(t)$ $(i = 1,2,\ldots,6)$ corresponding to velocity feedback gains. Moreover, $\mathcal{K}_{22}$ and $\mathcal{K}_{24}$ are the result of transforming diagonal matrices, with each diagonal element corresponding to a feedback term from the substructure modal equation similar in form to the rigid-body equations, to the configuration space using the substructure matrix of admissible functions; an example is given in detail in Appendix C. Of course, these gains are constant, because they are based on the independent, time-invariant substructure, and they are zero for the uncontrolled modes. The remaining blocks are zero matrices of appropriate dimension.

3.4.2.2 Mixed Control

The nonlinear case for Substructure-Decentralized Control is similar to the Collocated Control case for controlling the rigid-body motions. The flexible motion of each antenna is controlled by bang-off-bang controllers associated with substructure modes. Because the natural frequencies of a substructure are only indirectly related to the eigenvalues of the overall system, basing the switching curves solely on substructure eigenvalues would have little value. Nonlinear damping is added to each mode (i.e., on-off control based on velocity feedback) by means of a modal force similar to that used in Ref. 28, i.e., using the control law

$$f_r = \begin{cases} -k_r, & \dot{q}_r \geq c_r \\ 0, & |\dot{q}_r| < c_r \\ k_r, & \dot{q}_r \leq -c_r \end{cases}, \quad r = 1,2,3 \tag{3-25}$$

However, if the fundamental frequency of the system with stabilized rigid-body motions is so low that settling time requirements can be met only through added nonlinear stiffness (i.e., on-off control based on position feedback), then a more appropriate control law is

$$f_r = \begin{cases} -k_r, & q_r \geq d_r \cup [q_r \geq -d_r \cap \dot{q}_r \geq c_r] \\ 0, & |q_r| < d_r \cap |\dot{q}_r| < c_r \\ k_r, & q_r \leq -d_r \cup [q_r \leq d_r \cap \dot{q}_r \leq -c_r] \end{cases}, \quad r = 1,2,3 \tag{3-26}$$

In this case, position feedback is used when large displacements occur, while velocity feedback is employed for small amplitude motions. Figure 4 is a state plane description of this criterion.

3.4.2.3 Nonlinear Control

The fully nonlinear case simply combines the nonlinear controllers for each appendage described in the previous section with the nonlinear rigid-body controller used in the nonlinear collocated control case in Sec. 3.4.1.3.

4 STOCHASTIC DISCRETE-TIME CONTROL

4.1 Introduction

In an effort to address some of the problems involved in applying the previously discussed control techniques, in this section I consider the use of noisy actuators and sensors. In addition, I remove the assumption of full-state feedback, resulting in the need to estimate unmeasured states and filter system noise for the time-varying system.

4.2 Sensors

Whereas rigid-body motions of the main structure can be measured using conventional techniques, such as gyros or star sensors, measurement of elastic deformations in an antenna subject to independent slewing maneuvers presents unique difficulties. This dissertation is concerned only with the selection of sensors for measuring antenna elastic motions. Ideally, these measurement devices should be able to account for the changing nominal antenna position by either sensing deformations directly in the antenna local coordinate frame or by measuring positions in the rigid-body frame and then performing a simple transformation. Accelerometers, for example, which measure inertial accelerations, require significant processing of the output to separate antenna local

accelerations. This output, in turn, depends on other measured and estimated values, such as rigid-body angular rotations and rates, making accelerometers a poor choice as sensors for elastic motions.

4.2.1 Strain Gauges

Among sensors already used in flexible structure control experiments, strain gauges are particularly attractive. Indeed, they can measure antenna strains, from which displacements relative to the local frame can be easily derived. The strain gauge output voltage is proportional to the bending strain, ϵ of the antenna outer fibers. The beam strains corresponding to bending about the x_e- and y_e-axis are given by

$$\epsilon_x(z_{e_i}) = h_x \frac{\partial^2 u_x(z_{e_i},t)}{\partial z_e^2}, \quad \epsilon_y(z_{e_i}) = h_y \frac{\partial^2 u_y(z_{e_i},t)}{\partial z_e^2}, \quad i = 1,2,\ldots,p_e \tag{4-1}$$

where h_x and h_y are the half-thicknesses of the beam, whose undeformed neutral axis coincides with the local z_e axis, and i denotes the p_e strain gauge locations. Recalling Eq. (2-3), we can write

$$\frac{\partial^2 \underline{u}_{e_i}(z_{e_i},t)}{\partial z_e^2} = \Phi_e''(z_{e_i})\underline{q}_e(t), \quad e = 1,2,\ldots,N \tag{4-2}$$

Assuming a circular cross-section $h_x = h_y = h$ and solving for the vectors of elastic generalized displacements of the antenna, we obtain

$$\underline{q}_e(t) = \left\{\left[\Phi_e^{T''}(z_{e_1}) \quad \Phi_e^{T''}(z_{e_2}) \quad \cdots \quad \Phi_e^{T''}\left(z_{e_{p_e}}\right)\right]^T\right\}^{-1}\left(\frac{\underline{\epsilon}_e}{h}\right) = S_e^{-1}\left(\frac{\underline{\epsilon}_e}{h}\right) \quad (4-3)$$

where

$$S_e = \left[\Phi_e^{T''}(z_{e_1}) \quad \Phi_e^{T''}(z_{e_2}) \quad \cdots \quad \Phi_e^{T''}\left(z_{e_{p_e}}\right)\right]^T \quad (4-4)$$

and

$$\underline{\epsilon}_e = \left[\epsilon_x(z_{e_1}) \quad \epsilon_y(z_{e_1}) \quad \epsilon_x(z_{e_2}) \quad \epsilon_y(z_{e_2}) \quad \cdots \quad \epsilon_x\left(z_{e_{p_e}}\right) \quad \epsilon_y\left(z_{e_{p_e}}\right)\right]^T \quad (4-5)$$

is the vector of strain outputs from the $2p_e$ gauges located on antenna e.

Unfortunately, strain gauge outputs tend to be noisy, due primarily to the quality of the associated electronic equipment and low-output signal strength. Use of a Kalman filter to compensate for this drawback will be discussed in Sec. 4.3.

4.2.2 Optical Sensors

Another convenient choice is a photogrammetric sensor (Ref. 49). In this case, two or more sensors are placed on the main spacecraft for each antenna. Small infrared light

emitting diodes (LEDs) are then placed at desired locations on the antenna and fired sequentially. As an LED fires, its position is sensed by a planar photodiode. Combining data from two of these sensors and comparing this information with the known sensor and undeformed antenna position yields the elastic deformation at each source point. One shortcoming of an optical system, such as that described above, is a sample-rate limitation that depends not only on the type of sensors, but also on the number of light sources. Because all sources are tracked by the same set of sensors, only one source per antenna-sensor set can be active at any given instant.

Another optical technique would use the same type of sensors, but the optical signal would be provided using a combination of lasers mounted on the main rigid-body and small mirrors placed at desired points on the antenna. Reference 43 demonstrated that such a system can generate high accuracy output at high frequencies (>900Hz), though its ability to sense large deflections is somewhat limited.

4.3 Kalman Filter Design

Independent of the measurement technique used, we assume that the output includes only elastic displacements, and not velocities. Likewise, rigid-body translations and rotations are available while rates are not. All measurements are considered contaminated by "white" noise whose statistics are

known. The system itself is also subject to white noise due to actuator errors, unknown disturbances, etc. In light of this assumption, an estimate is required of both the unmeasured and noisy states.

Because construction of separate substructure estimators is meaningless, a standard full-order step-varying discrete-time Kalman filter approach is proposed (Refs. 11,13,20). In fact, unless a method to directly measure elastic displacements and velocities is available, thus rendering additional processing to recover incomplete or noisy states or for compensation of the time-varying nominal position of the antennas unnecessary, some type of global state estimation for feedback will be required. Implications of a requirement for global estimation on control law design are addressed in later sections.

Kalman filter design requires that the discrete-time equivalent of the system matrices $A(t)$ and $B(t)$, as well as the filter gains, be calculated at each time step. The corresponding closed-loop discrete-time state equations are given by

$$\underline{x}(k+1) = \mathcal{A}(k)\underline{x}(k) + \mathcal{B}(k)\underline{u}(k) + \mathcal{B}_1(k)\underline{w}(k), \quad k = 0,1,2,\ldots \qquad (4-6)$$

$$\underline{y}(k) = C\underline{x}(k) + \underline{v}(k) \qquad (4-7)$$

where k denotes the time $t = t_k = kT$, in which T is the sampling period, $\underline{x}(k)$ is the state vector and $\underline{u}(k)$ is the control input vector at step k. Moreover, $\underline{w}(k)$ and $\underline{v}(k)$ are corresponding actuator and sensor noise vectors, respectively, and $\mathcal{A}(k)$ and $\mathcal{B}(k)$ are again the discrete-time coefficient matrices given in Eqs. (3-7,8). In the case in which rigid-body displacements are measured directly and strain gauges are used to detect flexible motion in a system with one antenna, C has the form

$$C = \begin{bmatrix} I_{6\times 6} & 0 & 0 & 0 \\ 0 & S_1 & 0 & 0 \end{bmatrix} \tag{4-8}$$

where S_1 was defined in Eq. (4-4).

The state estimate $\hat{\underline{x}}(k)$ is given by

$$\hat{\underline{x}}(k) = \tilde{\underline{x}}(k) + \mathcal{M}(k)C^T[C\mathcal{M}(k)C^T + R]^{-1}[\underline{y}(k) - C\tilde{\underline{x}}(k)] \tag{4-9}$$

where

$$\tilde{\underline{x}}(k) = \mathcal{A}(k-1)\hat{\underline{x}}(k-1) + \mathcal{B}(k-1)\underline{u}(k-1) \tag{4-10}$$

is the estimate of the state based on the previous state estimate and input,

$$\mathcal{M}(k) = \mathcal{A}(k-1)\mathcal{P}(k-1)\mathcal{A}^T(k-1) + \mathcal{B}_1^T(k-1)Q\mathcal{B}_1(k-1) \tag{4-11}$$

and

$$\mathcal{P}(k-1)=M(k-1)-M(k-1)C^{T}[CM(k-1)C^{T}+R]^{-1}CM(k-1) \quad (4-12)$$

where $M(0)$ is known and R and Q are the covariance matrices associated with the sensor and actuator noise intensities $\underline{v}(k)$ and $\underline{w}(k)$, respectively.

For more accurate state estimation, the discrete approximation of the known inertial disturbance $\mathrm{D}(t)\underline{d}(t)$ can be added to Eq. (4-6), so that

$$\underline{\tilde{x}}(k)=\mathcal{A}(k-1)\underline{\hat{x}}(k-1)+\mathcal{B}(k-1)\underline{u}(k-1)+\mathcal{D}(k-1)\underline{d}(k-1) \quad (4-13)$$

where

$$\mathcal{D}(k)=\left[\mathrm{I}T+\frac{\mathrm{A}(k)T^{2}}{2!}+\frac{\mathrm{A}^{2}(k)T^{3}}{3!}+\cdots+\frac{\mathrm{A}^{i}(k)T^{i+1}}{(i+1)!}+\cdots\right]\mathrm{D}(k) \quad (4-14)$$

Moreover, $\underline{d}(k)$ is constant over each time interval $kT<t<(k+1)T$ and is equal to $\underline{d}(t)$ evaluated at $t=kT$. Equation (4-14) is obviated by the use of an open-loop disturbance-accommodating controller, as discussed in the next section.

4.4 Pseudo-Decentralized Control Law Design

As mentioned earlier, when incomplete and/or noisy measurements necessitate global estimation, true decentralized control is not possible. Instead, a pseudo-decentralized control is proposed where feedback controls are based on estimates of antenna and rigid-body motions. The system control

laws are pseudo-decentralized in the sense that substructure control inputs depend only on state estimates for that particular substructure. Those estimates, however, are calculated using a global observer - in our case, a Kalman filter.

This dissertation investigates two different approaches to pseudo-decentralized control. As in the case of the deterministic system discussed earlier, individual points corresponding to actuator locations on the antennas are controlled, based on observer estimates of the elastic states of the points in the antenna local coordinate frame (Pseudo-Collocated Control). In the second case, Substructure-Decentralized Control is employed. For Substructure-Decentralized Control, each appendage has an individual controller whose actuator forces are based solely on the globally derived state estimates associated with that particular appendage. In both cases, the rigid-body motions of the entire system are again controlled independently via actuators and sensors located on the main platform. Although the controls are designed by means of a pseudo-decentralized approach, the response is calculated by applying the decentralized control law to the full spacecraft.

Each of the six controllers responsible for the rigid-body motions of the spacecraft are designed separately, in the same fashion as in the deterministic cases. However, now the

estimated states from the Kalman filter are used as feedback for each controller. The closed-loop difference equation is therefore

$$\underline{x}(k+1) = \mathcal{A}(k)\underline{x}(k) + \mathcal{B}(k)[\mathcal{K}(k)\underline{\hat{x}}(k) + \underline{w}(k)], \quad k = 0,1,2,\ldots \quad (4-15)$$

where $\underline{w}(k)$ is the actuator noise vector and $\mathcal{K}(k)$ is chosen to yield satisfactory closed-loop response.

4.4.1 Pseudo-Collocated Control

The linear control law for the case in which point controllers are located on the appendage(s) is again based on the concept of Uniform Damping Control. For the stochastic system, the uniform damping control forces at points P_{e_ℓ} are given by

$$\underline{F}_{e_\ell}(k) = -\alpha^2 M_{e_\ell}\underline{\hat{U}}_{e_\ell}(k) - 2\alpha M_{e_\ell}\underline{\dot{\hat{U}}}_{e_\ell}(k), \quad \ell = 1,2,\ldots,n_e \quad (4-16)$$

where $\underline{\hat{U}}_{e_\ell}(k) = \underline{\hat{u}}(P_{e_\ell},k)$ and $\underline{\dot{\hat{U}}}_{e_\ell}(k) = \underline{\dot{\hat{u}}}(P_{e_\ell},k)$ are estimates of displacement and velocity, respectively, at points P_{e_ℓ}. Moreoever, $\underline{\hat{U}}_{e_\ell}(k)$ and $\underline{\dot{\hat{U}}}_{e_\ell}(k)$ are found using the Kalman filter estimate of antenna states, $\underline{\hat{q}}_e(k)$ and $\underline{\dot{\hat{q}}}_e(k)$. Hence,

$$\underline{\hat{U}}_{e_\ell}(k) = \Phi_e(P_{e_\ell})\underline{\hat{q}}_e(k), \quad \underline{\dot{\hat{U}}}_{e_\ell}(k) = \Phi_e(P_{e_\ell})\underline{\dot{\hat{q}}}_e(k), \quad e = 1,2,\ldots,N \quad (4-17)$$

On the other hand, M_{e_f} and α retain the same meaning as in the deterministic case.

Next, a nonlinear, bang-off-bang control law is implemented for the point controllers on the appendage using the same type of state-plane switching curve as in Section 3.4.1. Because the controls are now based on estimates of the local position and velocity, the deadzone "on" and "off" criteria become

$$\frac{\dot{\hat{U}}_{e_f}^2}{a_{off}^2} + \frac{\hat{U}_{e_f}^2}{b_{off}^2} \leq 1 \qquad (4-18)$$

$$\frac{\dot{\hat{U}}_{e_f}^2}{a_{on}^2} + \frac{\hat{U}_{e_f}^2}{b_{on}^2} \geq 1 \qquad (4-19)$$

For the fully nonlinear case, the rigid-body control is the same as that used in the deterministic case except, of course, that now the nonlinear controls are based on the estimated rigid-body states.

4.4.2 Substructure-Decentralized Control

Next, the system is controlled in a manner similar to the earlier Substructure-Decentralized Control (Sec. 3.4.2), except that the feedback control for a given flexible substructure is based on estimated states associated with that substructure as given by a global Kalman filter. Otherwise, the same control laws can be used for the linear, mixed and

nonlinear cases. For convenience, the term Substructure-Decentralized Control is retained although the technique is actually a pseudo-decentralized control.

5 NUMERICAL EXAMPLES

5.1 Introduction

The mathematical model considered consists of a rigid platform with one flexible antenna, represented by a uniform beam, hinged to the platform at one end and free at the other (Fig. 5). The antenna is slewed through a 45^{o} angle about the x_o-axis. The beam is discretized in space using five admissible functions for each displacement component. The admissible functions for the y_o-displacement component are taken in the form of cantilever modes

$$\phi_{y_j} = -(\cos\beta_j z - \cosh\beta_j z) + C_j(\sin\beta_j z - \sinh\beta_j z), \quad j = 1,2,3,4,5$$

This is consistent with the fact that the flexible antenna represents a slewing cantilever beam, where the slewing angle, is a given function of time. The admissible functions for the x_o-displacement component have the same form. The platform has one actuator corresponding to each rigid-body degree-of-freedom and the antenna has three sets of bi-directional actuators located at $z_i = l_o/3, 2l_o/3, l_o$. The following data was used in the computer simulation:

$$m_r = 10.0\,kg \qquad m_e = 1.0\,kg$$

$$l_e = 5.0\,m \qquad \underline{r}_{o_e} = 2.0\hat{k}\,m \qquad EI_e = 122.28\,N\cdot m^2$$

$$\mathbf{I}_e = \begin{bmatrix} 8.33 & 0 & 0 \\ 0 & 8.33 & 0 \\ 0 & 0 & 0 \end{bmatrix} kg\cdot m^2 \qquad \mathbf{I}_r = \begin{bmatrix} 20.0 & 0 & 0 \\ 0 & 20.0 & 0 \\ 0 & 0 & 20.0 \end{bmatrix} kg\cdot m^2$$

Structural damping equal to 0.2% of critical was added to the simulation model for each of the system elastic modes in the premaneuver configuration.

The time-optimal slewing profile is shown in Fig. 6. For all cases, the angular acceleration rate of the antenna was $\pm\pi/8$ rad/s, so that the entire maneuver is completed in about 2.8 s. The uncontrolled motion of the platform relative to the inertial space and the elastic displacement of the antenna tip are shown in Fig. 7.

When only the rigid-body modes are controlled linearly, the resulting deterministic uncontrolled tip displacement of the antenna in the y_o-direction is quite large, as can be seen in Fig. 8.

5.2 Deterministic Control

In the case of control using the step-varying LQR, the weighting matrices $\mathbf{P} = \mathbf{Q} = 100 \times [\mathbf{I}]_{24\times 24}$ and $\mathbf{R} = .001 \times [\mathbf{I}]_{12\times 12}$ were used. Figure 9 shows the tip displacement for the case in which open-loop disturbance accommodation is employed together

with the LQR. Figure 10 shows the same information without disturbance accommodation. In all cases, except for full nonlinear control, the rigid-body displacements were insignificant when compared to the elastic displacements of the antenna.

Linear Collocated Control using Uniform Damping was implemented using a decay rate $\alpha = 5.0$. The rigid-body motion was controlled using a linear control law with $\omega_n = 10 rad/s$ and $\zeta = 0.70$. Figures 11 and 12 show displacements with and without the open-loop disturbance accommodating control, respectively.

For the case of nonlinear antenna control using the parameters

$$f_1 = 0.18N \quad f_2 = 0.5N \quad f_3 = 0.22N$$

$$c_r = .05 m/s, \quad a_{off_r} = .001 m/s \quad a_{on_r} = .01 m/s$$

$$b_{off_r} = .003 m/s \quad b_{on_r} = .03 m/s, \quad r = 1,2,3$$

the resulting tip displacement is as shown in Figure 13. Figures 14-16 display the time history of the substructure actuator forces.

In the case of nonlinear control of both the rigid-body and the elastic motions, the parameters used were as follows:

$$f_1 = 0.18N \quad f_2 = 0.5N \quad f_3 = 0.22N$$

$$c_r = .04m/s \quad a_{off_r} = .01m/s \quad a_{on_r} = .02m/s$$

$$b_{off_r} = .05m/s \quad b_{on_r} = .10m/s, \quad r = 1,2,3$$

$$F_x = F_y = F_z = 0.8N \quad M_x = M_y = M_z = 1.6N$$

$$a_{\dot{x}} = a_{\dot{y}} = a_{\dot{z}} = .001m/s \quad a_{\theta_x} = a_{\theta_y} = a_{\theta_z} = .001rad/s$$

$$b_x = b_y = b_z = .003m \quad b_{\theta_x} = b_{\theta_y} = b_{\theta_z} = .003rad$$

The corresponding antenna displacement and actuator histories are shown in Figs. 17-20. Because the most significant rigid-body motion is rotation in the plane of the maneuver, Figs. 21 and 22 show the in-plane rotation and the actuator torque, respectively.

In the case of linear Substructure-Decentralized Control, the discrete-time control gains for each of the three controlled substructure modes were designed so as to yield an exponential decay rate of $\alpha = 5.0$. The antenna tip displacement with and without disturbance accommodation is shown in Figs. 23 and 24, respectively.

A nonlinear control next replaces the linear Substructure-Decentralized Control with the following switching parameters:

$$c_1 = c_2 = c_3 = .005m/s, \quad k_1 = 0.80N, \quad k_2 = k_3 = 0.40N$$

Nonlinear damping, as described earlier, was used for the first substructure mode with $d_1 = 0.01m$. The resulting tip displacements are shown in Figure 25 and the actuator force histories are shown in Figures 26-28.

In the case in which both the rigid-body and the elastic control is nonlinear, use of the parameters

$$k_1 = 0.80N \quad k_2 = k_3 = 0.40N$$

$$c_1 = c_2 = c_3 = .005m/s \quad d_1 = 0.01m$$

$$F_x = F_y = F_z = 1.0N \quad M_x = M_y = M_z = 2.0N$$

$$a_{\dot{x}} = a_{\dot{y}} = a_{\dot{z}} = .001m/s \quad a_{\theta_x} = a_{\theta_y} = a_{\theta_z} = .001rad/s$$

$$b_x = b_y = b_z = .003m \quad b_{\theta_x} = b_{\theta_y} = b_{\theta_z} = .001rad$$

resulted in the antenna tip displacements and actuator histories shown in Figs. 29-32. Figures 33 and 34 again display the rigid-body in-plane rotation and actuator torque.

5.3 Stochastic Control

The Kalman filter was based on a truncated model of the simulated system. In this case, the antenna was modeled by only three admissible functions in each direction, corresponding to the three controlled substructure modes. It was also assumed that the actuator noise manifests itself as unknown forces and torques on the system. Therefore, we choose

$$\mathcal{B}_1 = \begin{bmatrix} 0_{12\times 12} \\ I_{12\times 12} \end{bmatrix}$$

In the simulation, "white" noise was added to all outputs, $\underline{y}(k)$, at each sampling time to simulate sensor noise. A similar, uncorrelated "white" noise was added to each system state (including uncontrolled flexible states) at every simulation time step to simulate actuator noise and unknown disturbances. The "noise level" used for each term was $\mathcal{E}\{v_i^2(k)\} = \mathcal{E}\{w_j^2(k)\} = 10^{-4}$. For simplicity, the sensor noise covariance matrix R is taken as an identity matrix of appropriate dimension and

$$\mathcal{B}_1 Q \mathcal{B}_1^T = \begin{bmatrix} 0 & 0 \\ 0 & I_{12\times 12} \end{bmatrix}$$

Linear Pseudo-Collocated Control using uniform damping was implemented first, again using a decay rate $\alpha = 5.0$. The rigid-body motion was also controlled using linear control with $\omega = 10$ rad/s and $\zeta = 0.70$, i.e., the same as in the deterministic case. Figure 35 shows the antenna tip displacement with and without the open-loop disturbance accommodating control, respectively.

Using the same parameters $k_\ell, c_\ell, a_\ell, b_\ell$, the resulting tip displacement is as shown in Fig. 36. For comparison, the case with only rigid-body control (Fig. 8) is also shown. Figures

37-39 display the time history of the substructure actuator forces.

For nonlinear control of both the rigid-body and the elastic motions, the parameters used were as follows:

$$f_1 = 0.18N \quad f_2 = 0.5N \quad f_3 = 0.22N$$

$$c_r = .04m/s \quad a_{off_r} = .01m/s \quad a_{on_r} = .02m/s$$

$$b_{off_r} = .05m/s \quad b_{on_r} = .10m/s, \quad r = 1,2,3$$

$$F_x = F_y = F_z = 0.8N \quad M_x = M_y = M_z = 1.6N$$

$$a_{\dot{x}} = a_{\dot{y}} = a_{\dot{z}} = .005m/s \quad a_{\theta_x} = a_{\theta_y} = a_{\theta_z} = .005rad/s$$

$$b_x = b_y = b_z = .015m \quad b_{\theta_x} = b_{\theta_y} = b_{\theta_z} = .015rad$$

The resulting antenna tip displacements, antenna actuator forces, in-plane rotation and actuator torque are shown in Figs. 40-45, respectively.

In the case of linear Substructure-Decentralized Control, the discrete-time control gains for each of the three controlled substructure modes were also chosen identical to those in the deterministic case. The antenna tip displacement with and without disturbance accommodation is shown in Fig. 46. In Figs. 46-56, the term Substructure-Decentralized Control (Pseudo) is used to distinguish between these and those from the deterministic cases.

The linear Substructure-Decentralized Control was then

replaced with the nonlinear control used in Sec. 5.2. The resulting tip displacement is shown in Fig. 47, again compared with rigid-body control alone (Fig. 8); the actual actuator force histories are shown in Figs. 48-50.

For the case in which both the rigid-body and the elastic control is nonlinear, use of the same parameters as in the deterministic case yields the results displayed in Figs. 51-56.

6 CONCLUSIONS

This dissertation considers the control of a spacecraft with retargetable flexible antennas using discrete-time techniques. It significantly expands upon earlier work that derived the continuous-time equations of motion for this type of systems and applied global control laws based on a noise-free, full state feedback system that was considered largely time-invariant. Chapter 3 of this dissertation presents a discrete-time approach for designing an adequate control law that accounts for the time-varying nature of the system, but still assumes full state feedback and no sensor or actuator noise. First, a global approach using a discrete-time, step-varying linear quadratic regulator was implemented to control the time-varying mathematical model. Because a global controller requires extensive computations, the step-varying feedback gains can be precalculated and stored for use during a known spacecraft maneuver of a system with many appendages. Next, two decentralized approaches were proposed: Collocated Control and a new method designated Substructure-Decentralized Control. Both offer the advantage of lower computational effort, while still accounting for the time-varying nature of the system. Whereas Collocated Control suppresses the elastic

motion at specific points, Substructure-Decentralized Control suppresses the elastic appendage substructure modes, taken as cantilever modes in the case of a beam-like antenna. In each of the decentralized cases, linear and nonlinear (on-off) schemes were presented for controlling the elastic motion of the antennas and the rigid-body motions of the system. The linear Collocated Control law was based on a discrete-time application of Uniform Damping. Note that on-off controls used to suppress elastic motions translate into quantized actual controls in the Substructure-Decentralized Control case. The nonlinear control of the rigid-body motions assumed full decoupling of the rigid-body modes and used a switching curve based on a discrete-time, step-varying interpretation of a time-optimal controller for a double-integrator system. In all global (LQR) and decentralized cases using fully linear control, a discrete-time disturbance-accommodating, control designed to counteract the inertial disturbances caused by the known antenna maneuver profile was also included.

Chapter 4 considers the effects of noisy actuators and sensors, as well as the reality of incomplete state feedback, was addressed. A step-varying, full-order discrete-time Kalman filter was developed to estimate the system states upon for feedback control. Strain gauges were selected to measure elastic deformation in the slewing antennas because of the small amount of processing required to determine system states

from their output. Pseudo-decentralized control was then proposed whereby control forces used to suppress the elastic motion of an individual antenna are based on the globally derived estimates of states corresponding to that specific antenna. Indeed, if any processing of antenna sensor outputs is required to account for the relative motion of the antenna local coordinate frame during a maneuver, true direct output feedback control with collocated sensors and actuators is not possible. Similarly, a requirement of state estimation due to noise of incomplete measurements would make true decentralized control in general impossible.

The decentralized controllers applied to the deterministic system were therefore selected for use on the stochastic system. The difference here is that control forces are based on estimates of substructure modal states in the case of Substructure-Decentralized Control and estimates of the position and velocity of specific points on the antenna, measured in the antenna local coordinate frame, in the case of pseudo-collocated control.

A numerical example using a deterministic system with one antenna was presented and the results of each case compared. In each of the linear cases, the spacecraft was controlled quite well, with both decentralized methods offering performance comparable to the more computationally intensive step-varying LQR. While the linear controls performed

significantly better than the mixed or nonlinear cases, as might be expected, the mixed controller methods performed adequately, reducing tip motion for the 5 m antenna to under 4 mm within one second of maneuver completion, with minimal limit-cycle behavior. The fully nonlinear controller case using Substructure-Decentralized Control also performed well, converging quickly with little noticeable limit-cycle behavior. The Collocated Control case exhibited more limit-cycle behavior.

Next, numerical examples using a stochastic version of the same system with one antenna was presented. Strain gauges to sense elastic motion and a step-varying Kalman filter were used and the results for each different control law again displayed. Both linear pseudo-decentralized methods controlled the spacecraft quite well, with performance comparable to earlier results based on noise-free full-state feedback. Once again, the linear controls performed much better than the mixed and nonlinear ones. Both mixed control methods performed adequately, comparable to the determistic applications of the same controllers. The fully nonlinear controllers performance was also similar to that of their deterministic counterparts.

In conclusion, simulations confirm that for both the deterministic and stochastic case, linear and nonlinear discrete-time antenna controls based on Substructure-Decentralized Control are able to suppress elastic motions of

a slewing appendage in a time-varying spacecraft effectively. Strain gauges can conveniently sense elastic states associated with each appendage and, when coupled with a global step-varying estimator (or Kalman filter for a noisy system), can provide feedback for pseudo-decentralized substructure-decentralized controllers. Based on globally estimated states, each controller, in turn, effectively controls the elastic motions of its individual antenna.

REFERENCES

1. Athans, M. and Falb, P.L., *Optimal Control: An Introduction to the Theory and its Applications*, McGraw-Hill, New York, 1966.

2. Balas, M.J., "Active Control of Flexible Systems," *Journal of Optimization Theory and Applications*, Vol 25, No 3, July 1978, pp. 415-436.

3. Balas, M.J., "Direct Velocity Feedback of Large Space Structures," *Journal of Guidance, Control and Dynamics*, Vol 2, No 3, May-June 1979, pp. 252-253.

4. Balas, M.J., "Trends in Large Space Strucure Control Theory: Fondest Hopes, Wildest Dreams," *IEEE Transactions on Automatic Control*, Vol 27, 1982, pp. 522-535.

5. Baruh, H. and Silverberg, L., "Maneuver of Distributed Spacecraft," *Proceedings of the AIAA Guidance and Control Conference*, Seattle, WA, Aug 20-22, 1984, pp. 637-647.

6. Baruh, H. and Meirovitch, L., "Implementation of the IMSC Method by Means of a Varying Number of Actuators," *Proceedings of the 4th VPI&SU/AIAA Symposium on Dynamics and Control of Large Structures*, Blacksburg, VA, 1985.

7. Baruh, H. and Silverberg, L., "Implementation Problems Associated with Simultaneous Maneuver and Vibration Suppression of Flexible Spacecraft," *Proceedings of the Fifth VPI&SU/AIAA Symposium on Dynamics and Control of Large Structures*, Blacksburg, VA, 1985, pp. 585-599.

8. Breakwell, J.A., "Optimal Feedback Slewing of Flexible Spacecraft," *Journal of Guidance and Control*, Vol 4, No 5, 1981, pp. 472-479.

9. Bickle, L.W., "An Introduction to the Use of Strain Gages for the Measurement of Propogating Strain Waves," SC-DC-70-5193, Sandia Laboratories, Albuquerque, NM, 1970.

10. Fairman, F.W. and Luk, L., "On Reducing the Order of Kalman Filters for Discrete-Time Stochastic Systems Having Singular Measurement Noise," *IEEE Transactions on Automatic Control*, AC-30, No 11, Nov 1985, pp. 1150-1152.

11. Franklin, G.F. and Powell, J.D., *Digital Control of Dynamic Systems*, Addison-Wesley, Reading, MA, 1980.

12. Friedland, B., Richman, J. and Williams, D.E., "On the Adiabatic Approximation for Design of Control Laws for Linear, Time-Varying Systems," *IEEE Transactions on Automatic Control*, AC-32, No 1, Jan 1987, pp. 62-63.

13. Hostetter, G.H., *Digital Control System Design*, Holt, Rinehart and Winston, Inc., New York, NY, 1988.

14. Hughes, P.C., *Spacecraft Attitude Dynamics*, Wiley-Interscience, New York, 1986.

15. Juang, J.-N., Horta, L.G. and Robertshaw, H.H., "A Slewing Experiment for Flexible Structures," *Journal of Guidance, Control and Dynamics*, Vol 9, No 5, Sept-Oct 1986, pp. 599-607.

16. Kane, T.R. and Levinson, D.A., "Formulation of Equations of Motion for Complex Spacecraft," *Journal of Guidance and Control*, Vol 3, No 2, March-April 1980, pp. 99-112.

17. Kirk, D.E., *Optimal Control Theory*, Prentice-Hall Inc., Englewood Cliffs, NJ, 1970.

18. Koshiro, O., "Transient Response of Bonded Strain Gages," *Experimental Mechanics*, Vol 6, No 9, Sept 1966, pp. 463-469.

19. Kwak, M.K., "Dynamics and Control of Spacecraft with Retargeting Flexible Antennas," Ph.D. Dissertation, VPI&SU 1989.

20. Kwakernaak, H. and Sivan, R., *Linear Optimal Control Systems*, Wiley-Interscience, New York, 1972.

21. Leondes, C.T. and Novak, L.M., "Reduced-Order Observers for Linear Discrete-Time Systems," *IEEE Transactions on Automatic Control*, Feb 1974, pp. 42-46.

22. Lindner, D.K. and Reichard, K., "A Survey of Decentralized Control Techniques for Large Space Structures," *Proceedings of the Sixth VPI&SU/AIAA Symposium on Dynamics and Control of Large Structures*, Blacksburg, VA, 1987, pp. 89-102.

23. Meirovitch, L., *Methods in Analytical Dynamics*, McGraw-Hill Book Co., New York, 1970.

24. Meirovitch, L., *Computational Methods in Structural Dynamics*, Sijthoff & Noordhoff, The Netherlands, 1980.

25. Meirovitch, L. and Baruh, H., "Control of Self-Adjoint Distributed Parameter Systems," *Journal of Guidance, Control and Dynamics*, Vol 5, No 1, Jan-Feb 1982, pp. 60-66.

26. Meirovitch, L., Baruh, H., and Öz, H., "A Comparison of Control Techniques for Large Flexible Systems," *Journal of Guidance, Control and Dynamics*, Vol 6, No 4, July-Aug 1983, pp. 302-310.

27. Meirovitch, L. and Öz, H., "Digital Stochastic Control of Distributed Parameter Systems," *Journal of Optimization Theory and Applications*, Vol 43, No 2, June 1984, pp. 307-325.

28. Meirovitch, L., Baruh, H., Montgomery, R.C., and Williams, J.P., "Nonlinear Natural Control of an Experimental Beam," *Journal of Guidance, Control, and Dynamics*, Vol 7, No 4, July-August 1984, pp. 437-442.

29. Meirovitch, L., Quinn, R.D. and Norris, M.A., "Maneuvering of Flexible Spacecraft with Application to SCOLE," *Proceedings of the 5th VPI&SU/AIAA Symposium on Dynamics and Control of Large Structures*, Blacksburg, VA, 1985, pp. 525-546.

30. Meirovitch, L. and Sharony, Y., "Optimal Vibration Control of a Flexible Spacecraft During a Minimum-Time Maneuver," *Proceedings of the 6th VPI&SU/AIAA Symposium on Dynamics and Control of Large Structures*, Blacksburg, VA, 1987, pp. 579-601.

31. Meirovitch, L. and Quinn, R.D., "Maneuvering and Vibration Control of Flexible Spacecraft," *The Journal of the Astronautical Sciences*, Vol 35, No 3, 1987, pp. 301-328.

32. Meirovitch, L. and Kwak, M.K., "Dynamics and Control of a Spacecraft with Retargeting Flexible Antennas," *Proceedings of the 29th AIAA/ASME/ASCE/AHS/ASC Structures, Structural Dynamics and Materials Conference*, Williamsburg, VA, April 18-20, 1988, pp. 1584-1592.

33. Meirovitch, L., "Equations of Motion for Flexible Bodies in Terms of Quasi-Coordinates," *IUTAM/IFAC Symposium on Dynamics of Controlled Mechanical Systems*, Zurich, Switzerland, May 30 - June 3, 1988.

34. Meirovitch L. and Kwak, M.K., "Control of Spacecraft with Multitargeted Flexible Antennas," *AIAA/AAS Astrodynamics Conference*, Minneapolis, MN, August 15-17, 1988.

35. Meirovitch, L. and Kwak, M.K., "State Equations for a Spacecraft with Maneuvering Flexible Appendages in Terms of Quasi-Coordinates," presented at the Pan-American Congress of Applied Mechanics, Rio de Janeiro, Brazil, January, 1989.

36. Meirovitch, L. and France, M.E.B., "Discrete-Time Control of a Spacecraft with Retargetable Flexible Antennas," *12th Annual AAS Guidance and Control Conference*, Keystone, CO, February 4-8, 1989.

37. Meirovitch, L., *Dynamics and Control of Structures*, Wiley-Interscience, 1989 (to appear).

38. Meirovitch, L. and France, M.E.B., "Discrete-Time Maneuvering of Flexible Spacecraft," *Proceedings of the Seventh VPI&SU/AIAA Symposium on Dynamics and Control of Large Structures*, Blacksburg, VA, 1989.

39. Modi, V.J., "Attitude Dynamics of Satellites with Flexible Appendages - A Brief Review," *Journal of Spacecraft and Rockets*, Vol 11, November 1974, pp. 743-751.

40. Montgomery, R.C. and Welch, S.S., "Application of Optical Distributed Sensing and Computation of a Large Flexible Structure," *Proceedings of the Seventh VPI&SU/AIAA Symposium on Dynamics and Control of Large Structures*, Blacksburg, VA, 1989.

41. Perry, C.C. and Lissner, H.R., *The Strain Gage Primer*, 2nd ed., McGraw-Hill, New York, 1970.

42. Quinn, R.D., "Maneuver and Control of Flexible Spacecraft," Ph.D. Dissertation, VPI&SU, 1985.

43. Schuda, F.J., "High Precision, Wide-Range, Dual-Axis Angle Monitoring System," *Review of Scientific Instrumentation*, Vol. 54, No. 12, 1983, pp. 1649-1652.

44. Sharony, Y. and Meirovitch, L., "Accommodation of Kinematic Disturbances During a Minimum-Time Maneuver of a Flexible Spacecraft," presented at the AIAA/AAS Astrodynamics Conference, Minneapolis, MN, Aug 15-17, 1988.

45. Silverberg, L., "Uniform Damping Control of Spacecraft," *Proceedings of the Fifth VPI&SU/AIAA Symposium on Dynamics and Control of Large Structures*, Blacksburg, VA, June 12-14, 1985, pp. 145-162.

46. Skaar, S.B., Tang, L. and Yalda-Mooshabad, I., "On-Off Attitude Control of Flexible Satellites," *Journal of Guidance, Control and Dynamics*, Vol 9, No 4, July-Aug 1986, pp. 507-510.

47. Turner, J.D. and Junkins, J.L., "Optimal Large-Angle Single-Axis Rotational Maneuvers of Flexible Spacecraft," *Journal of Guidance and Control*, Vol 3, No 6, 1980, pp. 578-585.

48. Turner, J.D. and Chun, H.M., "Optimal Distributed Control of a Flexible Spacecraft During a Large-Angle Maneuver," *Journal of Guidance, Control and Dynamics*, Vol 7, No 3, May-June 1984, pp. 257-264.

49. Welch, S.S., Montgomery, R.C. and Barsky, M.F., "The SCOLE Optical Attitude Measurement System," Unpublished work relayed by S.S. Welch, NASA-Langley, Hampton, VA 1989.

50. Welch, S.S., "A Flexible Beam Experiment to Develop Control Using Optical Distributed Sensing and Computation," *Proceedings of the Seventh VPI&SU/AIAA Symposium on Dynamics and Control of Large Structures*, Blacksburg, VA, 1989.

51. Young, K.D., "A Distributed Finite Element Modeling and Control Approach for Large Flexible Structures," *Proceedings of the AIAA Guidance, Navigation and Control Conference*, August 15-17, 1988, Minneapolis, MN, pp. 253-263.

FIGURES

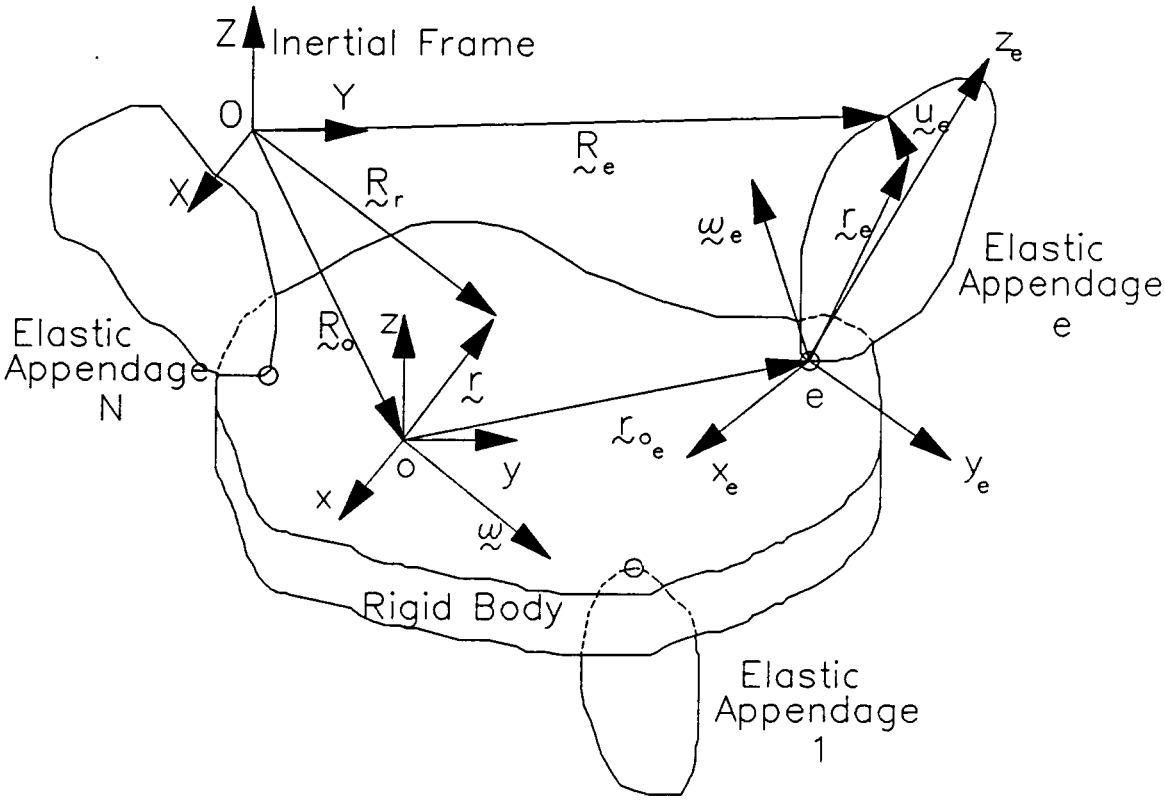

Fig. 1 Rigid Platform with Flexible Appendages

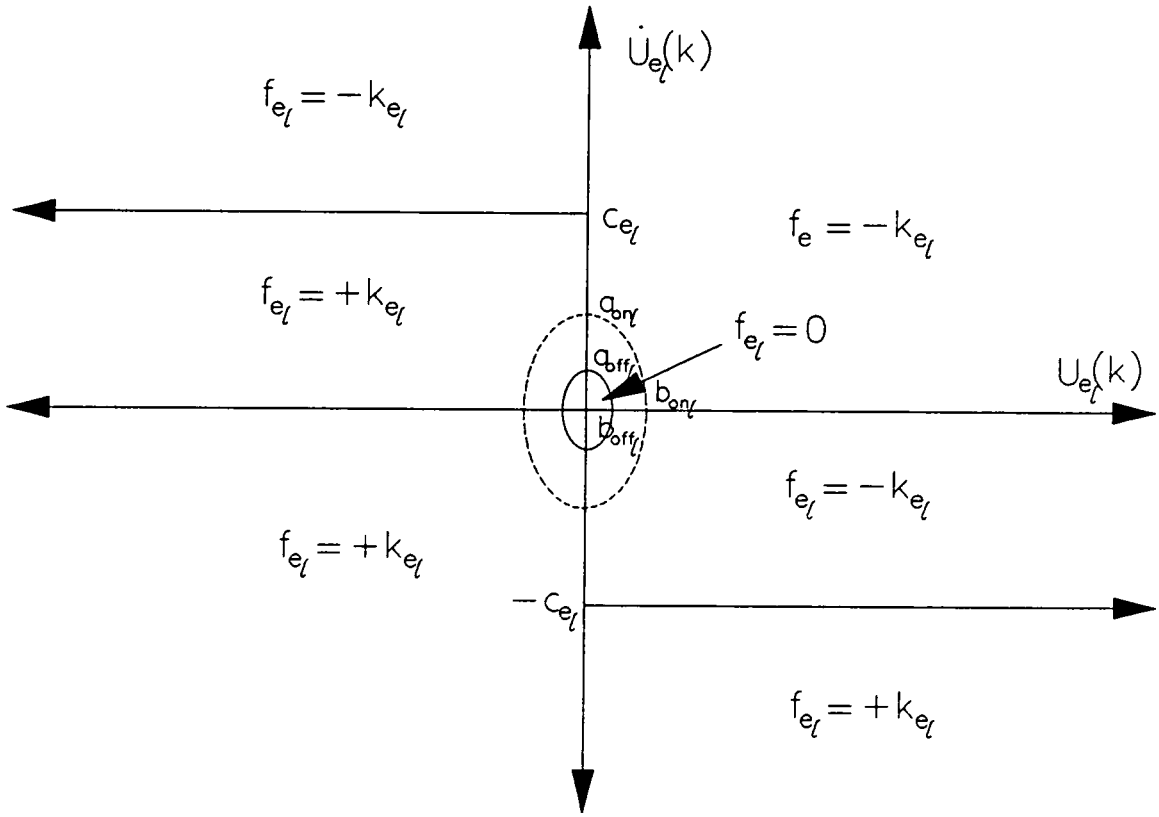

Fig. 2 Antenna Collocated Control Switching Curve

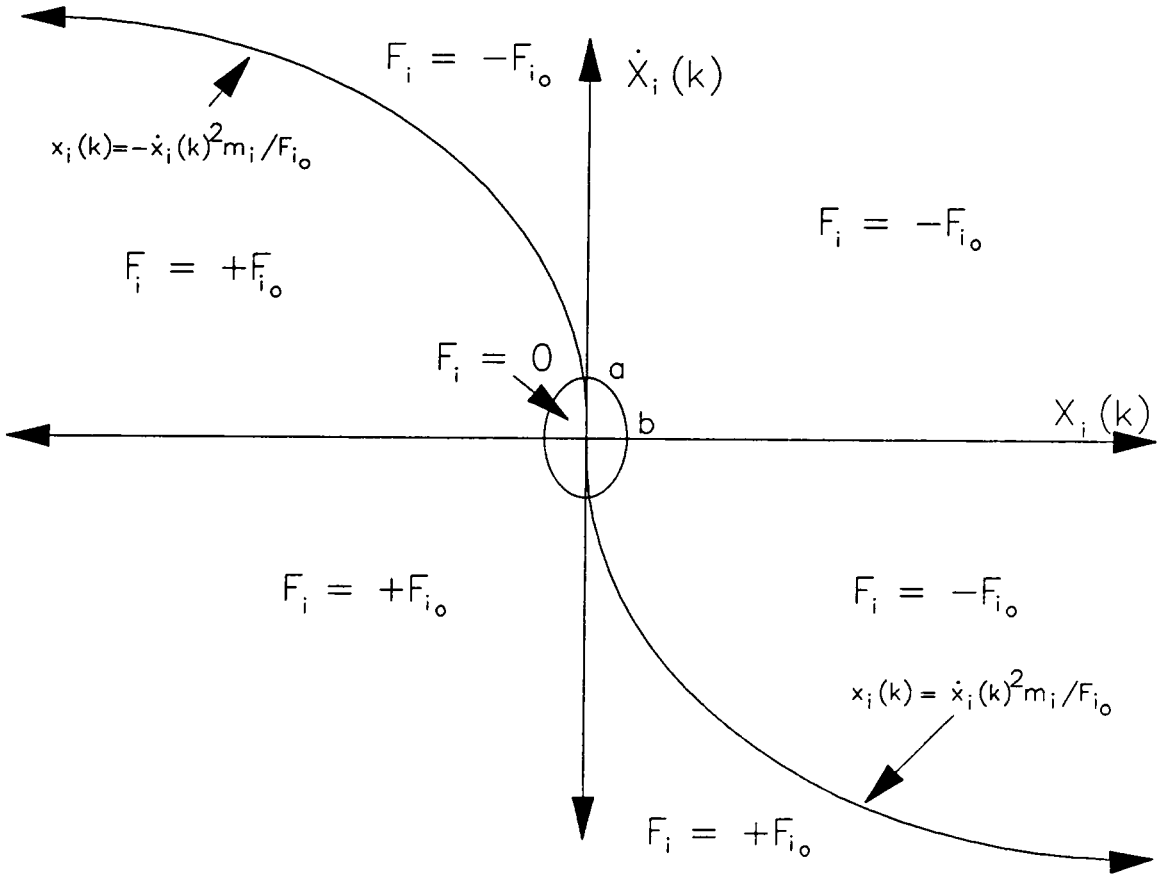

Fig. 3 Rigid-Body Motion Control Switching Curve

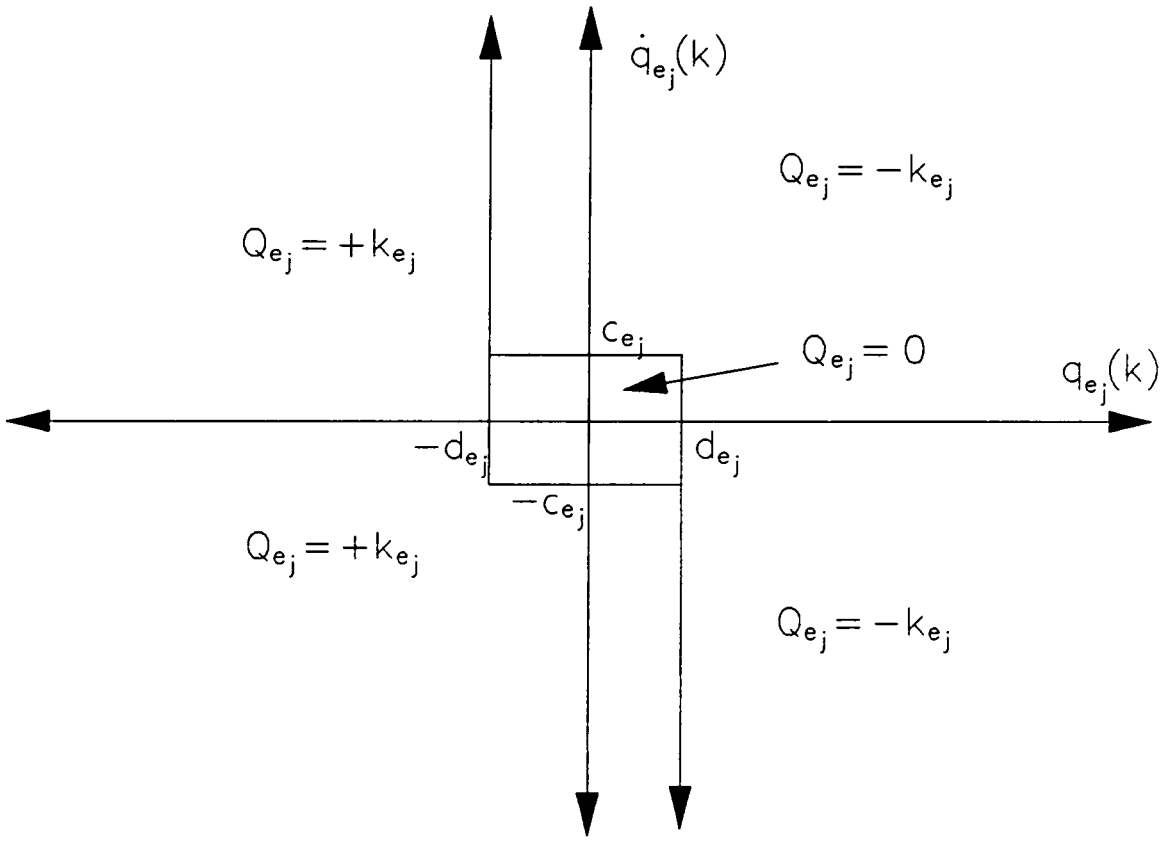

Fig. 4 Antenna Substructure Control Switching Curve

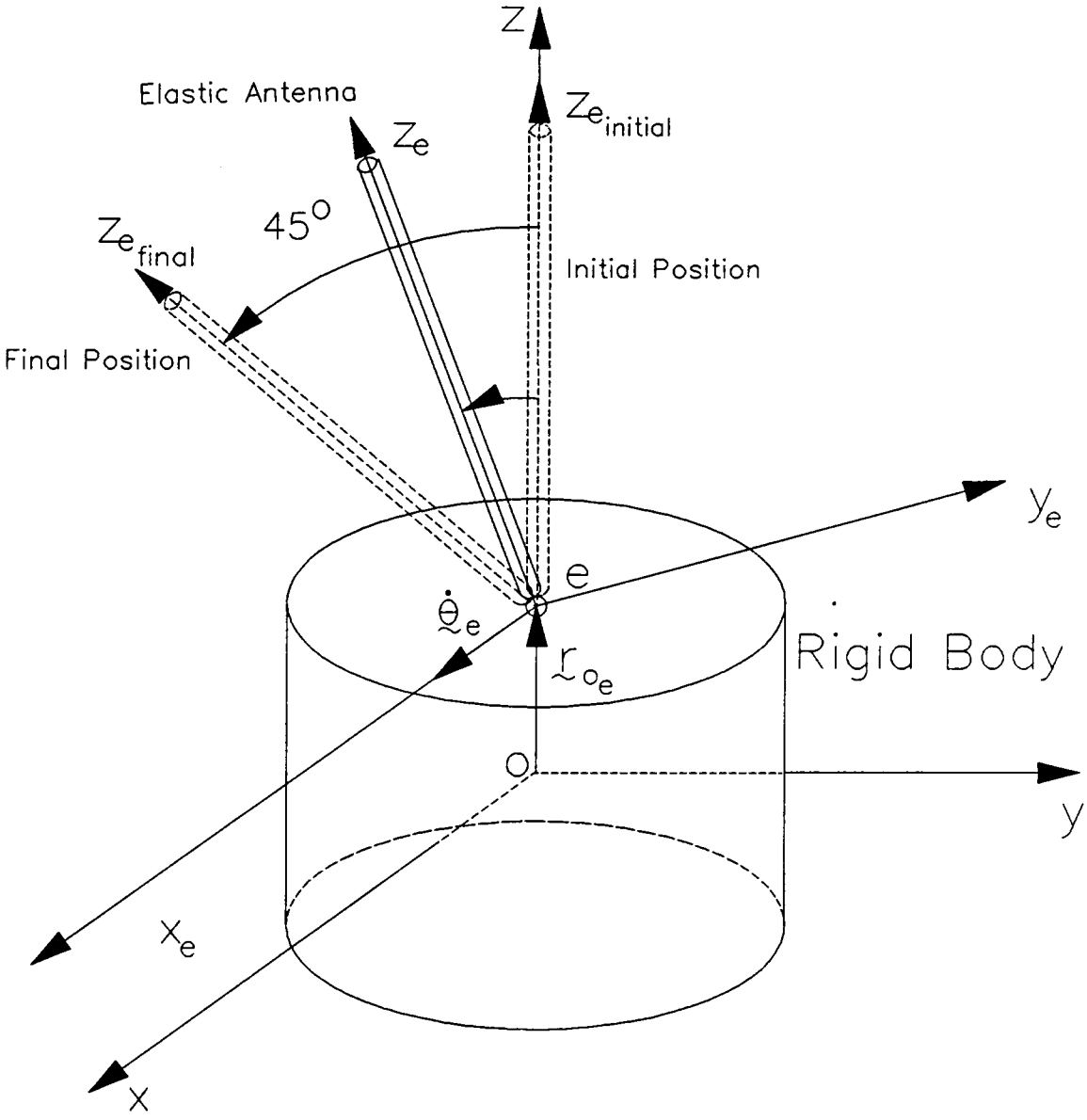

Fig. 5 Mathematical Model

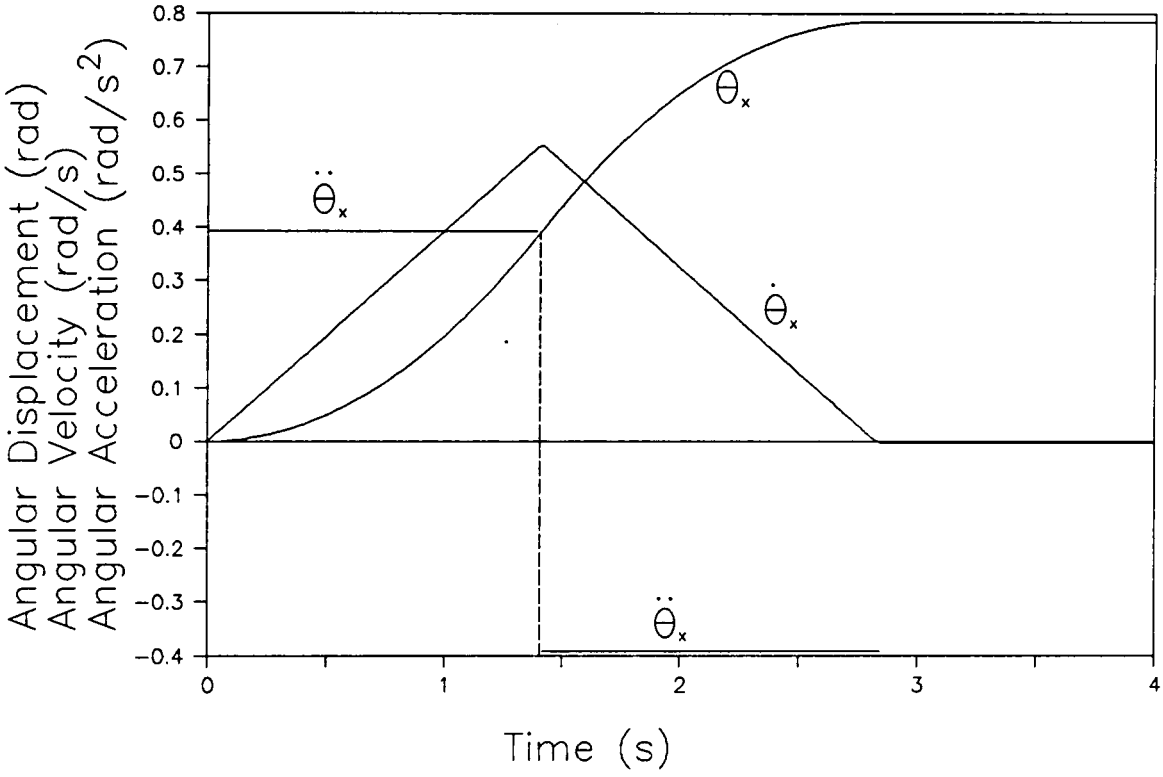

Fig. 6 Antenna Slewing Profile

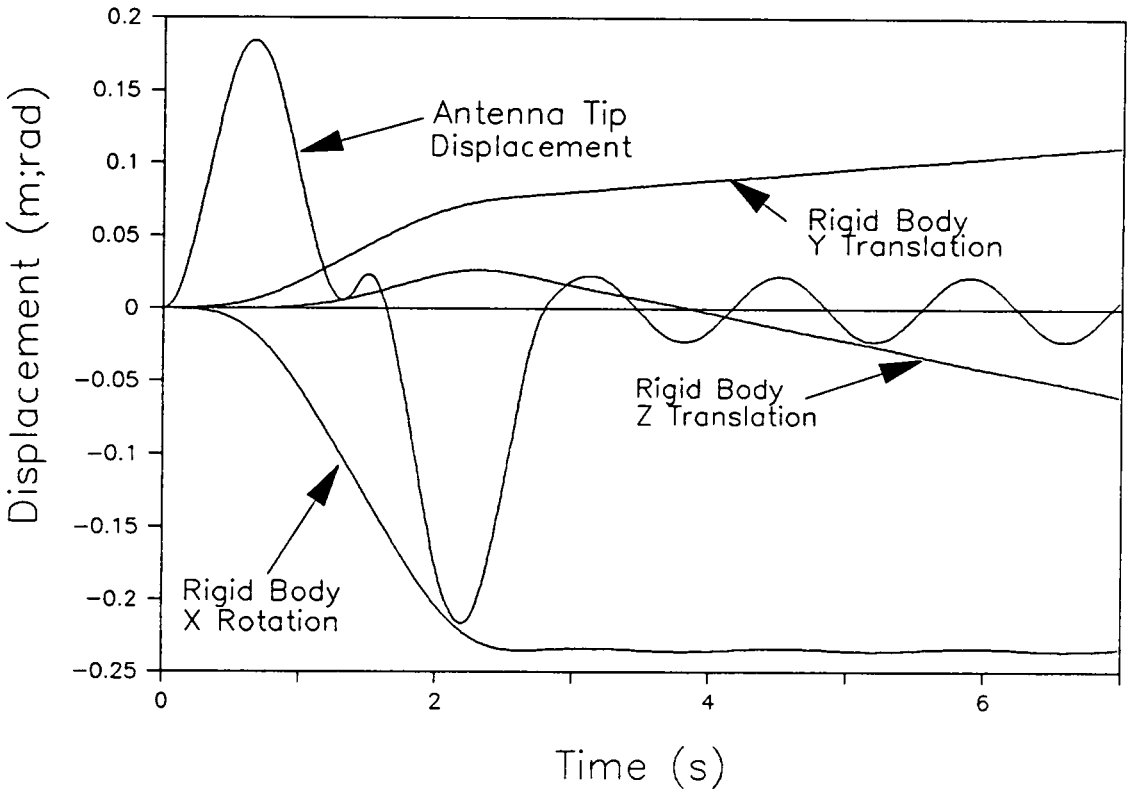

Fig. 7 Uncontrolled Platform and Antenna Displacements

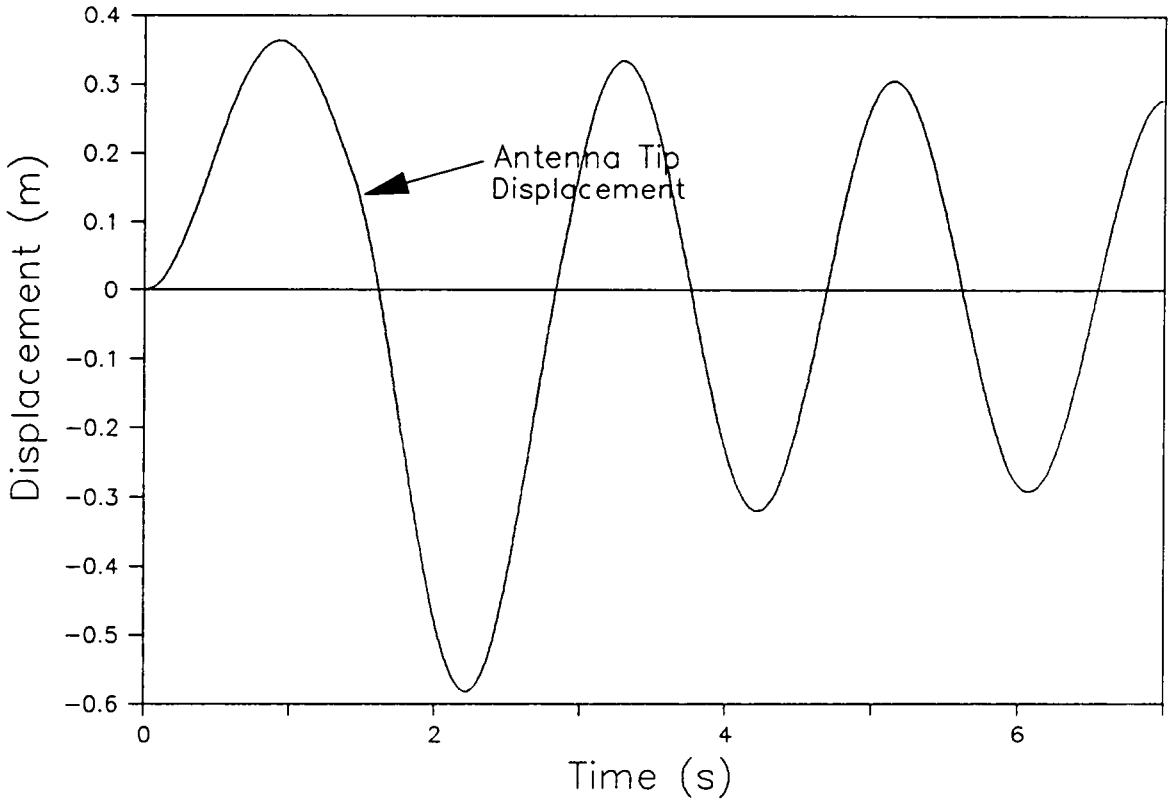

Fig. 8 Tip Displacement for Linear Rigid-Body Control, Uncontrolled Antenna

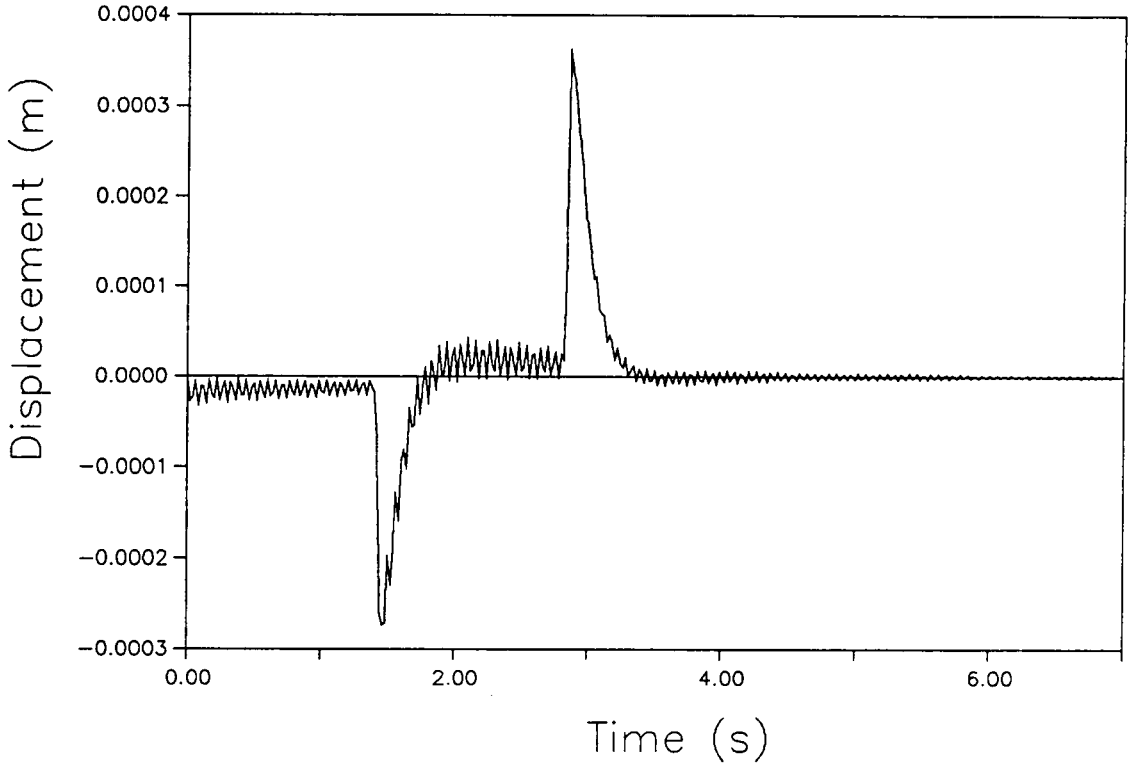

Fig. 9 Tip Displacement for LQR with Disturbance Accommodation

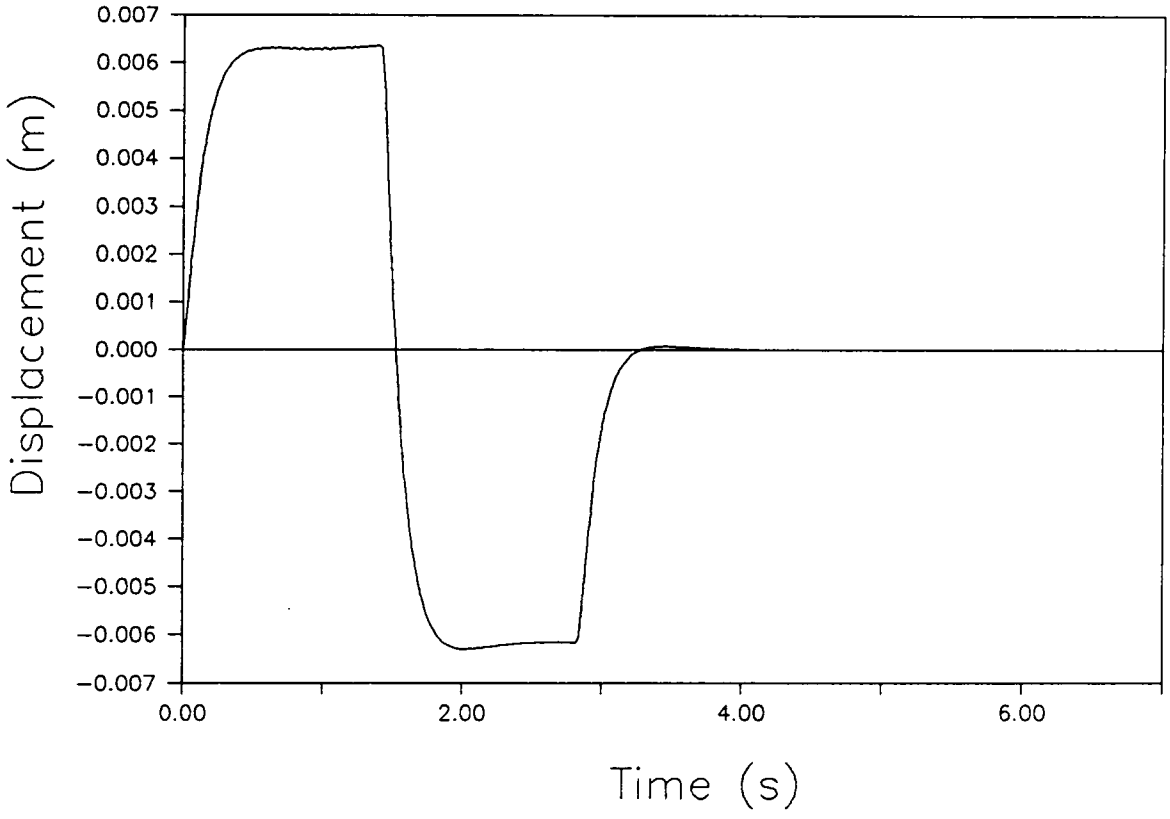

Fig. 10 Tip Displacement for LQR without Disturbance Accommodation

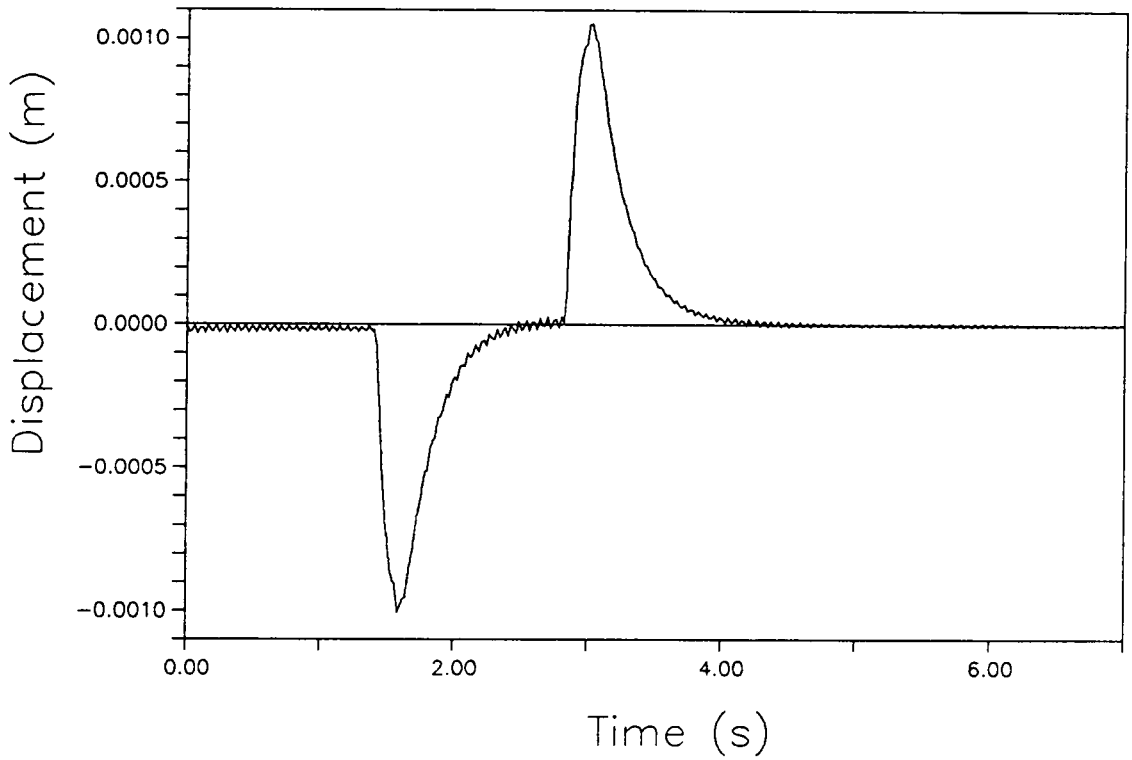

Fig. 11 Tip Displacement for Linear Collocated Control with Disturbance Accommodation

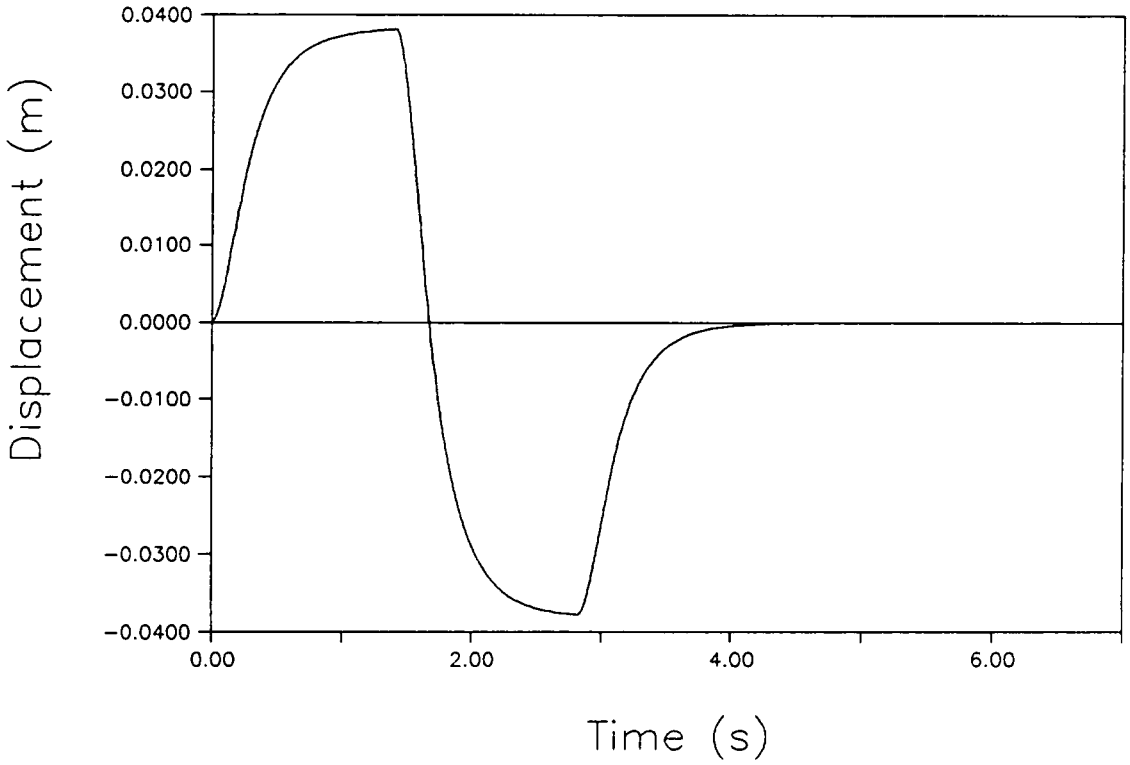

Fig. 12 Tip Displacement for Linear Collocated Control without Disturbance Accommodation

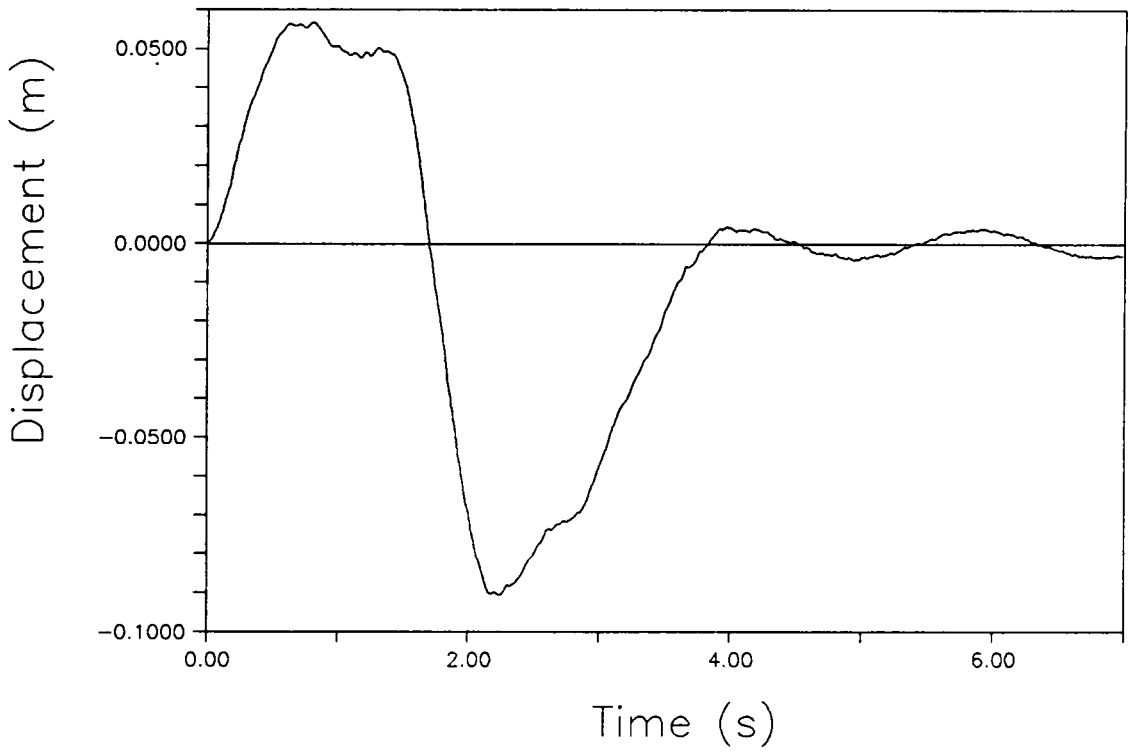

Fig. 13 Tip Displacement for Linear Rigid-Body Control, Nonlinear Collocated Antenna Control

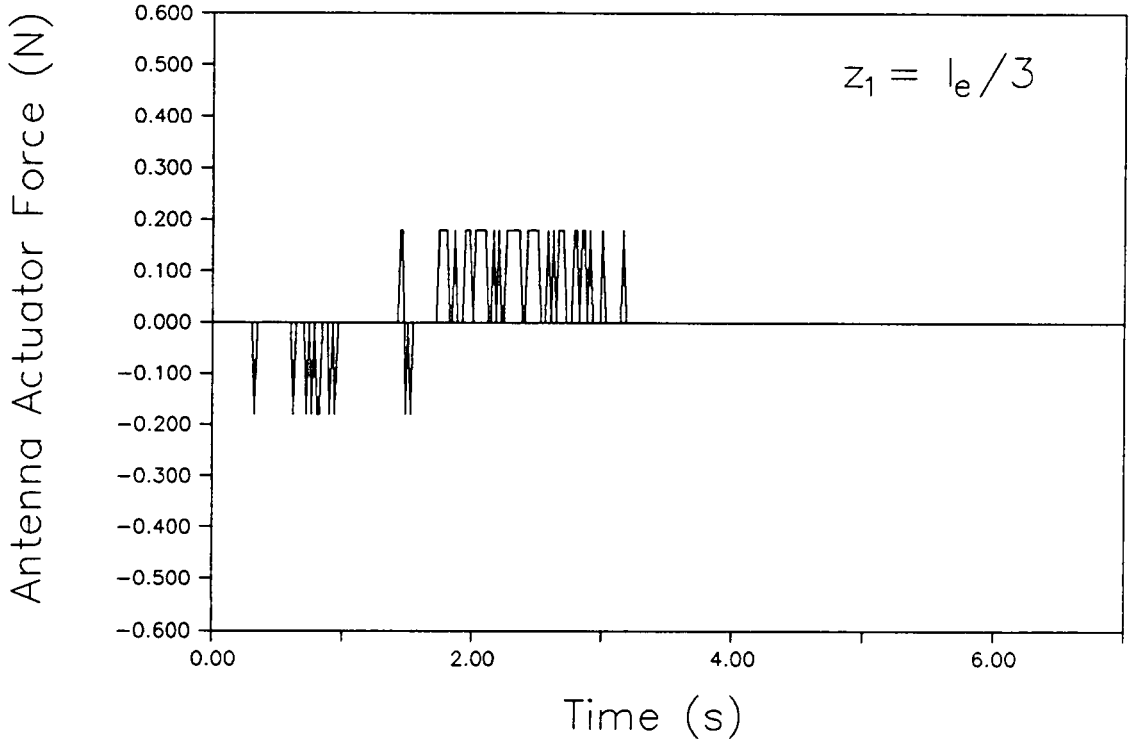

Fig. 14 Antenna Actuator Force for Linear Rigid-Body Control, Nonlinear Collocated Antenna Control, $z_1 = l_e/3$

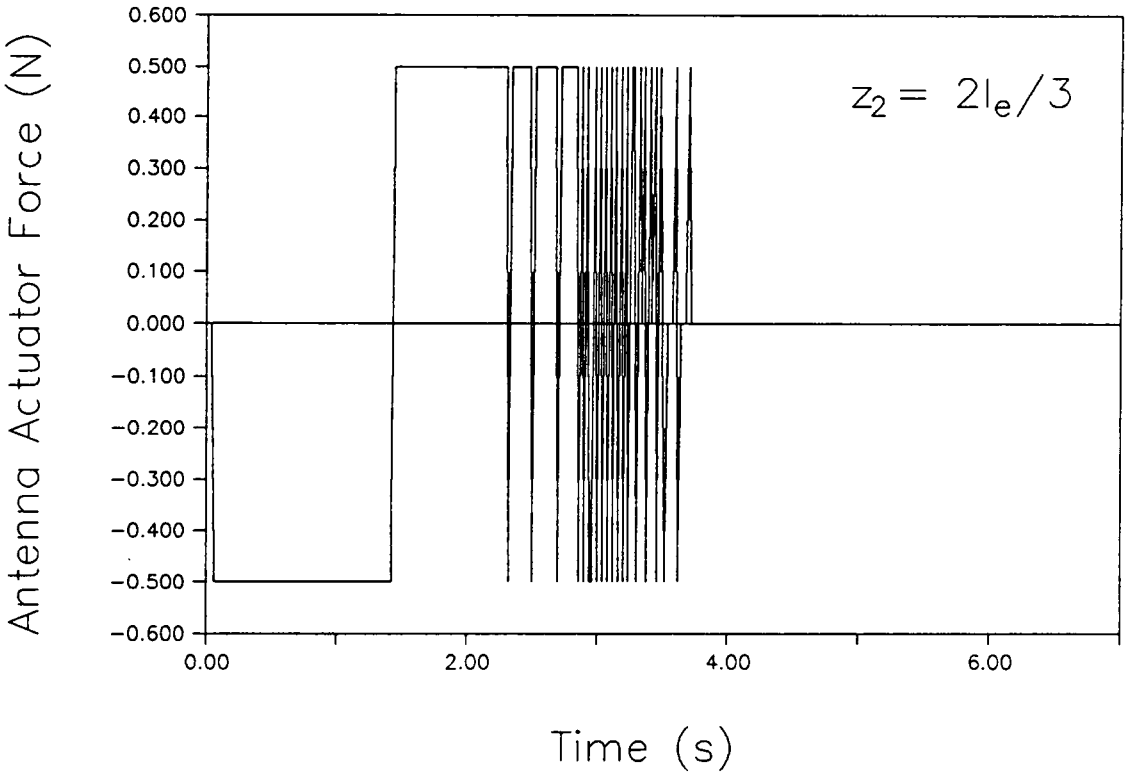

Fig. 15 Antenna Actuator Force for Linear Rigid-Body Control, Nonlinear Collocated Antenna Control, $z_2 = 2l_e/3$

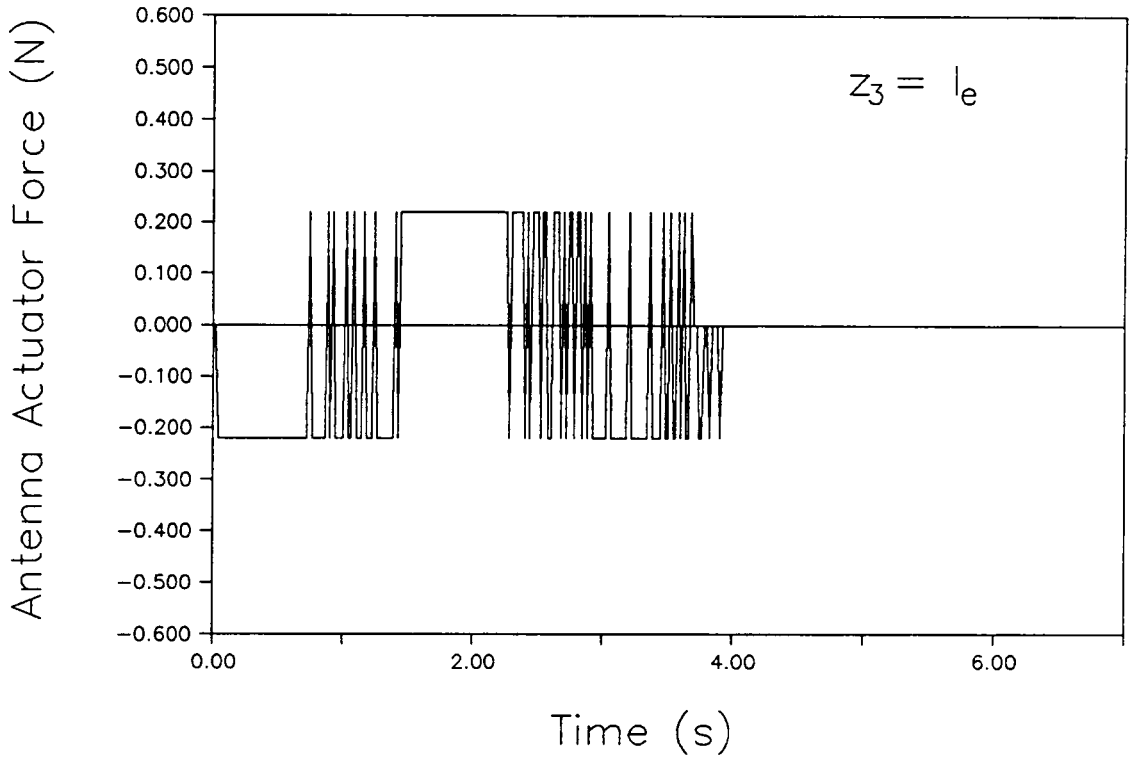

Fig. 16 Antenna Actuator Force for Linear Rigid-Body Control, Nonlinear Collocated Antenna Control, $z_3 = l_e$

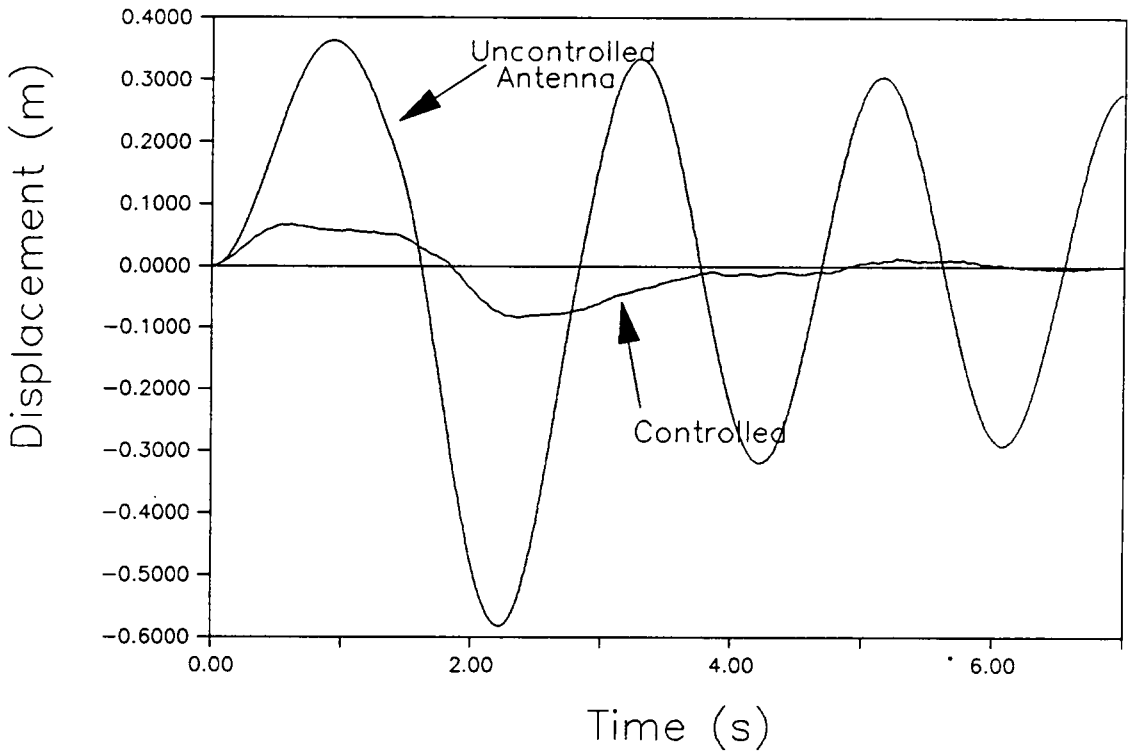

Fig. 17 Tip Displacement for Nonlinear Rigid-Body and Collocated Antenna Control

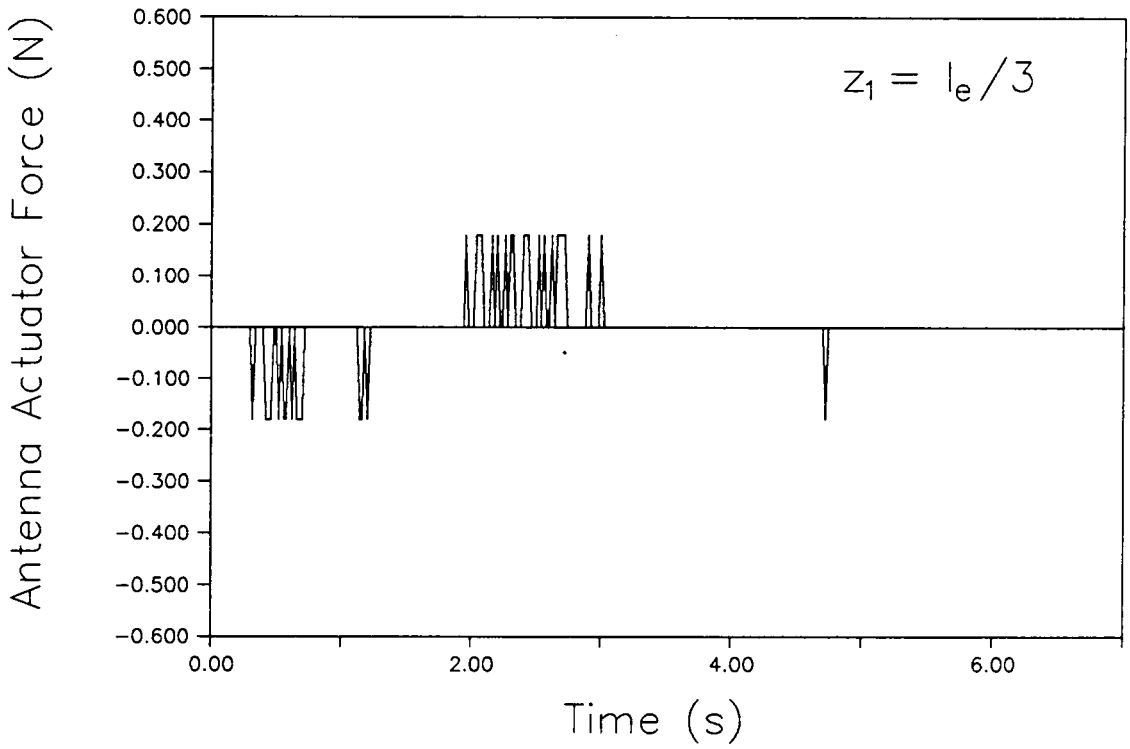

Fig. 18 Antenna Actuator Force for Nonlinear Rigid-Body and Collocated Antenna Control, $z_1 = l_e/3$

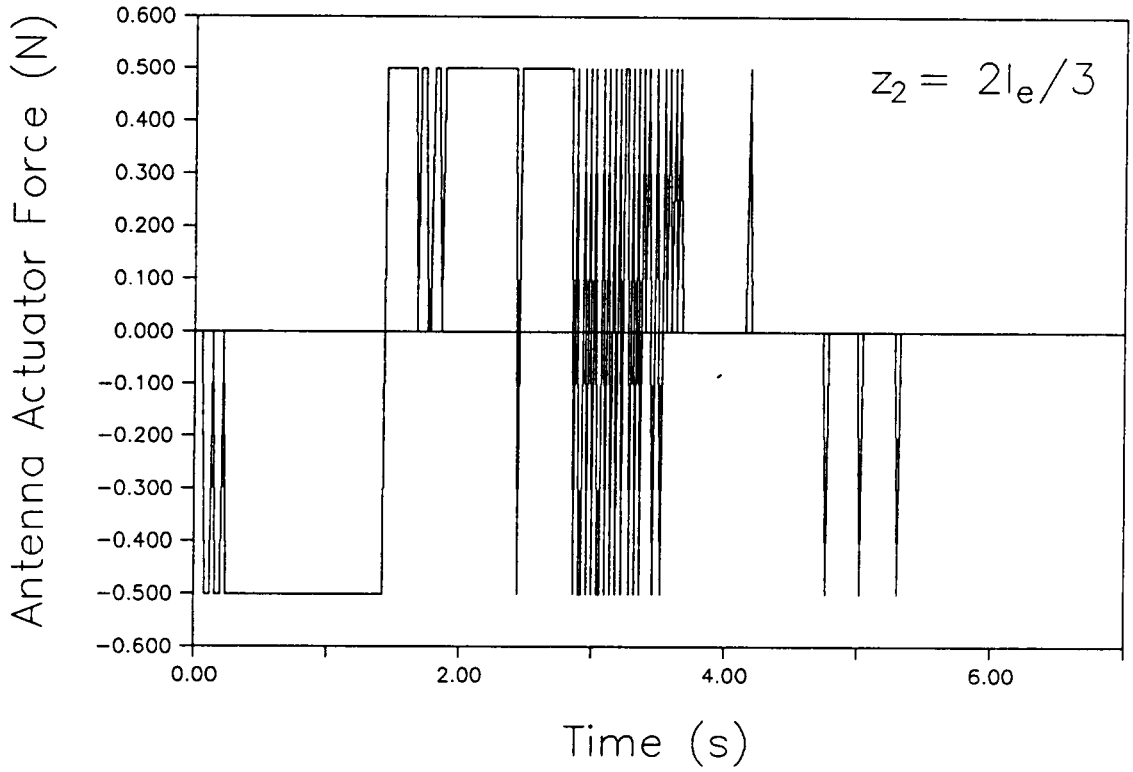

Fig. 19 Antenna Actuator Force for Nonlinear Rigid-Body and Collocated Antenna Control, $z_2 = 2l_e/3$

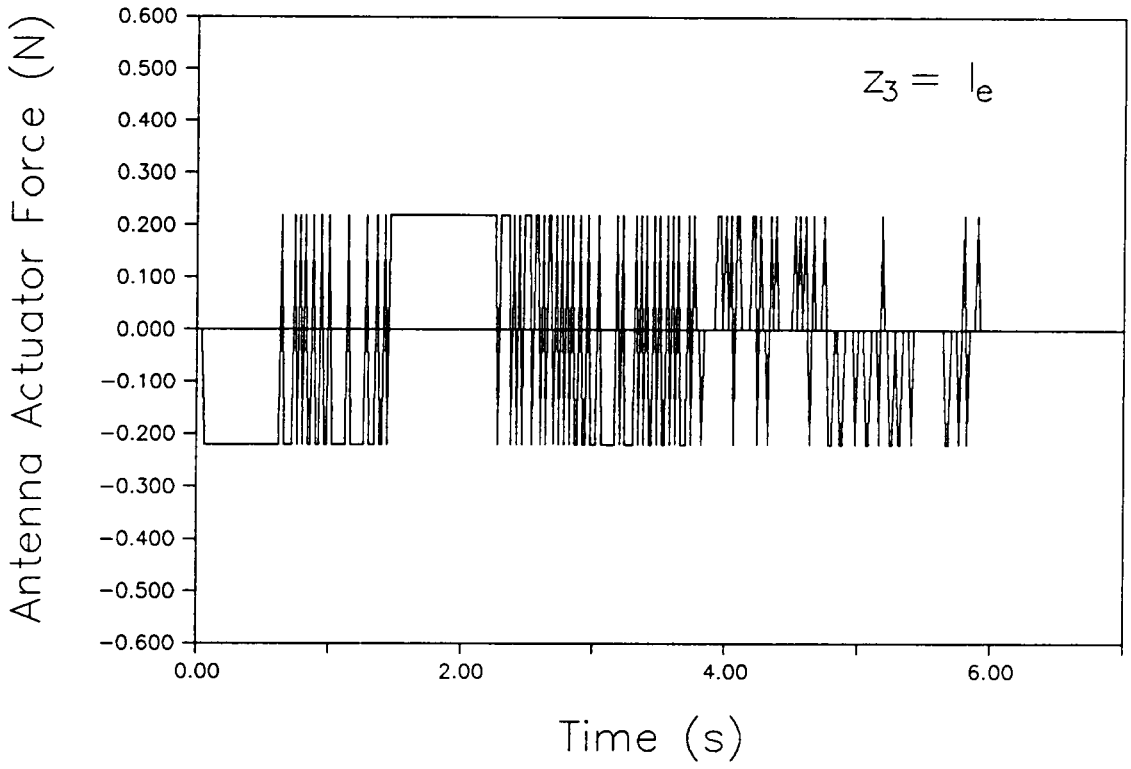

Fig. 20 Antenna Actuator Force for Nonlinear Rigid-Body and Collocated Antenna Control, $z_3 = l_e$

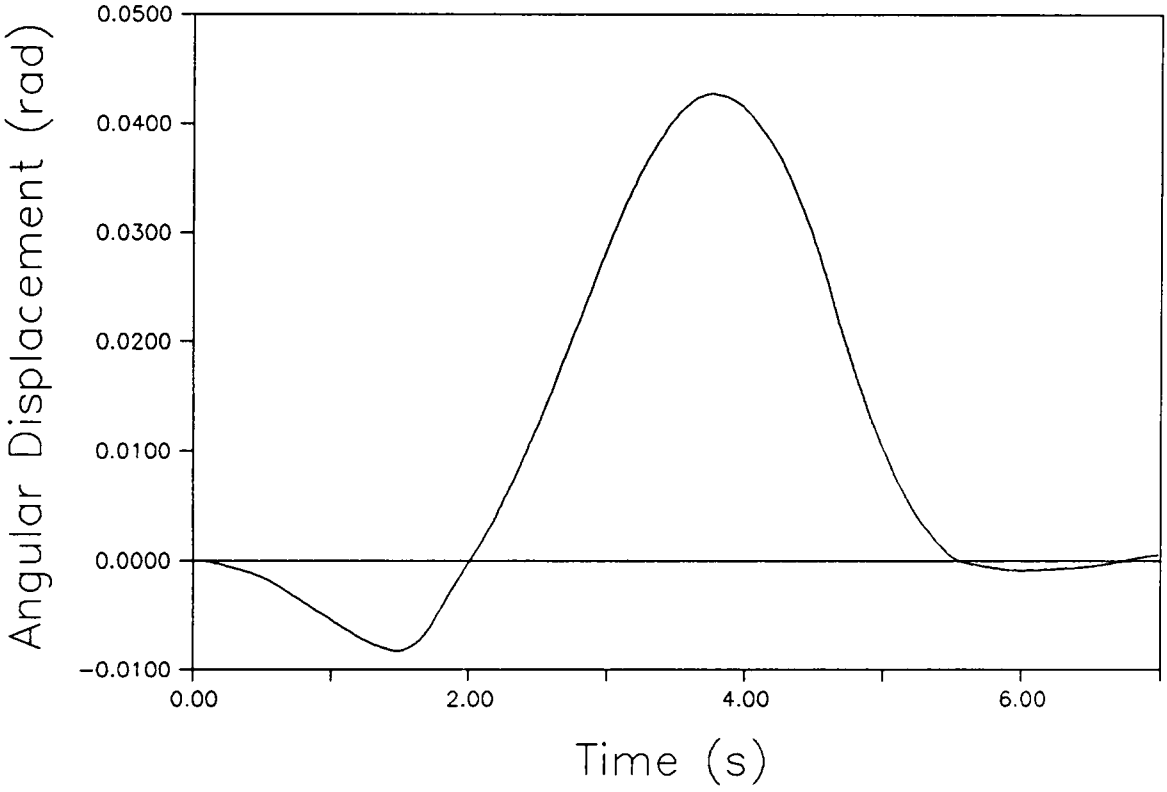

Fig. 21 x-Axis Angular Displacement for Nonlinear Rigid-Body and Collocated Antenna Control

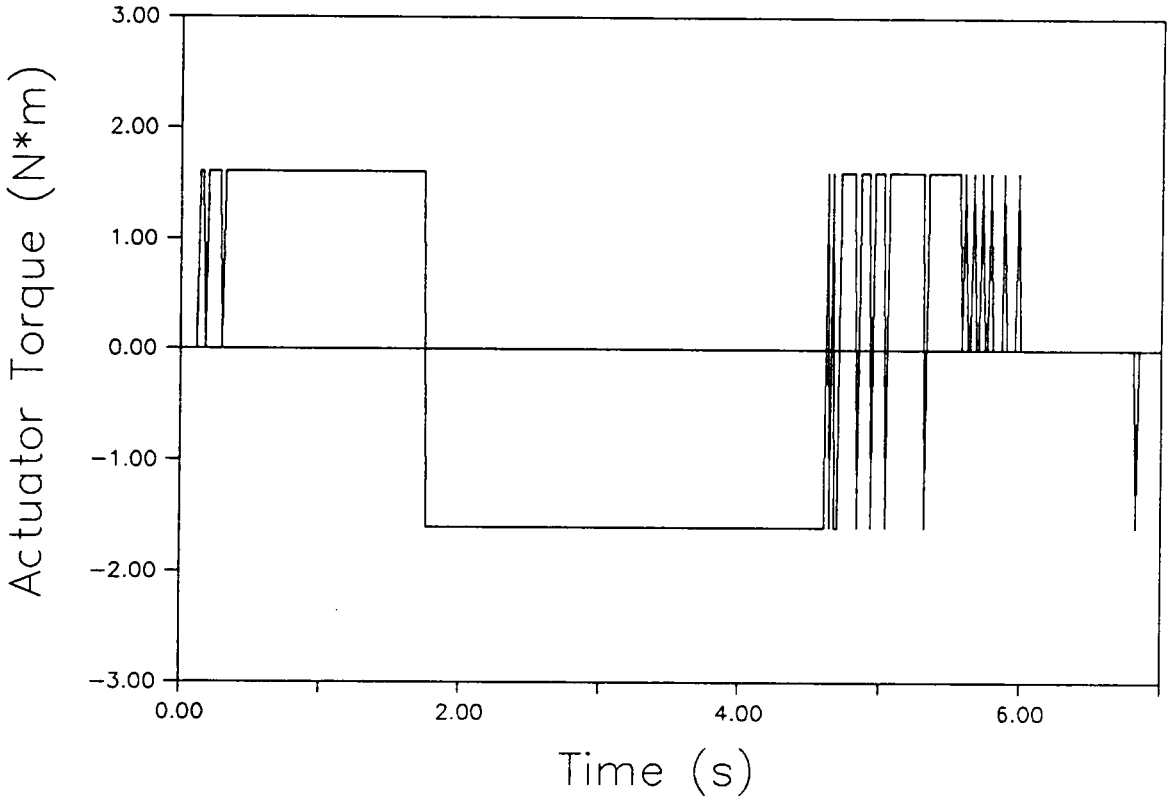

Fig. 22 x-Axis Actuator Torque for Nonlinear Rigid-Body and Collocated Antenna Control

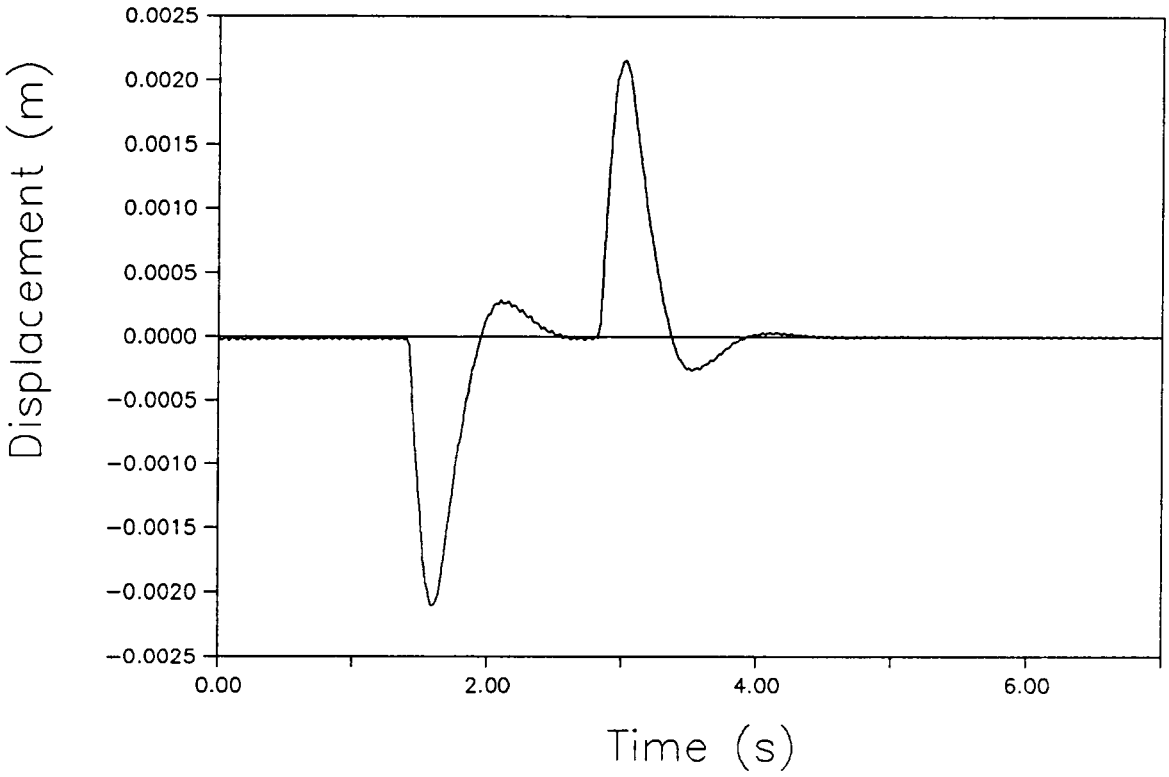

Fig. 23 Tip Displacement for Linear Substructure-Decentralized Control with Disturbance Accommodation

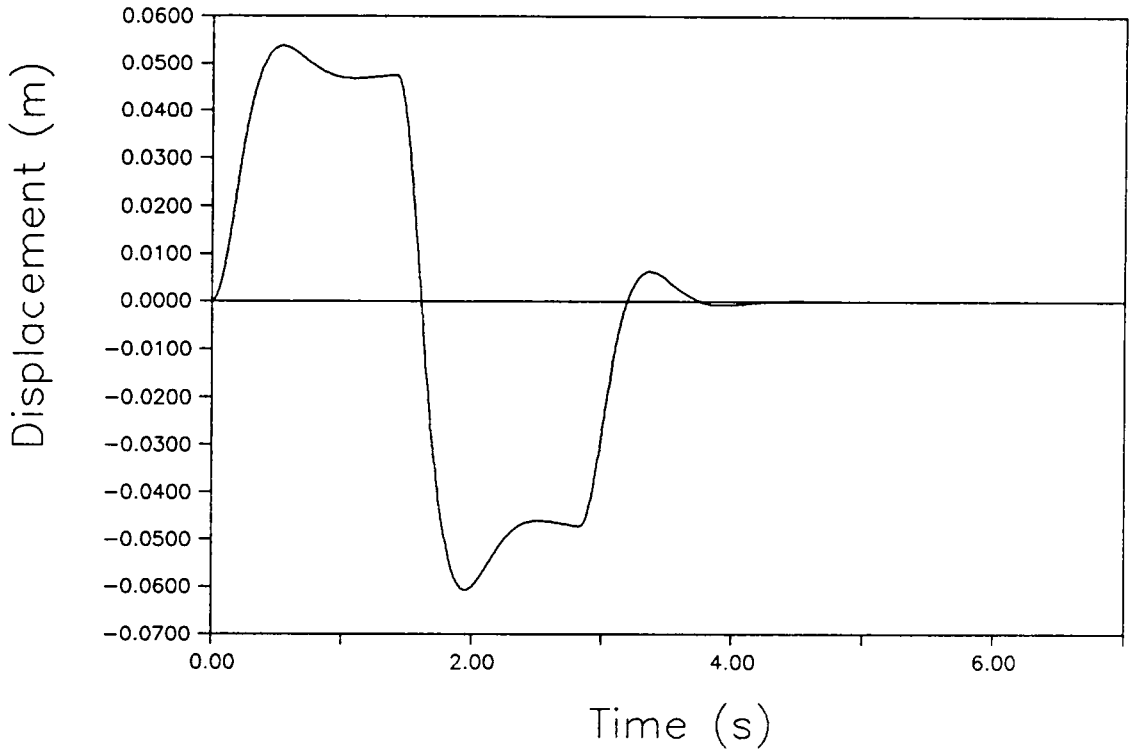

Fig. 24 Tip Displacement for Linear Substructure-Decentralized Control without Disturbance Accommodation

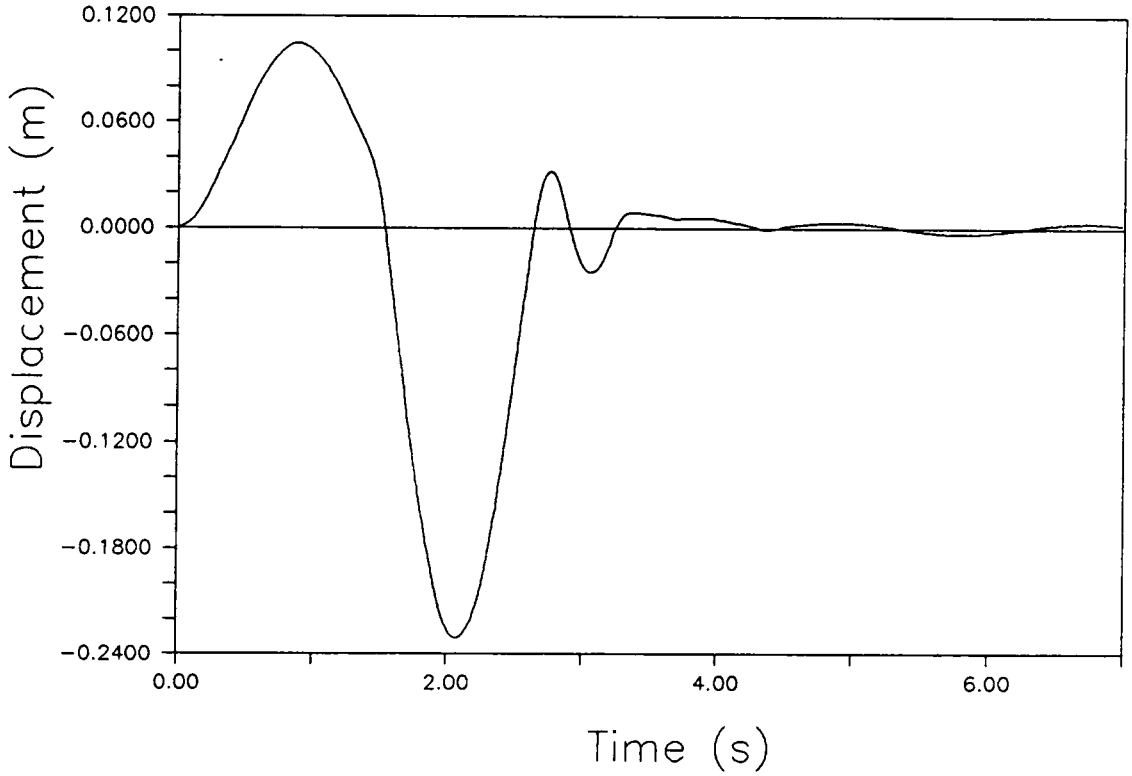

Fig. 25 Tip Displacement for Linear Rigid-Body Control, Nonlinear Substructure-Decentralized Control

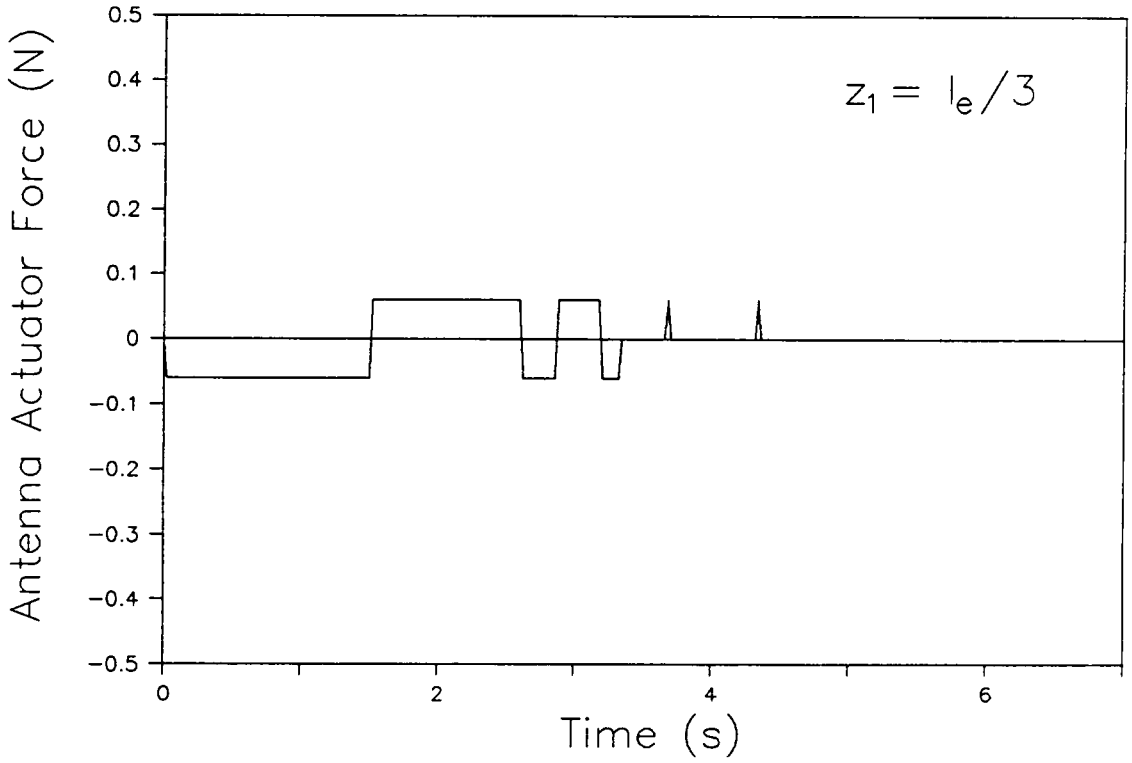

Fig. 26 Antenna Actuator Force for Linear Rigid-Body Control, Nonlinear Substructure-Decentralized Antenna Control, $z_1 = l_e/3$

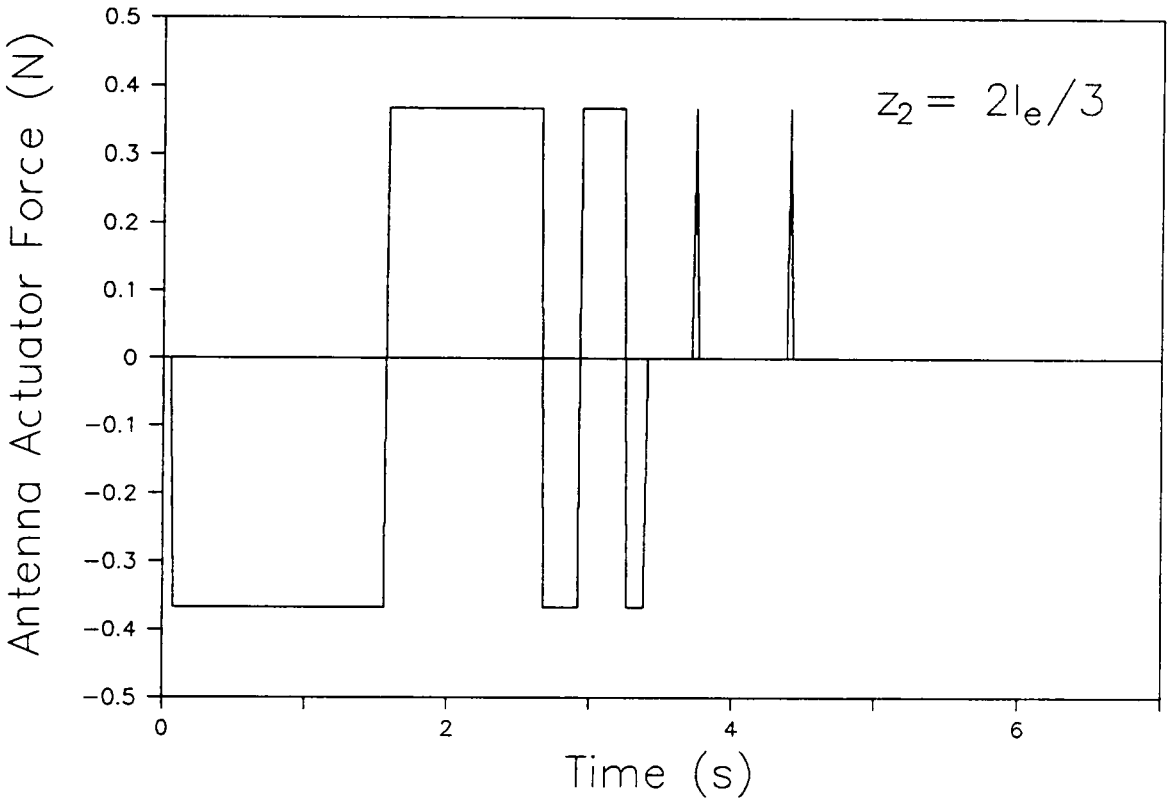

Fig. 27 Antenna Actuator Force for Linear Rigid-Body Control, Nonlinear Substructure-Decentralized Antenna Control, $z_2 = 2l_e/3$

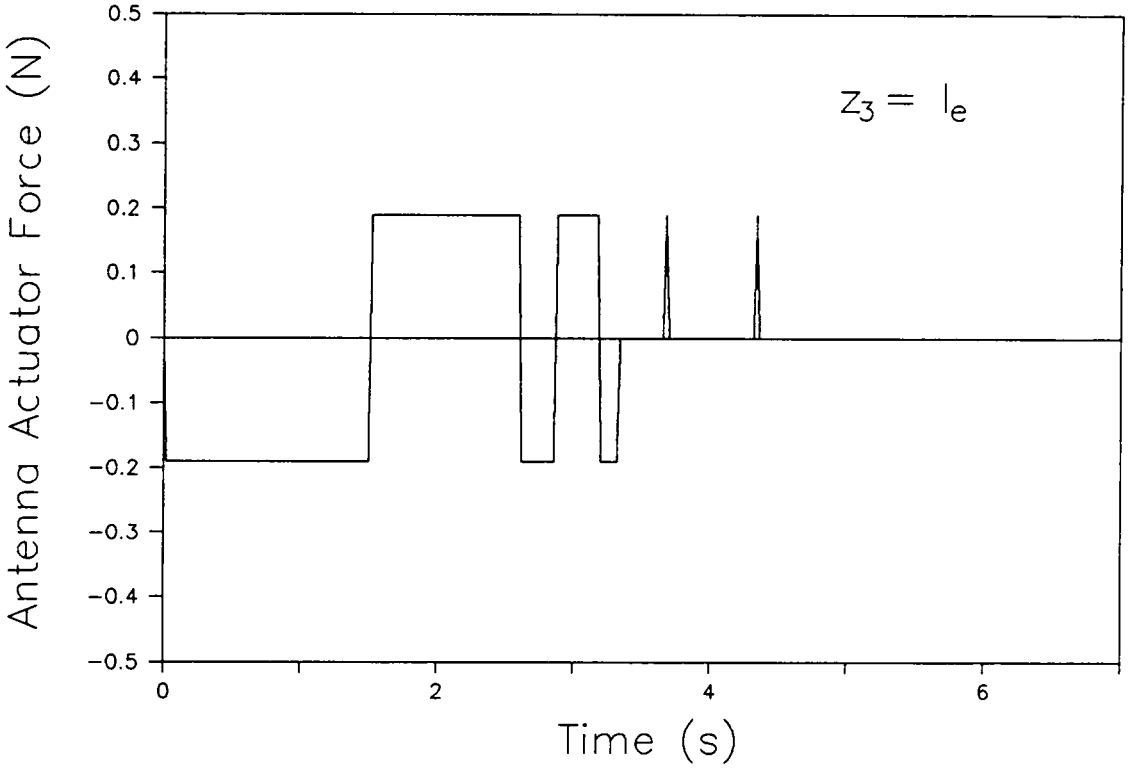

Fig. 28 Antenna Actuator Force for Linear Rigid-Body Control, Nonlinear Substructure-Decentralized Antenna Control, $z_3 = l_e$

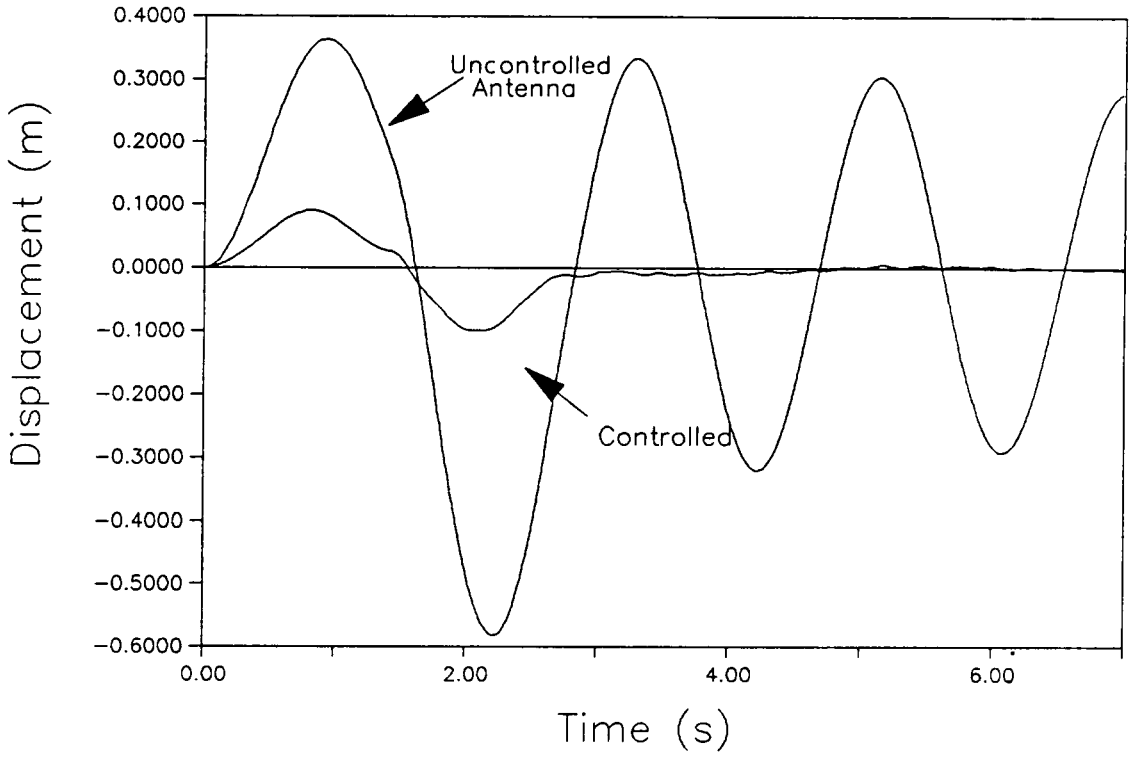

Fig. 29 Tip Displacement for Nonlinear Rigid-Body and Substructure-Decentralized Antenna Control

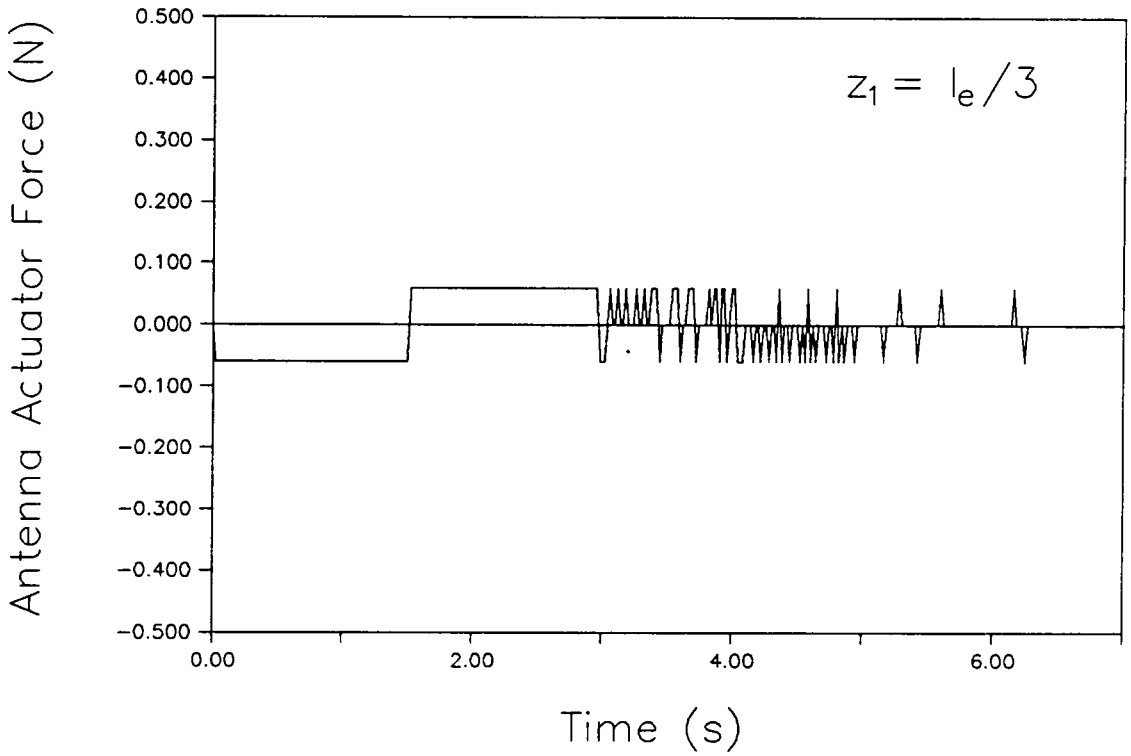

Fig. 30 Antenna Actuator Force for Nonlinear Rigid-Body and Substructure-Decentralized Antenna Control, $z_1 = l_e/3$

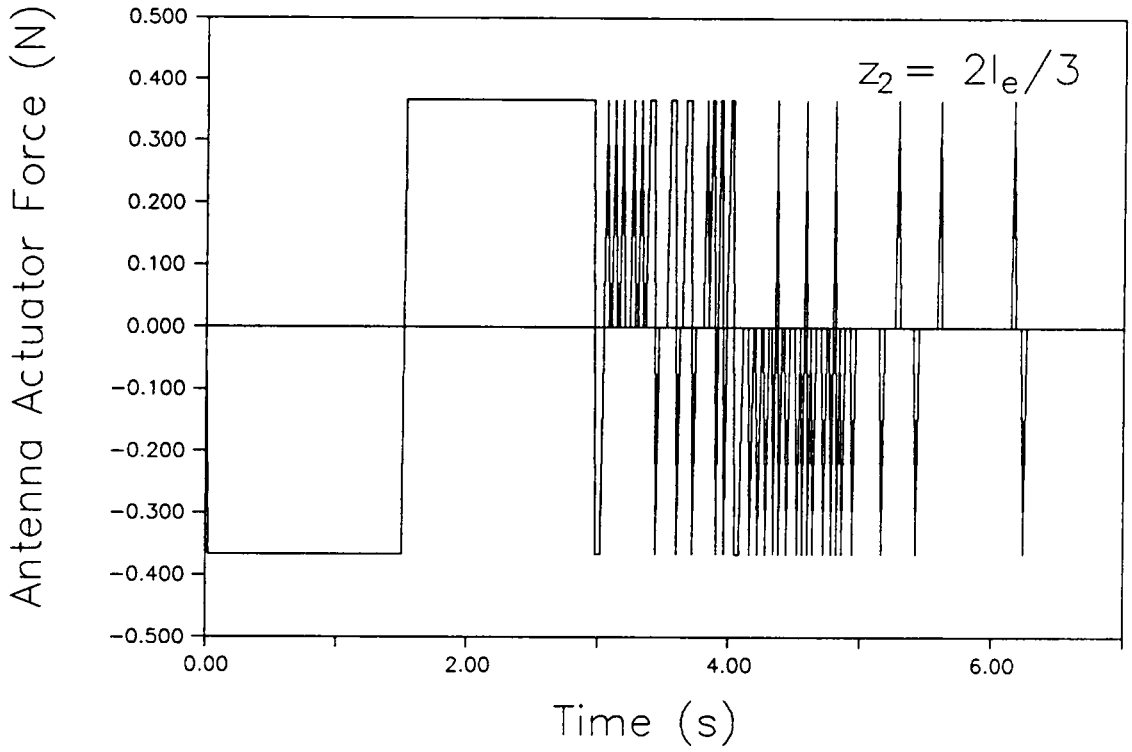

Fig. 31 Antenna Actuator Force for Nonlinear Rigid-Body and Substructure-Decentralized Antenna Control, $z_2 = 2l_e/3$

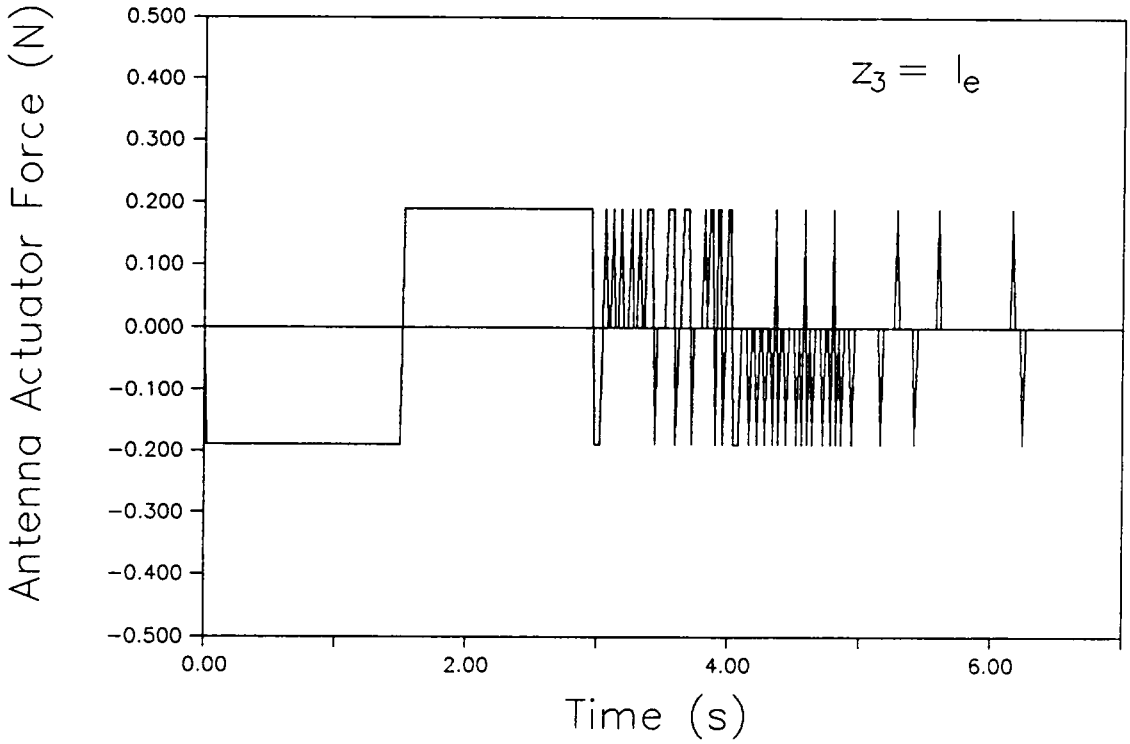

Fig. 32 Antenna Actuator Force for Nonlinear Rigid-Body and Substructure-Decentralized Antenna Control, $z_3 = l_e$

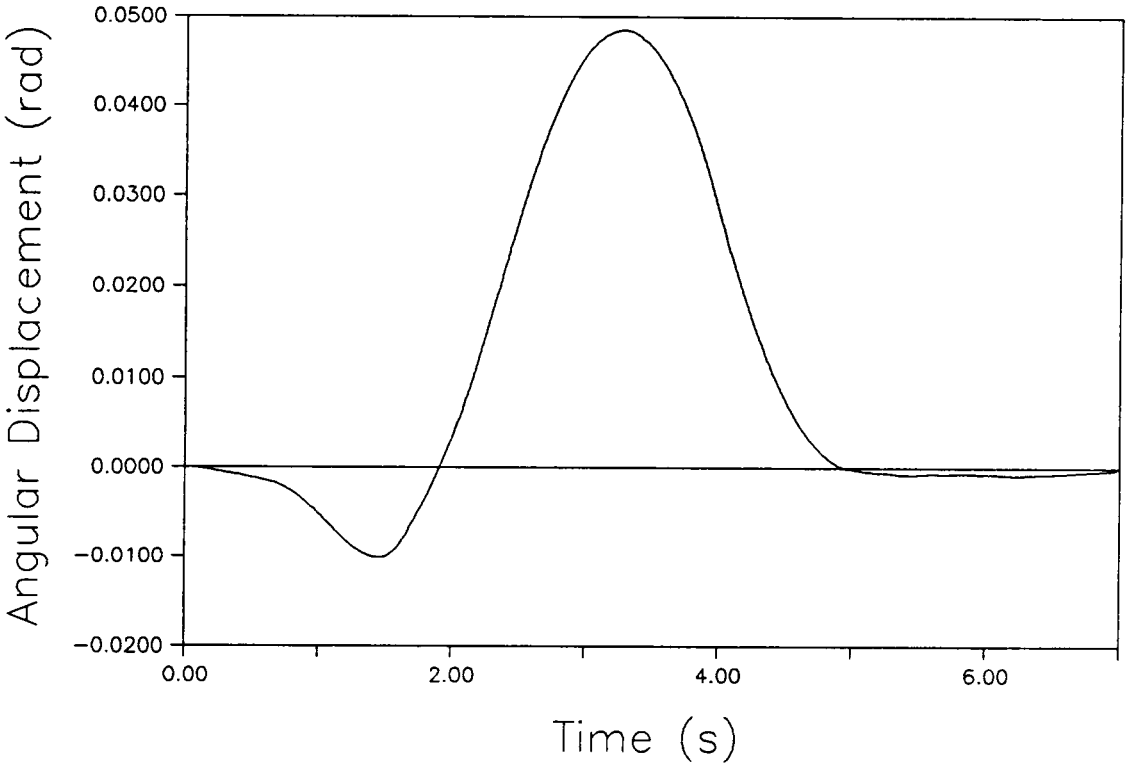

Fig. 33 x-Axis Angular Displacement for Nonlinear Rigid-Body and Substructure-Decentralized Antenna Control

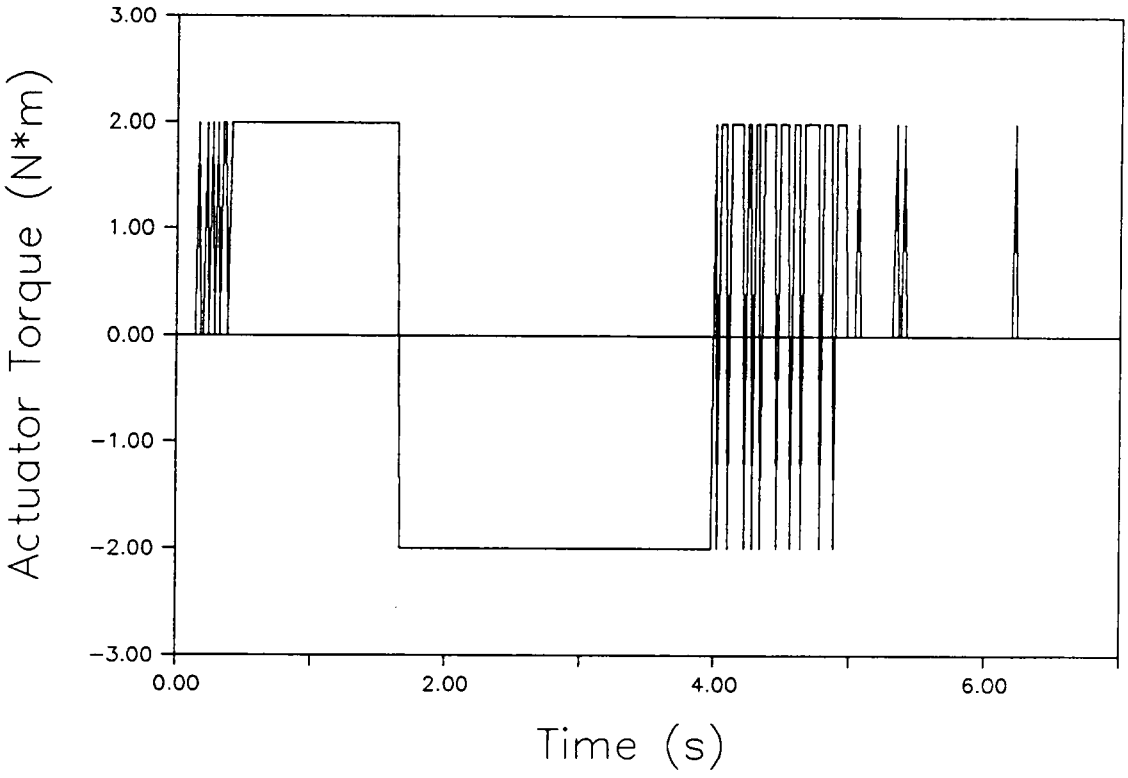

Fig. 34 x-Axis Actuator Torque for Nonlinear Rigid-Body and Substructure-Decentralized Antenna Control

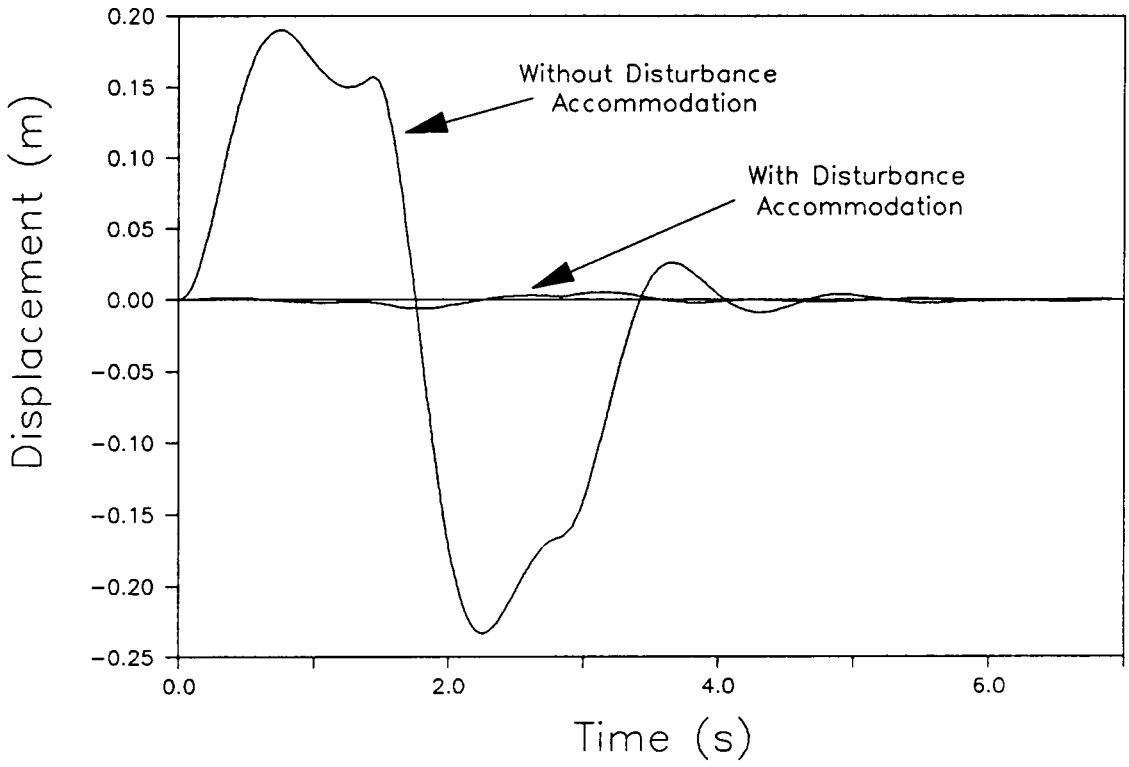

Fig. 35 Tip Displacement for Linear Pseudo-Collocated Control

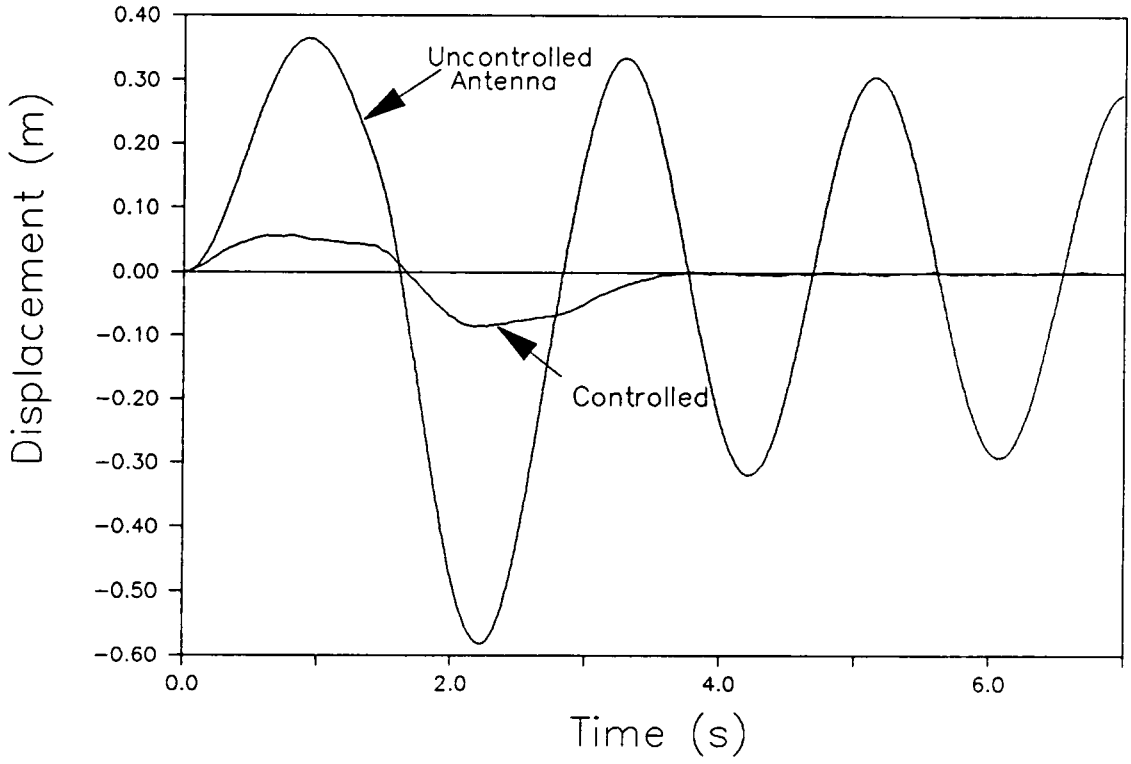

Fig. 36 Tip Displacement for Linear Rigid-Body Control, Nonlinear Pseudo-Collocated Antenna Control

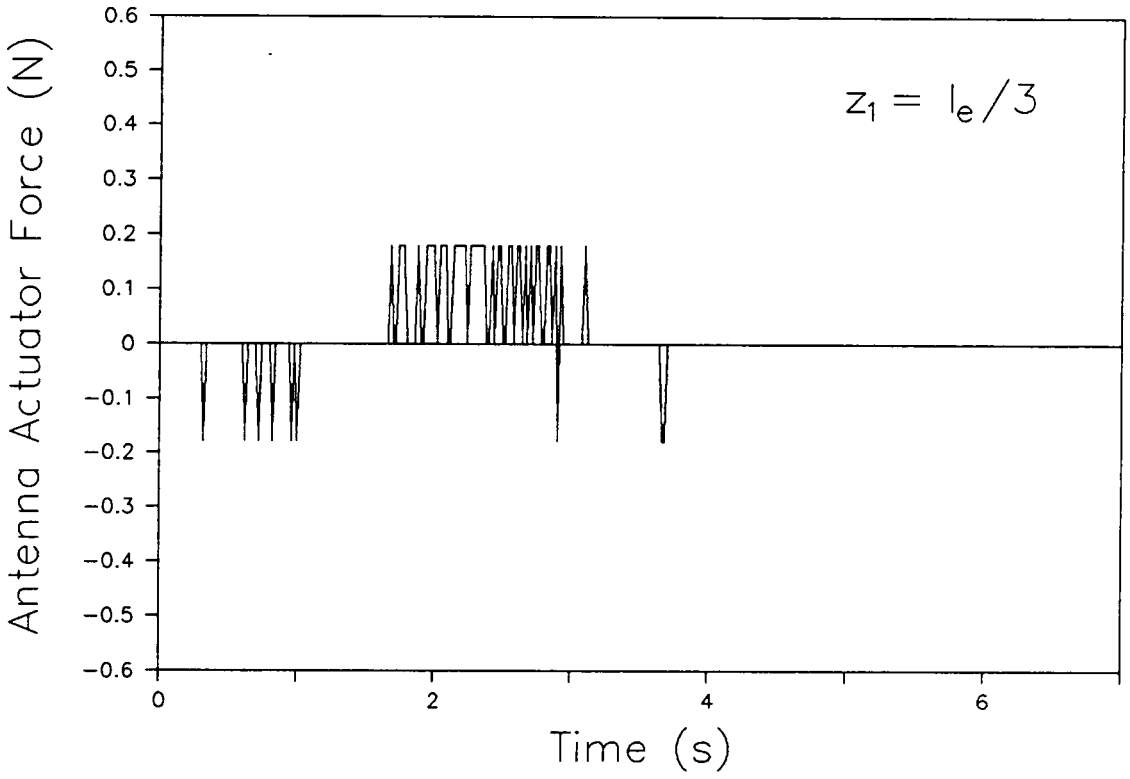

Fig. 37 Antenna Actuator Force for Linear Rigid-Body Control, Nonlinear Pseudo-Collocated Antenna Control, $z_1 = l_e/3$

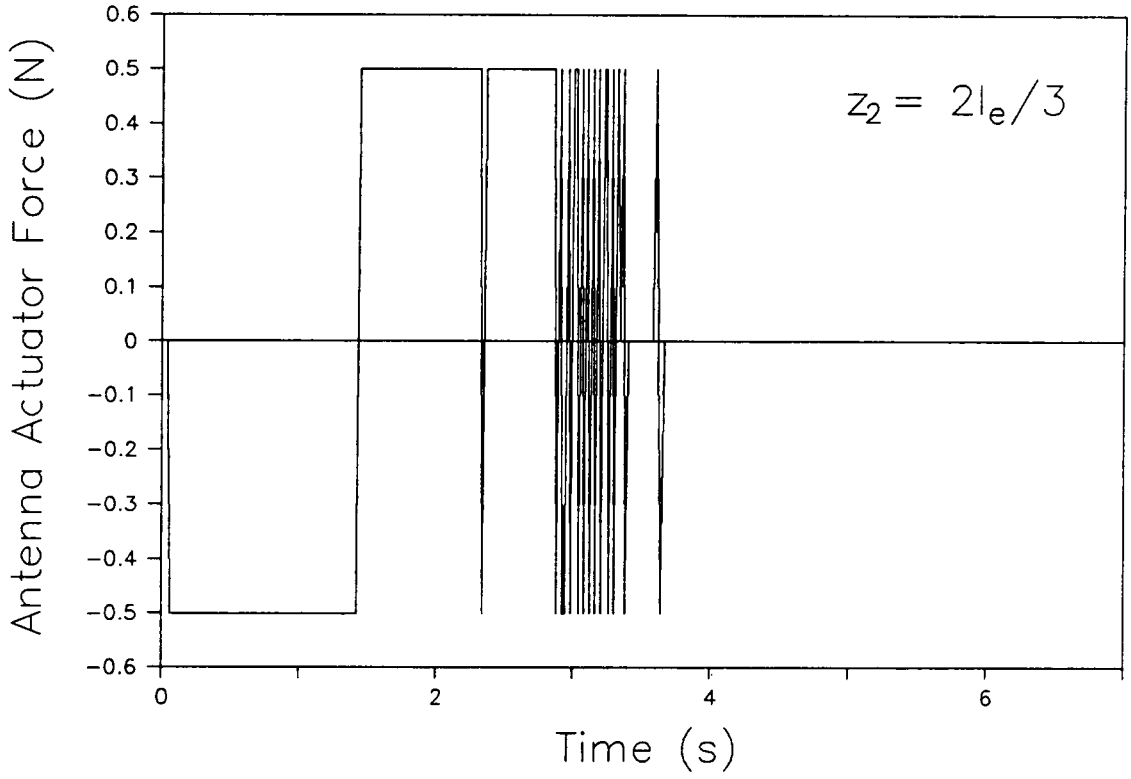

Fig. 38 Antenna Actuator Force for Linear Rigid-Body Control, Nonlinear Pseudo-Collocated Antenna Control, $z_2 = 2l_e/3$

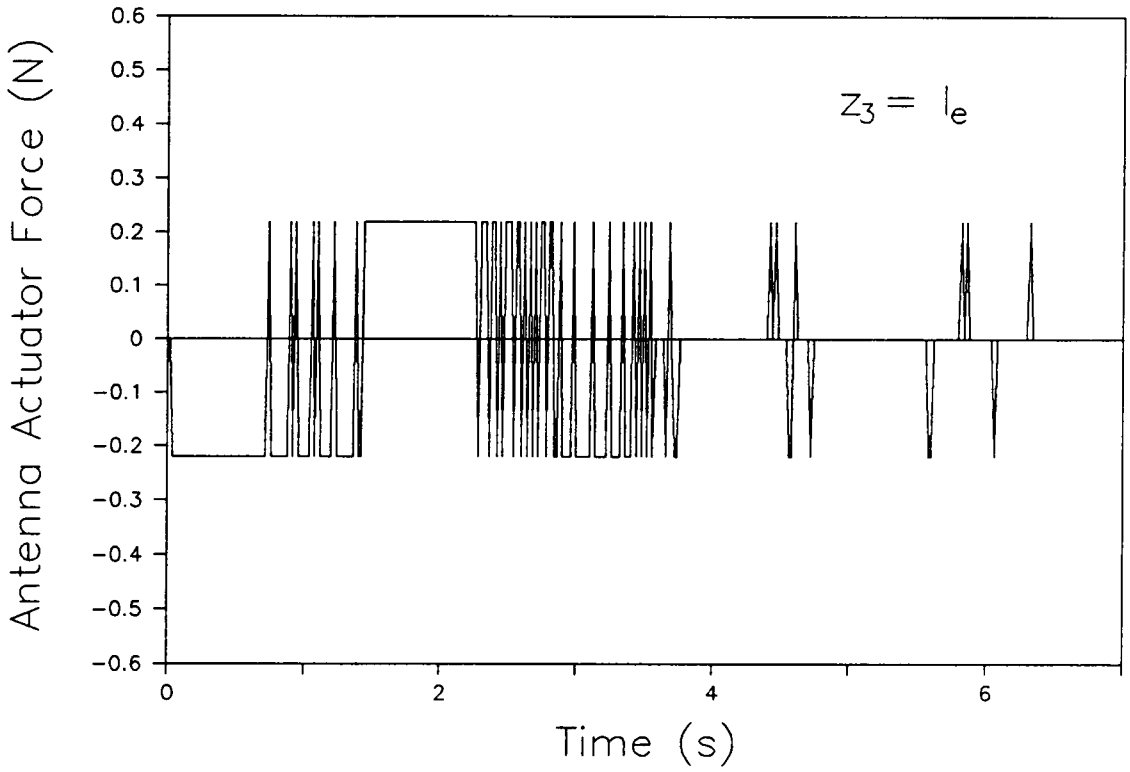

Fig. 39 Antenna Actuator Force for Linear Rigid-Body Control, Nonlinear Pseudo-Collocated Antenna Control, $z_3 = l_e$

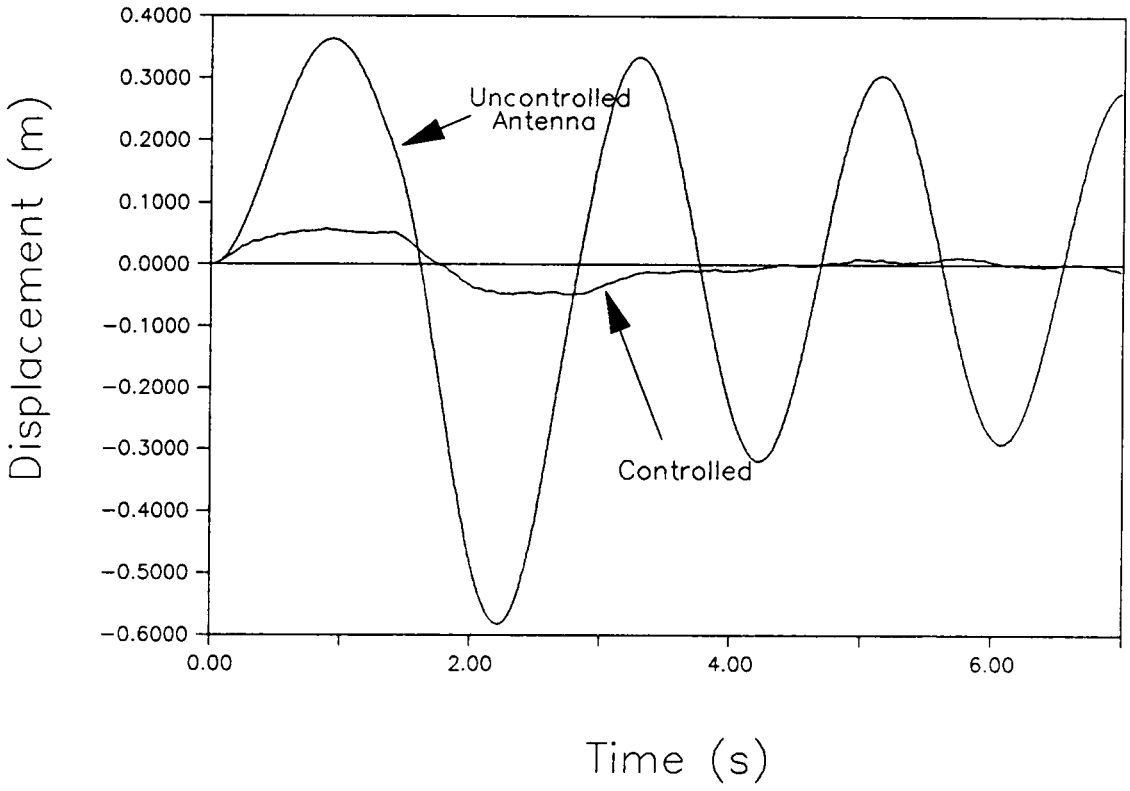

Fig. 40 Tip Displacement for Nonlinear Rigid-Body and Pseudo-Collocated Antenna Control

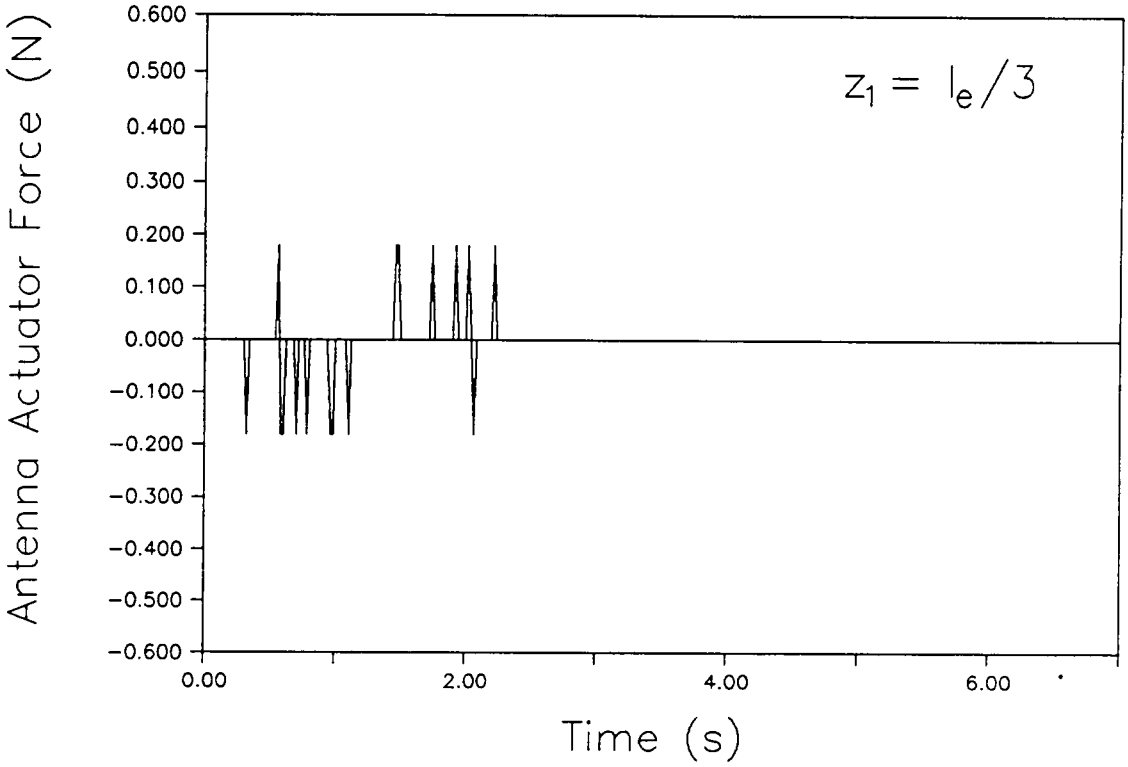

Fig. 41 Antenna Actuator Force for Nonlinear Rigid-Body and Pseudo-Collocated Antenna Control, $z_1 = l_e/3$

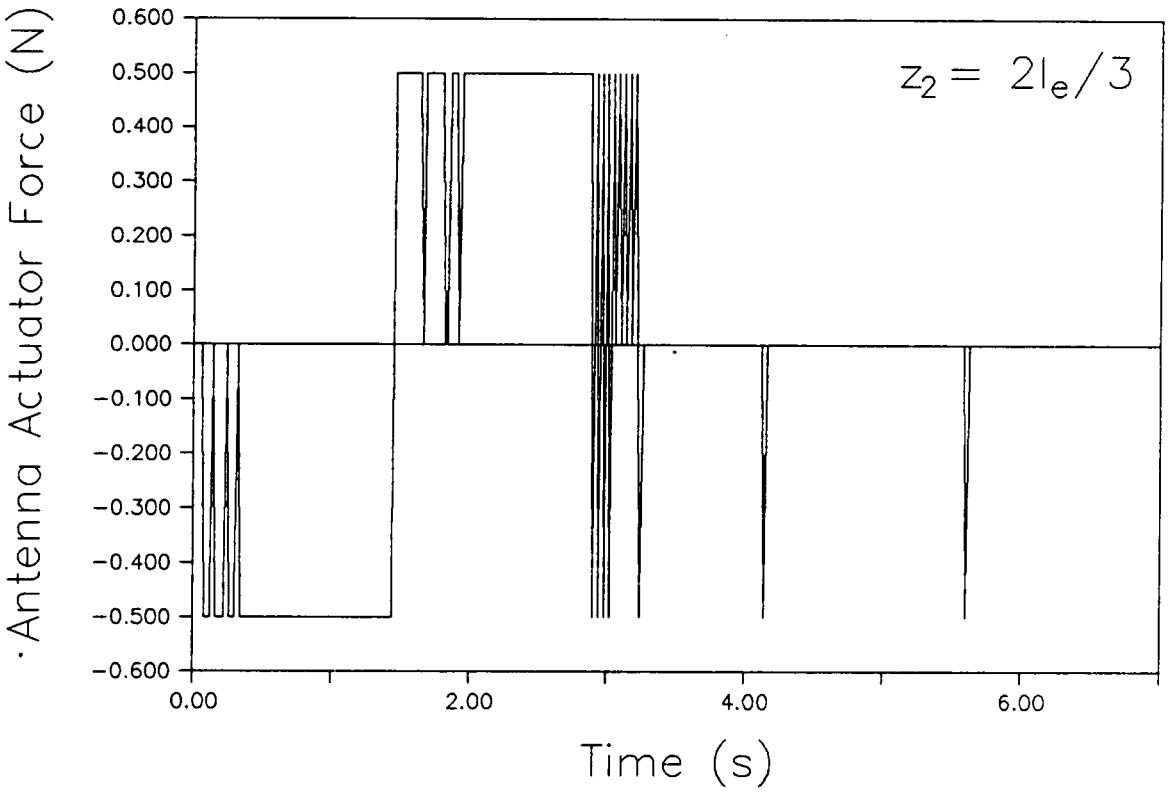

Fig. 42 Antenna Actuator Force for Nonlinear Rigid-Body and Pseudo-Collocated Antenna Control, $z_2 = 2l_e/3$

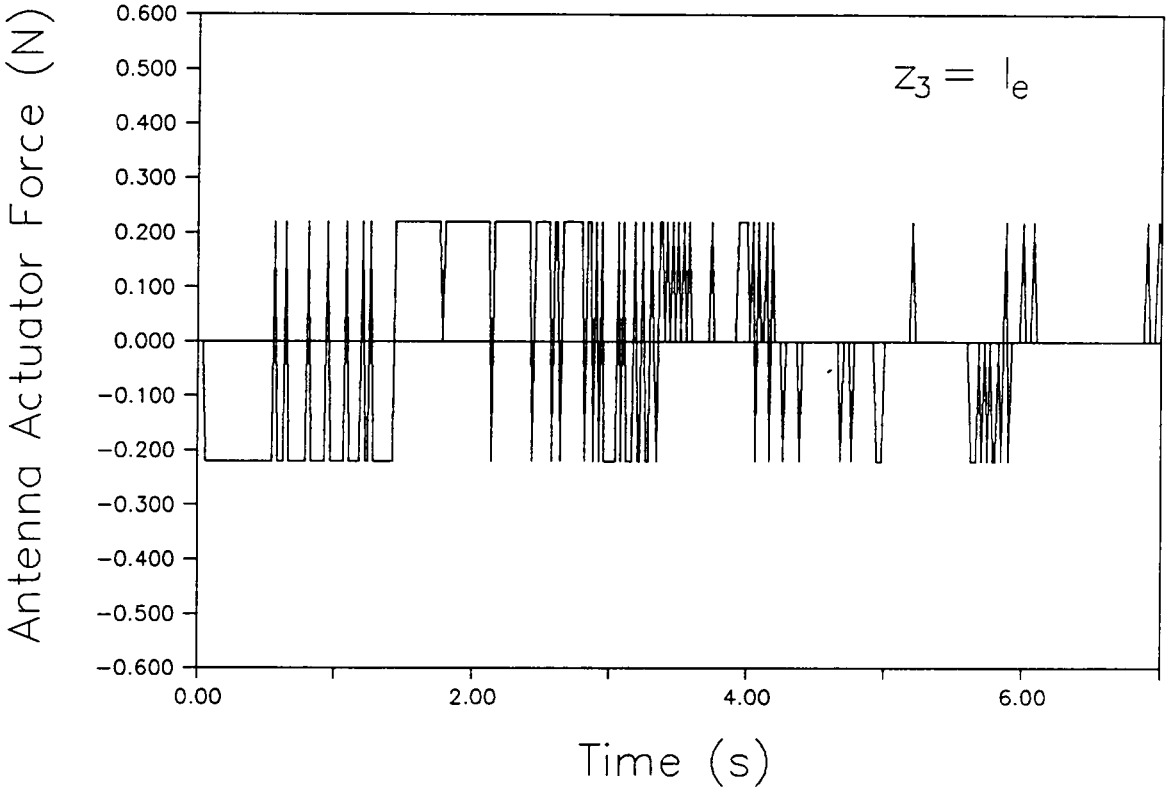

Fig. 43 Antenna Actuator Force for Nonlinear Rigid-Body and Pseudo-Collocated Antenna Control, $z_3 = l_e$

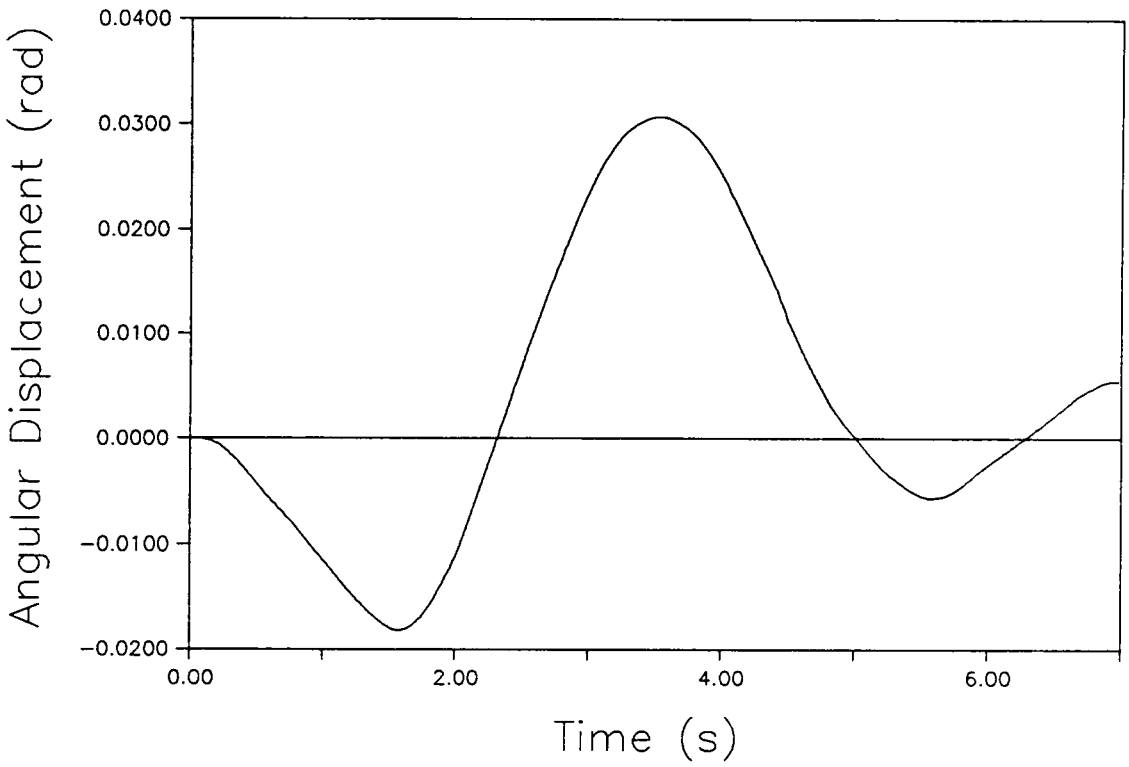

Fig. 44 X-Axis Angular Displacement for Nonlinear Rigid-Body and Pseudo-Collocated Antenna Control

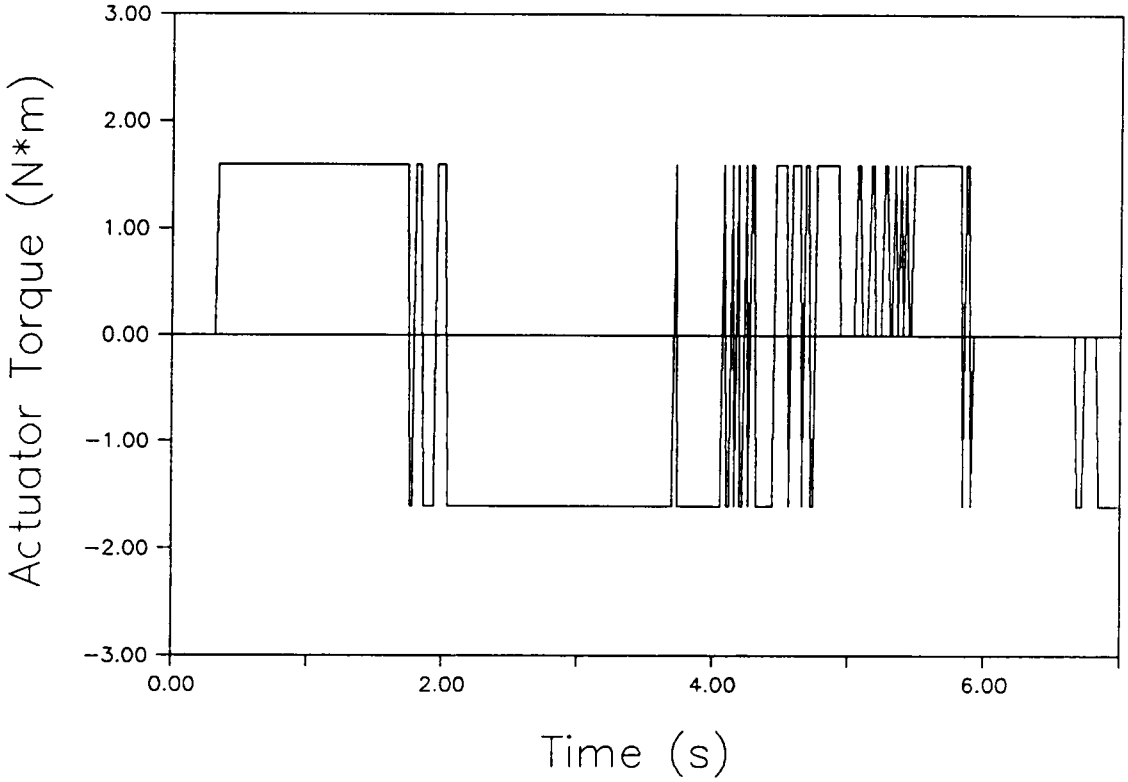

Fig. 45 x-Axis Actuator Torque for Nonlinear Rigid-Body and Pseudo-Collocated Antenna Control

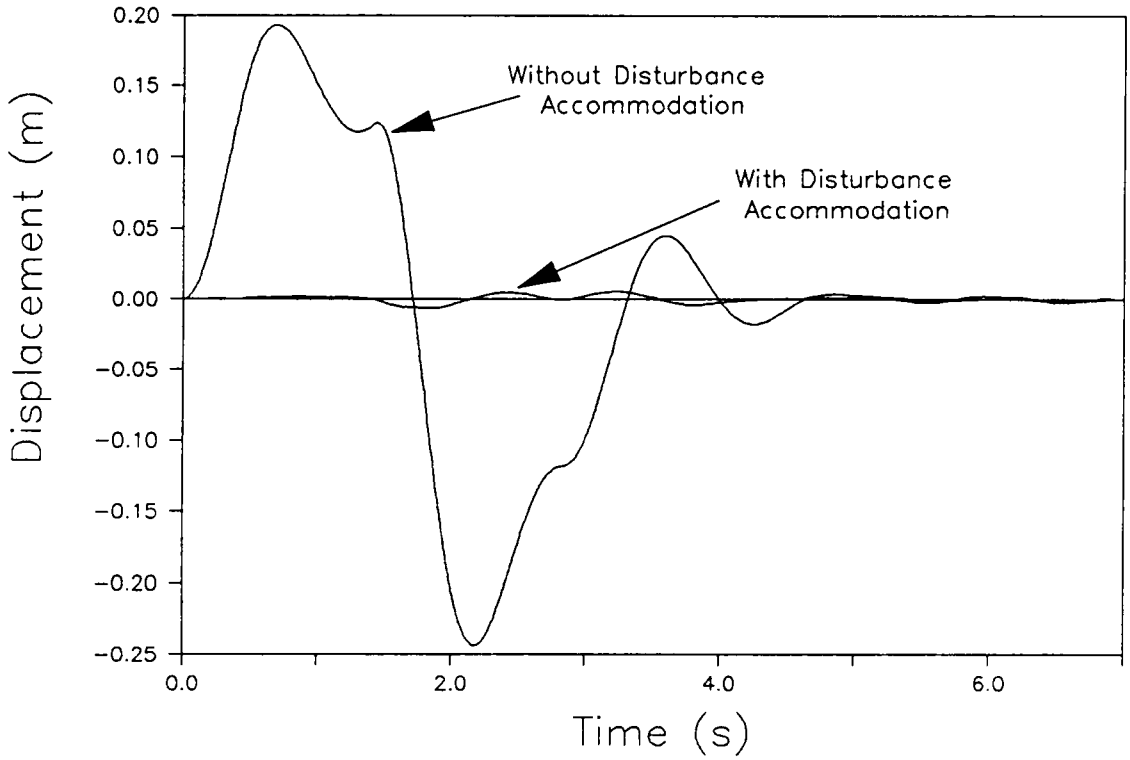

Fig. 46 Tip Displacement for Linear Substructure-Decentralized Control (Pseudo)

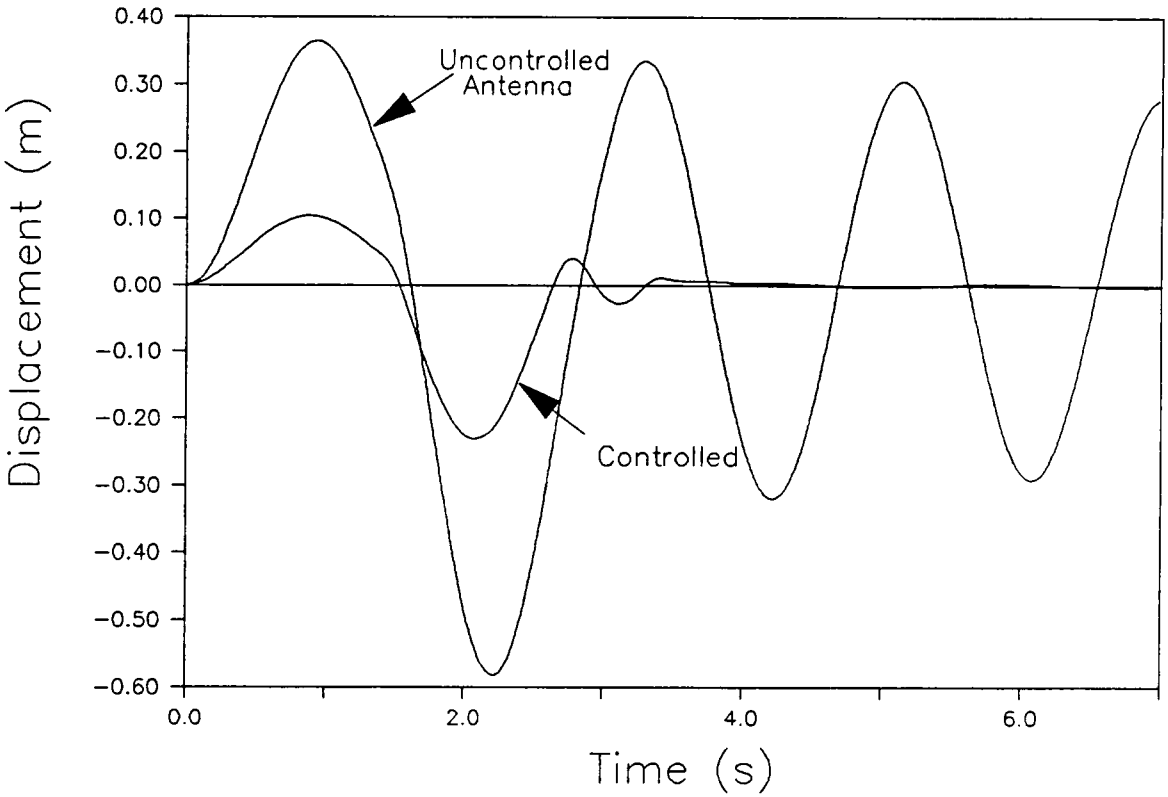

Fig. 47 Tip Displacement for Linear Rigid-Body Control, Nonlinear Substructure-Decentralized Antenna Control (Pseudo)

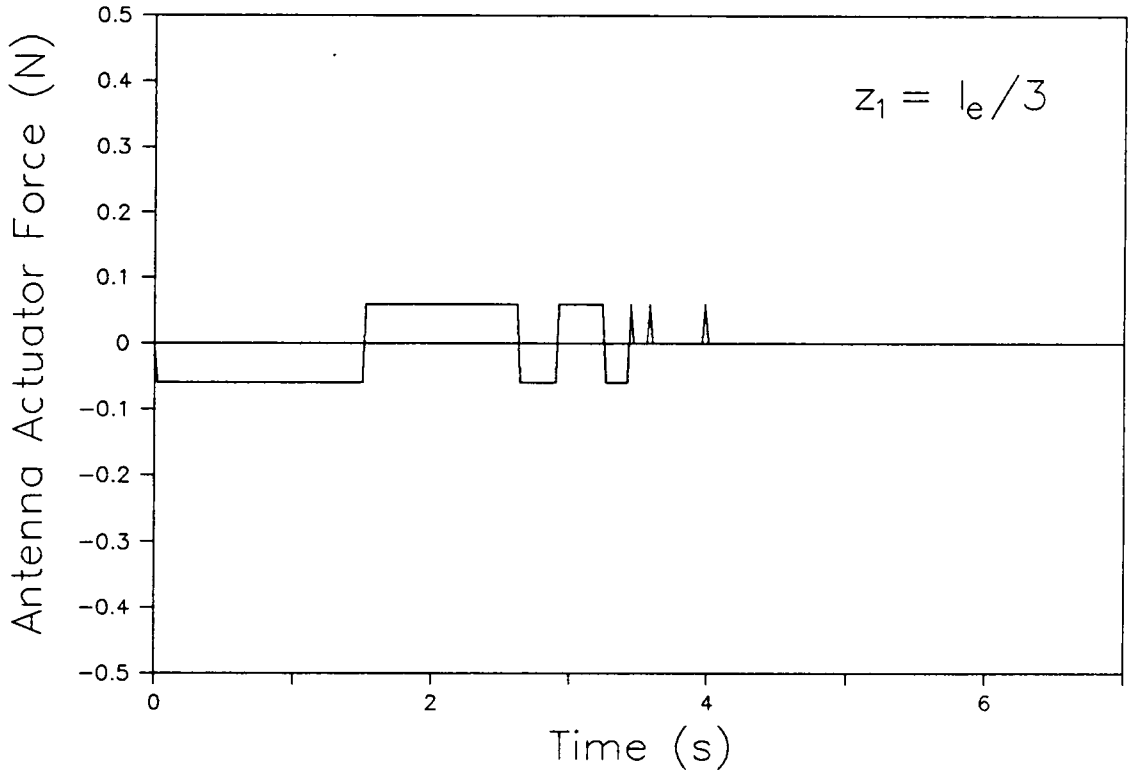

Fig. 48 Antenna Actuator Force for Linear Rigid-Body Control, Nonlinear Substructure-Decentralized Antenna Control (Pseudo), $z_1 = l_e/3$

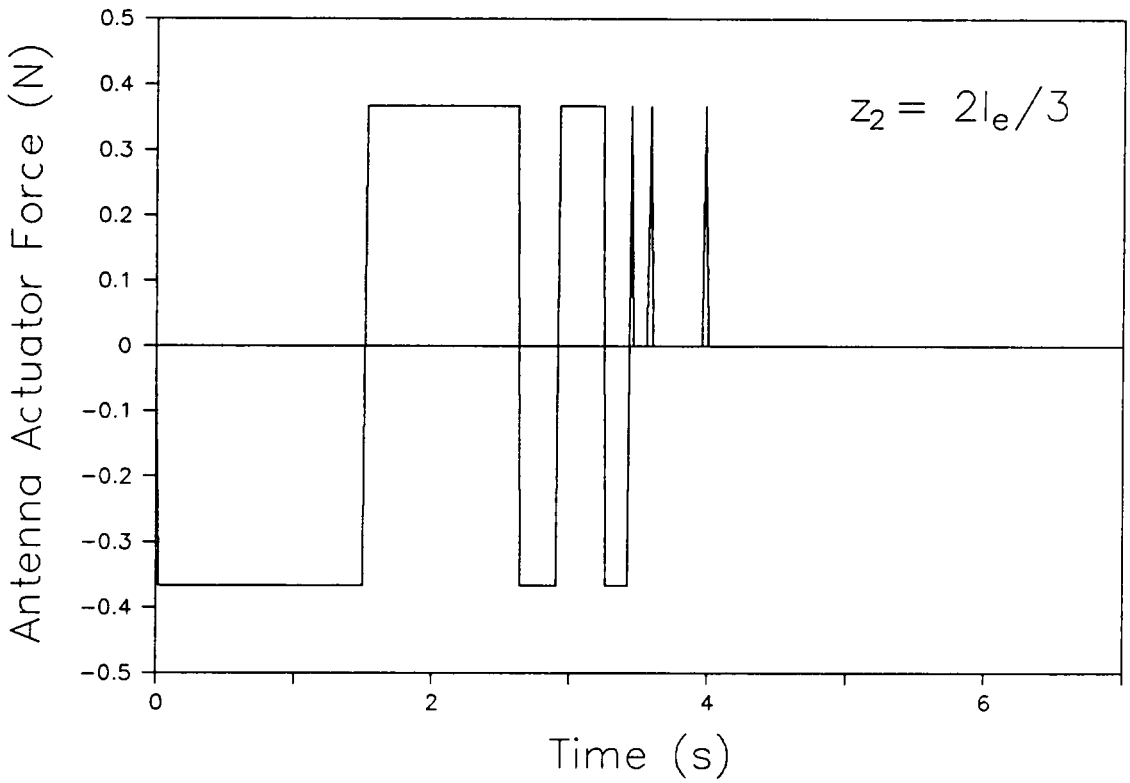

Fig. 49 Antenna Actuator Force for Linear Rigid-Body Control, Nonlinear Substructure-Decentralized Antenna Control (Pseudo), $z_2 = 2l_e/3$

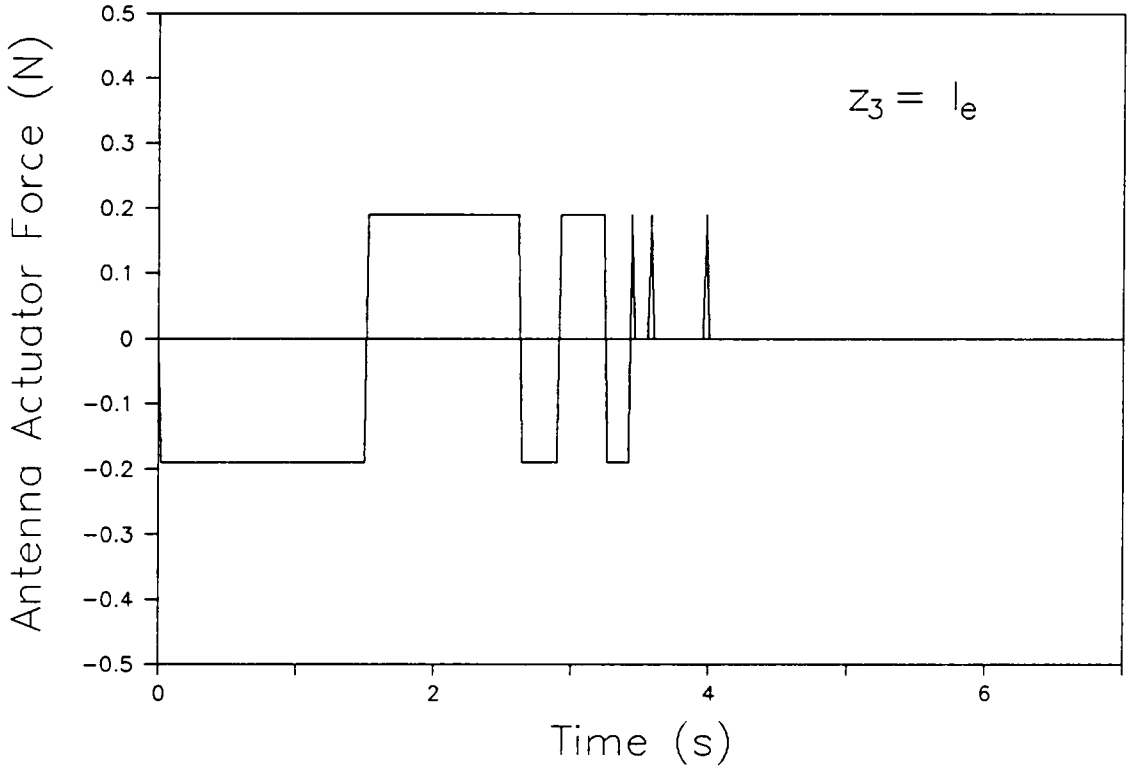

Fig. 50 Antenna Actuator Force for Linear Rigid-Body Control, Nonlinear Substructure-Decentralized Antenna Control (Pseudo), $z_3 = l_e$

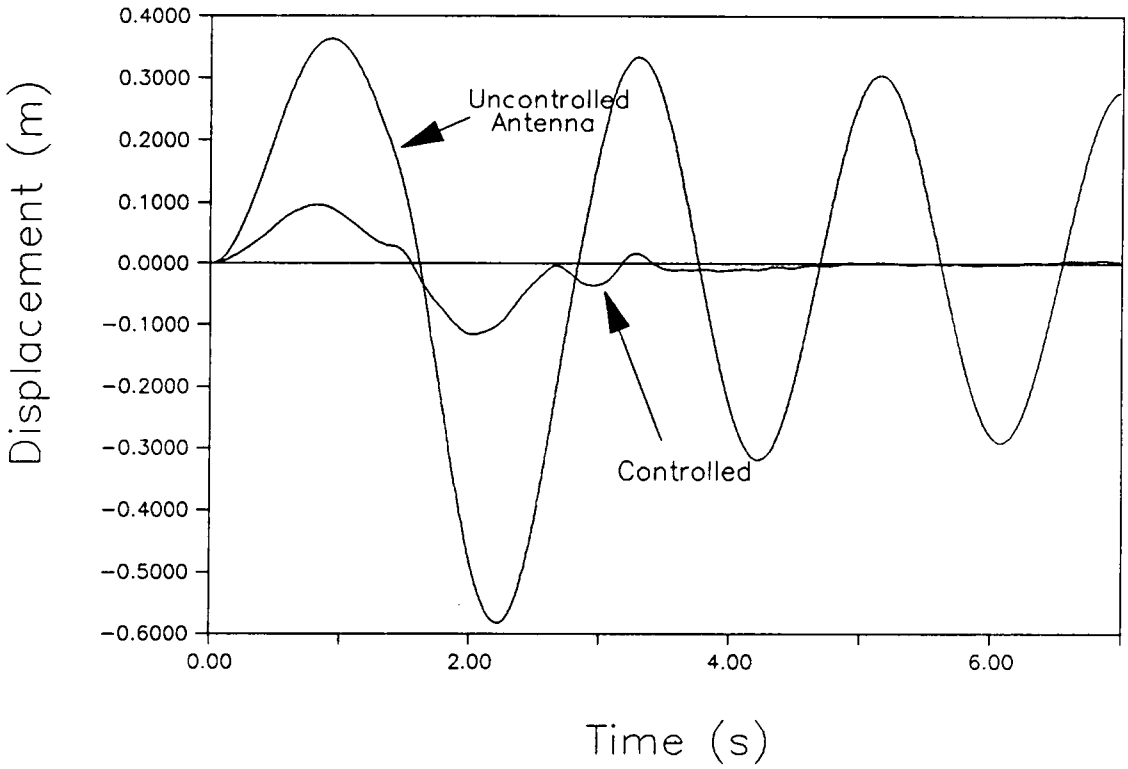

Fig. 51 Tip Displacement for Nonlinear Rigid-Body and Substructure-Decentralized Antenna Control (Pseudo)

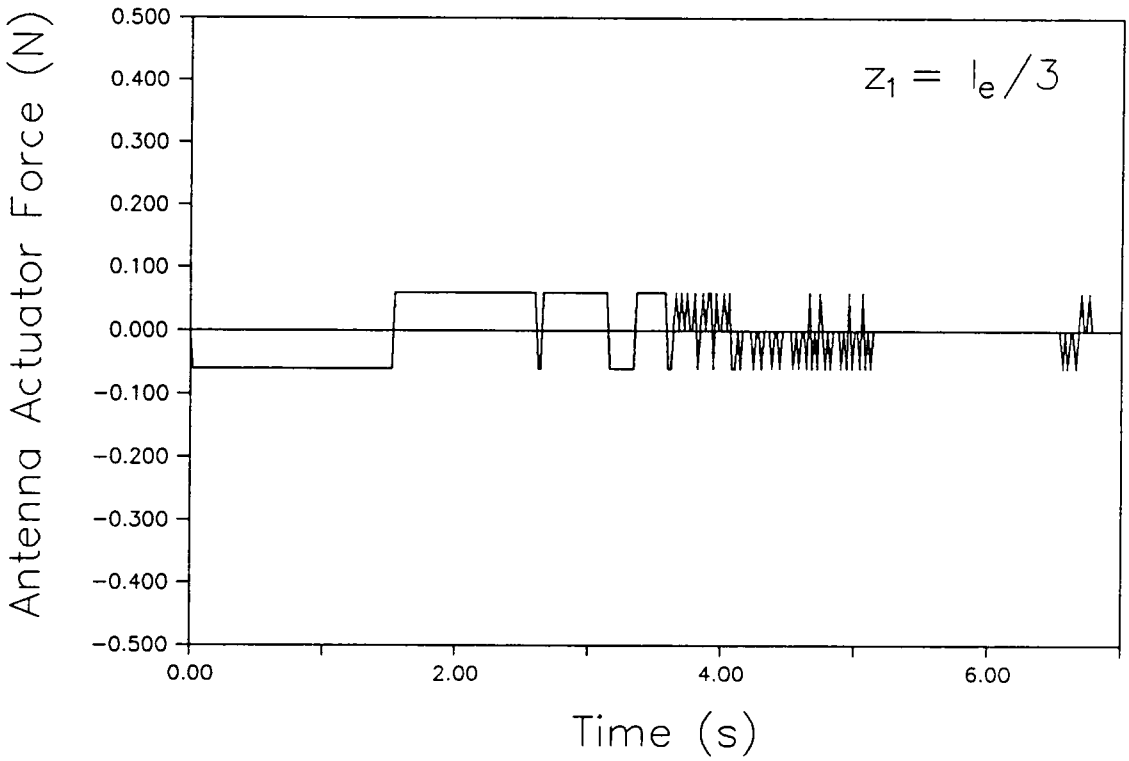

Fig. 52 Antenna Actuator Force for Nonlinear Rigid-Body and Substructure-Decentralized Antenna Control (Pseudo), $z_1 = l_e/3$

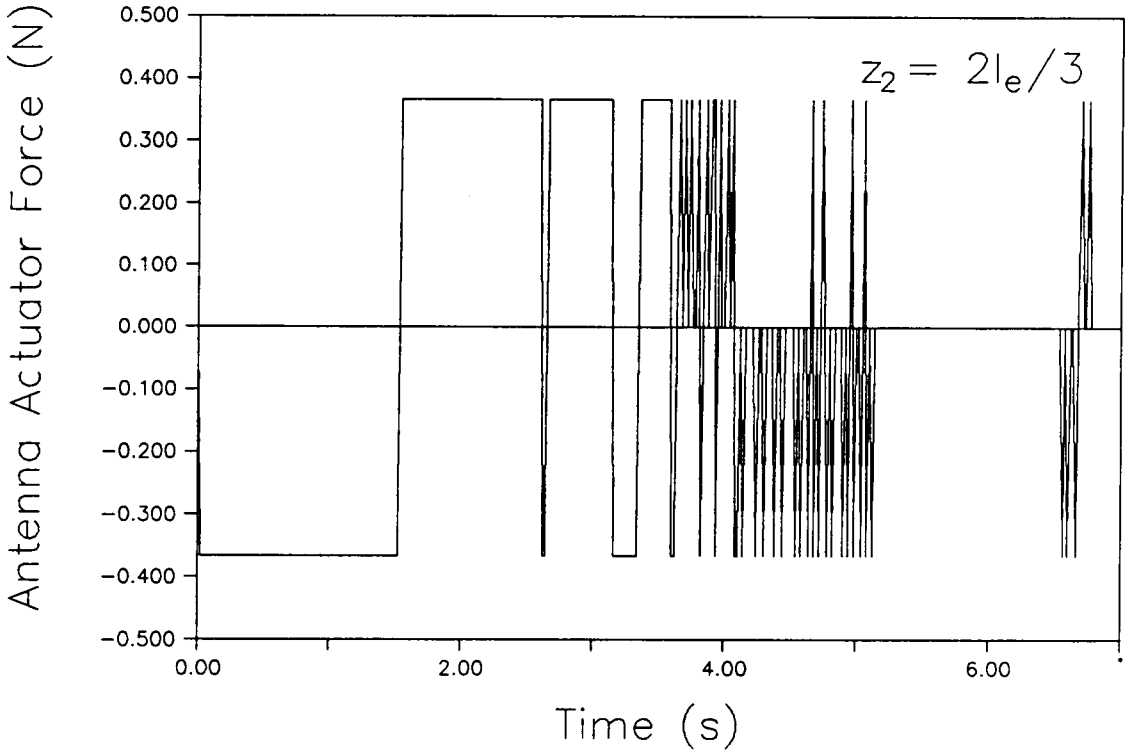

Fig. 53 Antenna Actuator Force for Nonlinear Rigid-Body and Substructure-Decentralized Antenna Control (Pseudo), $z_2 = 2l_e/3$

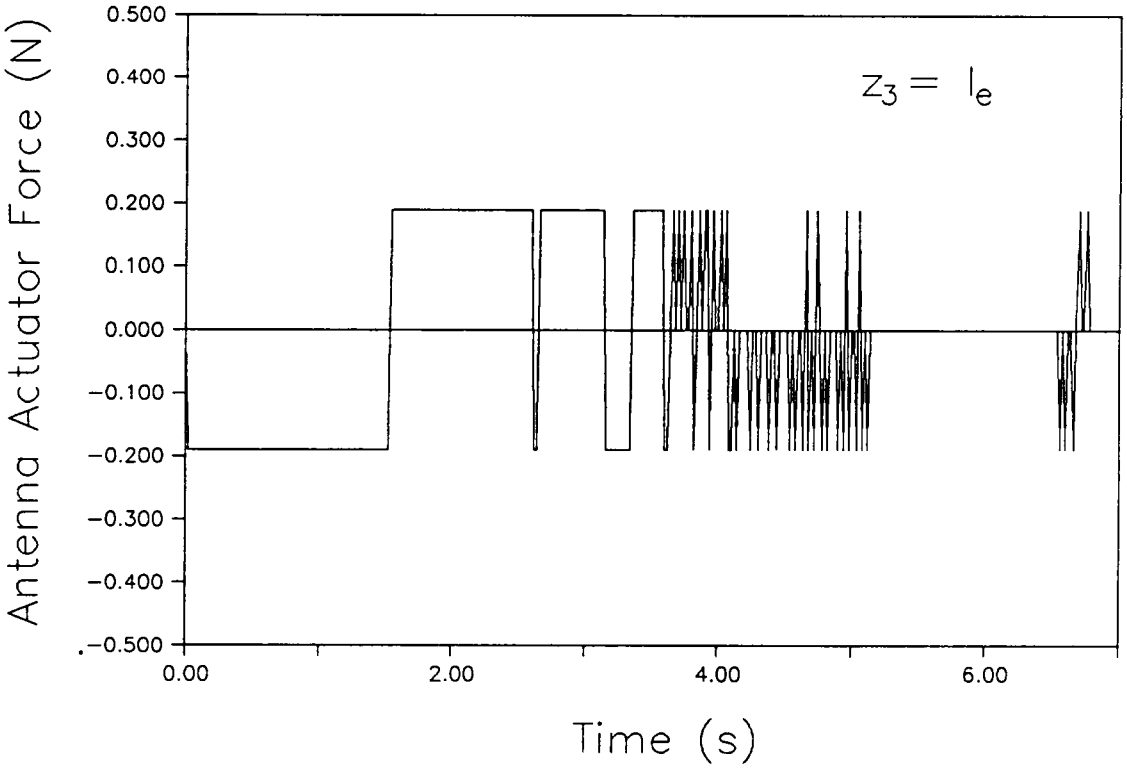

Fig. 54 Antenna Actuator Force for Nonlinear Rigid-Body and Substructure-Decentralized Antenna Control (Pseudo), $z_3 = l_e$

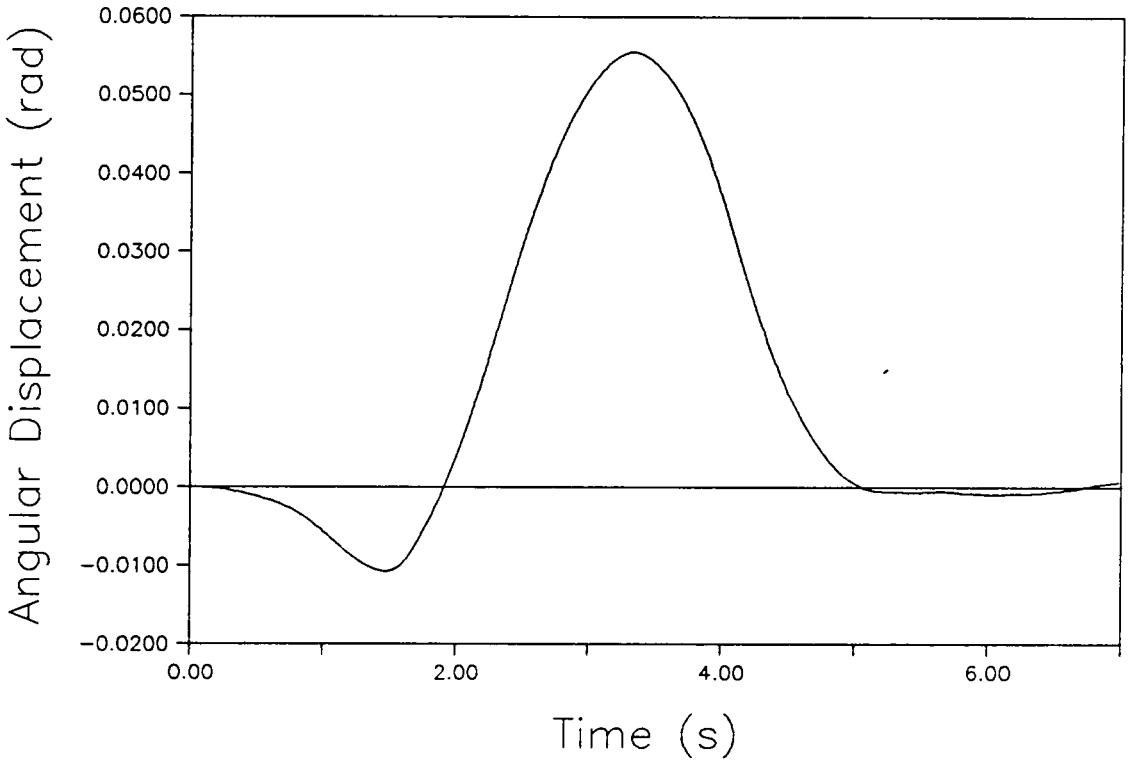

Fig. 55 X-Axis Angular Displacement for Nonlinear Rigid-Body and Substructure-Decentralized Antenna Control (Pseudo)

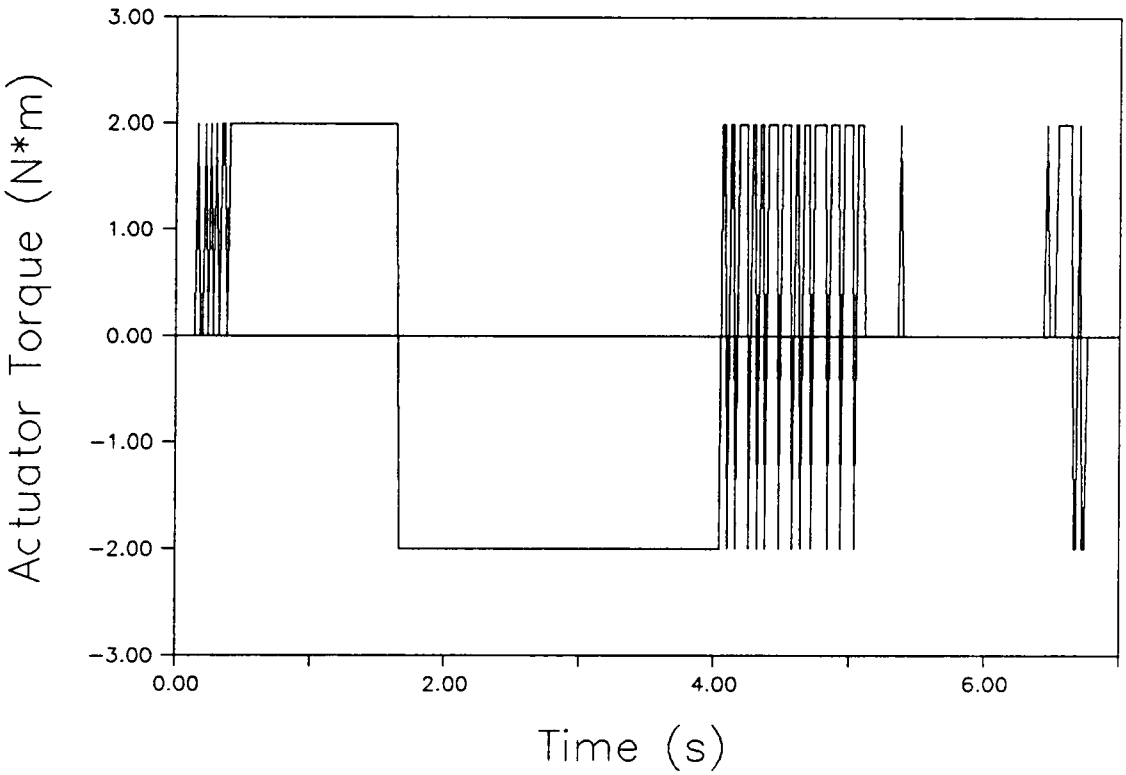

Fig. 56 X-Axis Actuator Torque for Nonlinear Rigid-Body and Substructure-Decentralized Antenna Control (Pseudo)

APPENDIX A

If $\underline{a}(t)$ is a three-dimensional vector, i.e., $\underline{a}(t)=[a_1(t)a_2(t)a_3(t)]^T$, then the skew symmetric matrix $\tilde{a}(t)$, called the vectrice (Ref. 14) is defined as

$$\tilde{a}(t)=\begin{bmatrix} 0 & -a_3(t) & a_2(t) \\ a_3(t) & 0 & -a_1(t) \\ -a_2(t) & a_1(t) & 0 \end{bmatrix} \qquad (A-1)$$

Using this expression, the cross product of two vectors is then given by

$$\underline{a}(t)\times\underline{r}=\tilde{a}(t)\underline{r}=-\tilde{r}\underline{a}(t) \qquad (A-2)$$

Furthermore, the skew symmetric matrix of the cross-product is

$$[\tilde{a}\underline{b}]=\tilde{a}\tilde{b}-\tilde{b}\tilde{a} \qquad (A-3)$$

and the time derivative of a direction cosine matrix, for example

$$C(t)=\begin{bmatrix} c\theta_2c\theta_3 & c\theta_1s\theta_3+s\theta_1s\theta_2c\theta_3 & s\theta_1s\theta_3-c\theta_1s\theta_2c\theta_3 \\ -c\theta_2s\theta_3 & c\theta_1c\theta_3-s\theta_1s\theta_2s\theta_3 & s\theta_1c\theta_3+c\theta_1s\theta_2s\theta_3 \\ s\theta_2 & -s\theta_1c\theta_2 & c\theta_1c\theta_2 \end{bmatrix} \qquad (A-4)$$

where $c\theta_i=\cos\theta_i$, $s\theta_i=\sin\theta_i$, can be expressed as

$$\dot{C} = -\tilde{\omega} C \tag{A-5}$$

or

$$\dot{C}^T = C^T \tilde{\omega} \tag{A-6}$$

where

$$\underline{\omega} = \mathcal{D}\dot{\underline{\theta}} \tag{A-7}$$

and

$$\mathcal{D}(t) = \begin{bmatrix} c\theta_2 c\theta_3 & s\theta_3 & 0 \\ -c\theta_2 s\theta_3 & c\theta_3 & 0 \\ s\theta_2 & 0 & 1 \end{bmatrix} \tag{A-8}$$

APPENDIX B MATRIX EXPRESSIONS

The components of the system state equations (Eq. 2-5a), $M(t)$, $K(t)$ and $G(t)$ have the form

$$M(t)=\begin{bmatrix} m_t\mathbf{I} & \tilde{S}_t^T & E_1^T\bar{\Phi}_1 & \cdots & E_N^T\tilde{\Phi}_N \\ \tilde{S}_t & \mathbf{I}_t & E_1^T+\tilde{r}_{o_1}E_1^T\bar{\Phi}_1 & \cdots & E_N^T\tilde{\Phi}_N+\tilde{r}_{o_N}E_N^T\bar{\Phi}_N \\ \bar{\Phi}_1^TE_1 & \tilde{\Phi}_1^TE_1+\bar{\Phi}_1^TE_1\tilde{r}_{o_1}^T & M_1 & \cdots & 0 \\ \cdot & \cdot & \cdot & \cdots & \cdot \\ \cdot & \cdot & \cdot & \cdots & \cdot \\ \bar{\Phi}_N^TE_N & \tilde{\Phi}_N^TE_N+\bar{\Phi}_N^TE_N\tilde{r}_{o_N}^T & 0 & \cdots & M_N \end{bmatrix} \tag{B-1}$$

$$K(t)=\begin{bmatrix} 0 & 0 & E_1^T(\dot{\tilde{\omega}}_1+\tilde{\omega}_1^2)\bar{\Phi}_1 & \cdots & E_N^T(\dot{\tilde{\omega}}_N+\tilde{\omega}_N^2)\bar{\Phi}_N \\ 0 & 0 & \tilde{r}_{o_1}E_1^T(\tilde{\omega}_1^2+\dot{\tilde{\omega}}_1)\bar{\Phi}_1+E_1[\tilde{\omega}_1J_1(\underline{\omega}_1)+J_1(\dot{\underline{\omega}}_1)] & \cdots & \tilde{r}_{o_N}E_N^T(\tilde{\omega}_N^2+\dot{\tilde{\omega}}_N)\bar{\Phi}_N+E_N[\tilde{\omega}_NJ_N(\underline{\omega}_N)+J_N(\dot{\underline{\omega}}_N)] \\ 0 & 0 & K_1+\bar{H}_1(\underline{\omega}_1)+\tilde{H}_1(\dot{\underline{\omega}}_1) & \cdots & 0 \\ \cdot & \cdot & \cdot & \cdots & \cdot \\ \cdot & \cdot & \cdot & \cdots & \cdot \\ 0 & 0 & 0 & \cdots & K_N+\bar{H}_N(\underline{\omega}_N)+\tilde{H}_N(\dot{\underline{\omega}}_N) \end{bmatrix} \tag{B-2}$$

$$G(t)=\begin{bmatrix} 0 & 2\sum_{e=1}^{N}E_e^T[\widetilde{\tilde{S}_e\underline{\omega}_e}] & 2E_1^T\tilde{\omega}_1\bar{\Phi}_1 & \cdots & 2E_N^T\tilde{\omega}_N\bar{\Phi}_N \\ 0 & G_{22} & G_{23}^1 & \cdots & G_{23}^N \\ 0 & \left[\tilde{\Phi}_1^T\tilde{\omega}_1^T-J_1^T(\underline{\omega}_1)\right]E_1 & 2\tilde{H}_1(\underline{\omega}_1) & \cdots & 0 \\ \cdot & \cdot & \cdot & \cdots & \cdot \\ \cdot & \cdot & \cdot & \cdots & \cdot \\ 0 & \left[\tilde{\Phi}_N^T\tilde{\omega}_N^T-J_N^T(\underline{\omega}_N)\right]E_N & 0 & \cdots & 2\tilde{H}_N(\underline{\omega}_N) \end{bmatrix} \tag{B-3}$$

where

$$m_t = m_r + \sum_{e=1}^{N} m_e \quad \underline{S}_e = \int_{m_e} \underline{r}_e \, dm_e \quad \tilde{S}_t = \sum_{e=1}^{N} \left(m_e \tilde{r}_{o_e} + E_e^T \tilde{S}_e E_e \right) \quad (B-4,5,6)$$

$$I_r = \int_{m_r} \tilde{r} \tilde{r}^T \, dm_r \qquad I_e = \int_{m_e} \tilde{r}_e \tilde{r}_e^T \, dm_e \qquad (B-7,8)$$

$$I_t = I_r + \sum_{e=1}^{N} \left(m_e \tilde{r}_{o_e} \tilde{r}_{o_e}^T + E_e^T I_e E_e + \tilde{r}_{o_e}^T E_e^T \tilde{S}_e E_e + E_e^T \tilde{S}_e E_e \tilde{r}_{o_e} \right) \qquad (B-9)$$

$$M_e = \int_{m_e} \Phi_e^T \Phi_e \, dm_e \quad \bar{\Phi}_e = \int_{m_e} \Phi_e \, dm_e \quad \tilde{\Phi}_e = \int_{m_e} \tilde{r}_e \Phi_e \, dm_e \quad (B-10,11,12)$$

$$\tilde{H}_e(\underline{\omega}_e) = \int_{m_e} \Phi_e^T \tilde{\omega}_e \Phi_e \, dm_e \qquad \bar{H}_e(\underline{\omega}_e) = \int_{m_e} \Phi_e^T \tilde{\omega}_e^2 \Phi_e \, dm_e \qquad (B-13,14)$$

$$J_e(\underline{\omega}_e) = \int_{m_e} (\tilde{r}_e \tilde{\omega}_e + [\widetilde{\tilde{r}_e \underline{\omega}_e}]) \Phi_e \, dm_e \qquad K_e = [\Phi_e, \Phi_e] \qquad (B-15,16)$$

in which the symbol [,] represents an energy inner product (Ref. 24).

$$G_{22} = \sum_{e=1}^{N} \left(E_e^T (2\tilde{\omega}_e I_e - \mathrm{tr} I_e \tilde{\omega}_e) E_e + 2\tilde{r}_{o_e} E_e^T [\widetilde{\tilde{S}_e \underline{\omega}_e}] E_e \right) \qquad (B-17)$$

$$G_{23}^e = 2\tilde{r}_{o_e} E_e^T \tilde{\omega}_e \bar{\Phi}_e + E_e^T \tilde{\omega}_e \tilde{\Phi}_e + E_e^T J_e(\underline{\omega}_e) \qquad (B-18)$$

The matrix $B^*(t)$ (Eq. 2-5b) is given by

$$\mathbf{B}^*(t)=\begin{bmatrix} \mathbf{I} & b^1 & b^2 & \cdot & \cdot & \cdot & b^N \\ \mathbf{0} & c^1 & \mathbf{0} & \cdot & \cdot & \cdot & \mathbf{0} \\ \mathbf{0} & \mathbf{0} & c^2 & \cdot & \cdot & \cdot & \mathbf{0} \\ \cdot & \cdot & \cdot & \cdot & \cdot & \cdot & \cdot \\ \cdot & \cdot & \cdot & \cdot & \cdot & \cdot & \cdot \\ \mathbf{0} & \mathbf{0} & \mathbf{0} & \cdot & \cdot & \cdot & c^N \end{bmatrix} \qquad (B-19)$$

where

$$b^e=\begin{bmatrix} \mathbf{E}_e^T & \mathbf{E}_e^T & \cdots & \mathbf{E}_e^T \\ \tilde{r}_{o_e}\mathbf{E}_e^T+\mathbf{E}_e^T\tilde{r}_{e_1} & \tilde{r}_{o_e}\mathbf{E}_e^T+\mathbf{E}_e^T\tilde{r}_{e_2} & \cdots & \tilde{r}_{o_e}\mathbf{E}_e^T+\mathbf{E}_e^T\tilde{r}_{e_{n_e}} \end{bmatrix} \qquad (B-20)$$

$$c^e=\begin{bmatrix} \Phi_e^T\left(\underline{r}_{e_1}\right) & \Phi_e^T\left(\underline{r}_{e_2}\right) & \cdots & \Phi_e^T\left(\underline{r}_{e_{n_e}}\right) \end{bmatrix} \qquad (B-21)$$

The inertial disturbance vector is defined as

$$\underline{d}(t)=\begin{bmatrix} \sum_{e=1}^{N}\mathbf{E}_e^T(\tilde{\mathbf{S}}_e\dot{\underline{\omega}}_e+\tilde{\omega}_e\tilde{\mathbf{S}}_e\underline{\omega}_e) \\ \sum_{e=1}^{N}\left[\tilde{r}_{o_e}\mathbf{E}_e^T(\tilde{\mathbf{S}}_e\dot{\underline{\omega}}_e+\tilde{\omega}_e\tilde{\mathbf{S}}_e\underline{\omega}_e)-\mathbf{E}_e^T(\mathbf{I}_e\dot{\underline{\omega}}_e+\tilde{\omega}_e\mathbf{I}_e\underline{\omega}_e)\right] \\ -\tilde{\Phi}_1\dot{\underline{\omega}}_1+\int_{m_1}\Phi_1^T\tilde{\omega}_1\tilde{r}_1\underline{\omega}_1\,\mathrm{d}m_1 \\ \vdots \\ -\tilde{\Phi}_N\dot{\underline{\omega}}_N+\int_{m_N}\Phi_N^T\tilde{\omega}_N\tilde{r}_N\underline{\omega}_N\,\mathrm{d}m_N \end{bmatrix} \qquad (B-22)$$

APPENDIX C SDC LINEAR FEEDBACK MATRICES

The submatrices (from Eq. 3-23) associated with the feedback gains for linear Substructure-Decentralized Control applied to the flexible appendages of the system in question are given by

$$\mathcal{K}_{22}(k)=\left[\Phi_o^T\left(\underline{\Gamma}_{o_1}\right)\quad \Phi_o^T\left(\underline{\Gamma}_{o_2}\right)\quad \cdots\quad \Phi_o^T\left(\underline{\Gamma}_{o_{n_o}}\right)\right]^{-1}[k_{22}]$$

$$\mathcal{K}_{24}(k)=\left[\Phi_o^T\left(\underline{\Gamma}_{o_1}\right)\quad \Phi_o^T\left(\underline{\Gamma}_{o_2}\right)\quad \cdots\quad \Phi_o^T\left(\underline{\Gamma}_{o_{n_o}}\right)\right]^{-1}[k_{24}]$$

where, for example, in the case of one antenna,

$$k_{22}=\begin{bmatrix} c_{x_{11}} & 0 & \cdot & \cdot & \cdot & \cdot & \cdot & 0 \\ 0 & c_{x_{22}} & 0 & \cdot & \cdot & \cdot & \cdot & 0 \\ \cdot & 0 & \cdot & 0 & \cdot & \cdot & \cdot & 0 \\ \cdot & \cdot & 0 & c_{x_{rr}} & 0 & \cdot & \cdot & 0 \\ \cdot & \cdot & \cdot & 0 & c_{y_{11}} & 0 & \cdot & 0 \\ \cdot & \cdot & \cdot & \cdot & 0 & c_{y_{22}} & 0 & 0 \\ \cdot & \cdot & \cdot & \cdot & \cdot & 0 & \cdot & 0 \\ 0 & 0 & 0 & 0 & 0 & 0 & 0 & c_{y_{rr}} \end{bmatrix} \quad k_{24}=\begin{bmatrix} b_{x_{11}} & 0 & \cdot & \cdot & \cdot & \cdot & \cdot & 0 \\ 0 & b_{x_{22}} & 0 & \cdot & \cdot & \cdot & \cdot & 0 \\ \cdot & 0 & \cdot & 0 & \cdot & \cdot & \cdot & 0 \\ \cdot & \cdot & 0 & b_{x_{rr}} & 0 & \cdot & \cdot & 0 \\ \cdot & \cdot & \cdot & 0 & b_{y_{11}} & 0 & \cdot & 0 \\ \cdot & \cdot & \cdot & \cdot & 0 & b_{y_{22}} & 0 & 0 \\ \cdot & \cdot & \cdot & \cdot & \cdot & 0 & \cdot & 0 \\ 0 & 0 & 0 & 0 & 0 & 0 & 0 & b_{y_{rr}} \end{bmatrix}$$

Note that $c_{y_{ii}}=b_{y_{ii}}=0$ if the ith substructure mode in the y_o-direction is uncontrolled, and the same can be said for substructure modes in the x_o-direction.

The vita has been removed from the scanned document